



REPUBLIC OF TURKEY
ACIBADEM MEHMET ALİ AYDINLAR UNIVERSITY
INSTITUTE OF HEALTH SCIENCES

**INVESTIGATING THE EFFECTS OF *5,10-*
METHYLENETETRAHYDROFOLATE REDUCTASE C677T
POLYMORPHISM ON HUMAN MESENCHYMAL STEM
CELLS BY USING CRISPR/CAS9 SYSTEM AS A GENE
EDITING TOOL**

BURCU TALUĞ

MASTER THESIS

DEPARTMENT OF MEDICAL BIOTECHNOLOGY

SUPERVISOR

Assist. Prof. Dr. Zeynep Tokcaer Keskin

SECOND SUPERVISOR

Assist. Prof. Dr. Emre Deniz

ISTANBUL-2019



REPUBLIC OF TURKEY
ACIBADEM MEHMET ALİ AYDINLAR UNIVERSITY
INSTITUTE OF HEALTH SCIENCES

**INVESTIGATING THE EFFECTS OF *5,10-*
METHYLENETETRAHYDROFOLATE REDUCTASE C677T
POLYMORPHISM ON HUMAN MESENCHYMAL STEM
CELLS BY USING CRISPR/CAS9 SYSTEM AS A GENE
EDITING TOOL**

BURCU TALUĞ

MASTER THESIS

DEPARTMENT OF MEDICAL BIOTECHNOLOGY

SUPERVISOR

Assist. Prof. Dr. Zeynep Tokcaer Keskin

SECOND SUPERVISOR

Assist. Prof. Dr. Emre Deniz

ISTANBUL-2019

Department: Institute of Health Sciences

Program: Medical Biotechnology

Thesis title: Investigating the Effects of *5,10-Methylenetetrahydrofolate Reductase C677T* Polymorphism on Mesenchymal Stem Cells by Using CRISPR/Cas9 System as a Gene Editing Tool

Students' name and surname: Burcu Taluğ

Date of defence: 10 / 05 / 2019

This is to certify that I have examined this copy of master thesis. I have found that she prepared after fulfilling requirements specified in the associated legislations before the final examining committee whose signatures are below.

Jury president
Prof. Dr. H. Uygur Tazebay
Gebze Technical University

Supervisor of the thesis
Assist. Prof. Dr. Zeynep Tokcaer Keskin
Acıbadem Mehmet Ali Aydınlar University

Second Supervisor of the thesis
Assist. Prof. Dr. Emre Deniz
Acıbadem Mehmet Ali Aydınlar University

Jury member
Assist. Prof. Dr. Beste Kınkoğlu Erol
Acıbadem Mehmet Ali Aydınlar University

Jury member
Assist. Prof. Dr. Hande Koçak
Demiroğlu Bilim University

This thesis has been approved by the above jury and it has been accepted by decision of Health Sciences Board of Directors.


Prof. Dr. Uğur Özbek

Director of the Institute

Acıbadem Mehmet Ali Aydınlar University

DECLARATION

I hereby declare that, this thesis has been written by me based on the data obtained in line with the scientific rules and ethical principles of responsible conduct of research. All information, data, comments, analyses have been collected and processed through scientific, academic writing style, and literature used have been duly shown by giving reference to the original sources in accordance with the publication ethics. I also announce and emphasize that I have not violated any rules secured by patent and copyrights whilst the conduct and writing of this research.



10.04.2019

Burcu Taluğ

ACKNOWLEDGEMENT

Firstly, I would like to express my deep gratitude to my supervisor Assist. Prof. Dr. Zeynep TOKCAER KESKİN, for her patient guidance, enthusiastic encouragement and useful critiques of this research work. She is more than just a good advisor and supervisor to me, she became also my mentor though life besides science. I am very lucky meet her and say that she was my supervisor. I would also like to thank my co-supervisor Assist. Prof. Dr. Emre DENİZ, all kinds of support, especially throughout the laboratory experiences and troubleshooting.

I would like to offer my special thanks to my colleagues Ömer Faruk TAŞTAN, Hazal YILMAZ, Fatma PINAR, Süleyman BOZKURT, Ayşegül EKMEKÇİOĞLU and especially Gülin BARAN for their help during my master studies and for giving me joy and strength to overcome the hard times. I was very lucky to have especially Gülin as a lab partner with helpful discussions on every single experiment and idea and as a friend with constant support.

Finally, I would like to thank my lovely dad, Mustafa TALUĞ and beloved mum, Şenay TALUĞ. I could not make it without their support and unconditional love. And I would like to thank Ömer Faruk TAŞTAN who has always been with me throughout the thesis, and who has always supported me. I am grateful for their support.

This thesis project was supported by Acıbadem Mehmet Ali Aydınlar University Scientific Research Fund ABAPKO 2017/01/12. Burcu Taluğ was supported by TÜBİTAK 1003 project entitled "Genome-Wide Screening With CRISPR/Cas9 and Modeling of Resistance Mechanisms Developed Against Cytotoxic Drugs in Cancer Treatment" with Grant Number: 216S404.

LIST OF CONTENTS

Page No

ACKNOWLEDGEMENT	iv
LIST OF CONTENTS	v
LIST OF ABBREVIATIONS	viii
LIST OF TABLES	xii
SUMMARY	xiii
ÖZET.....	xiv
1 AIM OF STUDY	1
2 INTRODUCTION	2
2.1 Stem Cells	2
2.1.1 Embryonic stem cells	2
2.1.2 Induced pluripotent stem cells	4
2.1.3 Adult stem cells.....	5
2.1.4 Mesenchymal stem cells	7
2.2 Genome Engineering Technologies	11
2.2.1 The CRISPR/Cas system	12
2.3 Metylenetetrahydrofolate Reductase Gene	15
2.3.1 MHTFR enzyme	16
2.3.2 C677T polymorphism	17
2.4 Aim of this thesis study.....	20
3 Materials and Methods	21
3.1 Cell Culture	21
3.1.1 Maintenance of human embriyonic kidney 293T cells	21
3.1.2 Cryopreservation of HEK293T cells.....	21
3.1.3 Maintenance of BMMSCs	22

3.1.4	Cryopreservation of BMMSCs	22
3.2	Differentiation of BMMSCs	23
3.2.1	Differentiation of BMMSCs into adipocytes	23
3.2.2	Differentiation of BMMSCs into osteocytes.....	23
3.2.3	Differentiation of BMMSCs into chondrocytes.....	24
3.3	CRISPR/Cas9 vector design for the HDR-mediated genome editing of cells to introduce C677T SNP in <i>MTHFR</i> gene	25
3.3.1	Bioinformatic design of the sgRNAs	25
3.3.2	Construction of CRISPR/Cas9 vector	29
3.4	DNA Isolation	37
3.5	Primer Design	37
3.6	Polymerase Chain Reaction (PCR)	38
3.7	Restriction Fragment Length Polymorphism (RFLP) Assay	39
3.8	Agarose Gel Electrophoresis.....	40
3.9	Transient Transfection of Human Cell Lines.....	40
3.9.1	Transient transfection of cell lines using polyethylenimine (PEI).....	40
3.9.2	Transient transfection of BMMSCs with electroporation.....	41
3.9.3	Transient transfection of cell lines with lipofectamine	41
4	RESULTS	42
4.1	Characterization of BMMSCs by Stem Cell Marker Expressions.....	42
4.2	Evaluating the Effect of C677T Polymorphisim on Mesencyhmal Stem Cell Properties.....	43
4.2.1	Genotyping of the BMMSCs	43
4.2.2	The effect of <i>MTHFR</i> C677T polymorphism on BMMSC morphology	45
4.2.3	The effect of <i>MTHFR</i> C677T polymorphism on differentiation of BMMSCs	46

4.3	Introducing the <i>MTHFR</i> gene C677T polymorphism to HEK293T cells with CRISPR/Cas9 gene editing system.....	53
4.3.1	Transient transfection of HEK293T cells	53
4.3.2	Genotyping of the mutant HEK 293T colonies with RFLP.....	56
4.3.3	Genotyping of the mutant HEK 293T colonies with T7 endonuclease1 assay	59
4.4	Introducing the <i>MTHFR</i> C677T polymorphism to BMMSCs by using CRISPR/Cas9 gene editing system	60
4.4.1	Optimization of transfection of BMMSCs.....	60
4.4.2	Transient transfection of BMMSCs with the CRISPR/Cas9 system ...	65
5	DISCUSSION AND CONCLUSION.....	68
6	REFERENCES.....	74
7	CURRICULUM VITAE	81

LIST OF ABBREVIATIONS

ASC	Adult Stem Cells
BMMSC	Bone Marrow Derived Mesenchymal Stem Cells
BNP	Brain Natriuretic Peptide
bp	Base Pairs
CD	Cluster Of Differentiation
CFU-F	Colony Forming Unit Fibroblasts
CRISPR	Clustered Regularly Interspaced Short Palindromic Repeats
crRNA	CRISPR RNA
DMEM	Dulbecco's Modified Eagle Medium
DMSO	Dimethyl Sulfoxide
dNTP	Deoxyribonucleotide Triphosphate
DPBS	Dulbecco's Phosphate Buffered Saline
EB	Embryoid Bodies
EDTA	Ethylenediaminetetraacetic Acid
ESCs	Embryonic Stem Cells
FBS	Fetal Bovine Serum
FGF	Fibroblast Growth Factor
GFP	Green Fluorescence Protein
HDR	Homology Directed Repair
HEK	Human Embryonic Kidney
HSC	Hematopoietic Stem Cells
ICM	Inner Cell Mass
ISCT	International Society for Cellular Therapy
iPSC	Induced Pluripotent Cells
LB	Lysogeny Broth
MEF	Mouse Embryonic Fibroblast Cells
MSC	Mesenchymal Stem Cells
<i>MTHFR</i>	Methylenetetrahydrofolate Reductase
NHEJ	Non-homologous End Joining
PAM	Protospacer Adjacent Motif

PBS	Phosphate Buffered Saline
PCR	Polymerase Chain Reaction
PD	Population Doublings
PEI	Polyethylenimine
PKA	Protein Kinase A
RFLP	Restriction Fragment Length Polymorphism
RT	Room Temperature
sgRNA	Single Guide RNA
SNP	Single Nucleotide Polymorphism
Sp1	Specificity Protein 1
ssODN	Single Stranded Oligodeoxynucleotide
T7E1	T7 Endonuclease1
TALEN	Transcription Activator Like Effector Nucleases
TGF	Transforming Growth Factor
THF	Tetrahydrofolate
tracrRNA	Trans Activating CRISPR RNA
UV	Ultra Violet
VEGF	Vascular Endothelial Growth Factor
ZFN	Zinc Finger Nucleases

LIST OF FIGURES

Page No

Figure 2.1 Characteristics of ESCs	3
Figure 2.2 Adult Stem Cells	6
Figure 2.3 Pathways involved in MSC differentiation.....	9
Figure 2.4 MSC differentiation	9
Figure 2.5 Schematic illustration of CRISPR/Cas9 mediated genome engineering .	14
Figure 3.1 Transcripts of MTHFR	25
Figure 3.2 Location of the SNP.....	26
Figure 3.3 Predicted gRNA sequences.....	26
Figure 3.4 Schematic presentation of CRISPR design with gRNAs and screening primers used for genotyping	28
Figure 3.5 Representative image of of pSpCas9(BB)-2A-Puro (PX459) vector	29
Figure 3.6 Agarose gel electrophoresis image of the sgRNA oligonucleotides.....	31
Figure 3.7 Confirmation digest for the cloning of annealed sgRNAs intoPX459 vector.....	32
Figure 3.8 Colony PCR result	34
Figure 3.9 Sequencing result of Colony-2	34
Figure 3.10 Sequencing result of Colony-8	35
Figure 4.1 Representative flow cytometry analysis of BMMSC marker expressions of Donor 1	43
Figure 4.2 RFLP assays of hBM-MSCs.....	45
Figure 4.3 Bright field microscopy images of first passage A) wild type, B) heterozygous and C) homozygous BMMSCs	46
Figure 4.4 Lipid droplets observed after Oil Red O staining of A) wild type, B) heterozygous, C) homozygous differentiated cells, respectively.....	47
Figure 4.5 Adipogenic differentiation of BMMSCs from all genotypes determined by Oil Red O staining.....	48
Figure 4.6 Comparison of adipogenic differentiation capabilities between three genotypes.	49
Figure 4.7 Calcium deposits observed after Alizarin red staining of A) wild type, B) heterozygous, C) homozygous differentiated cells	50

Figure 4.8 Osteogenic differentiation of BMMSCs from all genotypes determined by Alizarin Red staining.....	50
Figure 4.9 Comparison of osteogenic differentiation capabilities between three genotypes.	51
Figure 4.10 Representative images of chondrogenic aggregates observed after toluidine blue staining of A) differentiated wild type cells, B) differentiated homozygous cells.....	52
Figure 4.11 Fluorescent microscopy images of HEK293T cells transfected by using PEI 1:3 with PX458 vector	54
Figure 4.12 Fluorescent microscopy images of A) bright field, B)transfected HEK293T cells transfected with PX458 vector and 1.85 ug of ssODN by using PEI Max in a ratio of 1:4.....	55
Figure 4.13 Fluorescent microscopy images of A) bright field, B)transfected HEK293T cells transfected with pSpCas9(BB)-2A-GFP (PX458) vector by using PEI Max 1:4.	56
Figure 4.14 Genotyping results of mutant HEK293T colonies by RFLP assay	58
Figure 4.15 T7E1 assay of pool of transfected cell and two heterozygous (C/T) colonies	59
Figure 4.16 Fluorescent microscopy images of BMMCSs transfected with PX458 vector by using Lipofectamine with different lipofectamine:DNA amount rati.....	61
Figure 4.17 Fluorescent microscopy images of BMMCSs transfected with PX458 vector by using	62
Figure 4.18 Bright field images of BMMSCs treated with different puromycin concentrations.	64
Figure 4.19 Puromycin resistance death curve of BMMSCs	65
Figure 4.20 Fluorescent microscopy images of A) bright field, B)transfected BMMSCs transfected with PX458 vector by using PEI Max 1:4.....	66
Figure 4.21 T7E1 assay of BMMSCs	67

LIST OF TABLES

Page No

Table 3.1 gRNA sequences	27
Table 3.2 Sequence of ssODN repair template	27
Table 3.3 Annealing of sgRNA	30
Table 3.4 Annealing reaction	30
Table 3.5 Ligation reaction of sgRNA into the plasmid	31
Table 3.6 Ligation reaction condition	32
Table 3.7 Colony PCR reaction.....	33
Table 3.8 Colony PCR reaction conditions	33
Table 3.9 Primer sequences used in screening	37
Table 3.10 PCR conditions for <i>BNP</i> amplification	38
Table 3.11 PCR conditions for <i>MTHFR</i> amplification	38
Table 3.12 Thermal cyler conditions.....	39
Table 3.13 RFLP conditions.....	39
Table 3.14 Electroporation conditions for BMMSs	41
Table 4.1 Flow cytometry analysis of BMMSC marker expressions of Donors	43

SUMMARY

5,10-Methylenetetrahydrofolate reductase (MTHFR) enzyme plays an important role in folate metabolism and C677T single nucleotide polymorphism (SNP) is the most frequently seen mutation in Turkish population and it causes MTHFR enzyme activity to decrease. This SNP has been linked to many different diseases in the literature and accompanied with high homocysteine levels. The latter is considered as an indicator of bone diseases and triggers the osteoclast formation, leading to a decrease in bone density and causes apoptosis in bone marrow derived mesenchymal stem cells (MSCs). As MSCs are known to be the major source of bone, cartilage and adipose tissue regeneration, we hypothesized that there could be a link between *MTHFR* C677T polymorphism and MSC differentiation capacity. That is why in this project, we aim to investigate the effects of *MTHFR* C677T polymorphism on MSC viability, morphology, physiology and differentiation capacity. For this purpose, we obtained primary human bone marrow derived MSCs (BMMSCs) that are wild type (C/C), heterozygous (C/T) and homozygous (T/T) for *MTHFR* gene at the corresponding nucleotide position of C677T SNP. Our primary results revealed that these cells were different by their differentiation capacities. However, this may be due to different genetic backgrounds of the patients. To eliminate the differences in genetic background we designed a guide RNA and a template single stranded oligo nucleotide (ssODN) to introduce C677T polymorphism to the genomes of BMMSCs using CRISPR/Cas9 genome editing technology. However, the cells couldn't be obtained as single cells and died. As a result, this study was able to show that the C677T SNP of *MTHFR* has interference in the differentiation potentials of BMMSCs and it needs further work to investigate the underlying reasons.

Keywords: Human mesenchymal stem cells, CRISPR/Cas9, 5,10-Methylenetetrahydrofolate reductase, *MTHFR*, SNP

ÖZET

İnsan Mezenkimal Kök Hücrelerinde CRISPR/Cas9 Genom Düzenleme Yöntemi ile 5,10- Metilentetrahidrofolat Redüktaz C677T Polimorfizm Etkisinin Araştırılması

5,10-Metilenetrahidrofolat redüktaz (MTHFR) enzimi folat metabolizmasında önemli bir rol oynar ve C677T tekli nükleotit polimorfizmi(TNP), Türk popülasyonunda en sık görülen mutasyondur ve ilgili enzimin aktivitesinin azalmasına neden olur. Bu polimorfizm yüksek homosistein seviyeleri ile birlikte, literatürdeki birçok farklı hastalıkla ilişkilendirilmiştir. Ayrıca kemik hastalıklarının bir göstergesi olarak kabul edilir ve kemik yoğunluğunun azalmasına yol açarak kemik iliği kaynaklı mezenkimal kök hücrelerde (KİMKH'ler) apoptozise neden olan osteoklast oluşumunu tetikler. MKH'lerin başlıca kemik, kıkırdak ve adipoz doku rejenerasyon kaynağı olduğu bilindiğinden, *MTHFR* C677T polimorfizmi ile MKH farklılaşma kapasitesi arasında bir bağlantı olabileceği düşünülmüştür. Bu nedenle bu projede *MTHFR* C677T polimorfizminin MKH canlılığı, morfoloji, fizyoloji ve farklılaşma kapasitesi üzerine etkilerini araştırmayı hedefliyoruz. Bu amaçla, *MTHFR* geni C677T TNP'inin ilgili nükleotit pozisyonu için vahşi tip (C / C), heterozigot (C / T) ve homozigot (T / T) olan kemik iliği kaynaklı birincil insan mezenkimal kök hücrelerini (KİMKH) elde ettik. Birincil sonuçlarımız, bu hücrelerin farklılaşma kapasitelerine göre farklı olduğunu ortaya koydu. Ancak bu hastaların farklı genetik geçmişlerine bağlı olabilir. Genetik arka plandaki farklılıkları ortadan kaldırmak, C677T polimorfizmini tanıtmak ve istenen varyatı CRISPR/Cas9 genome düzenleme teknolojisini kullanarak KİMKH'lerin genomuna entegre etmek için bir kılavuz RNA ve bir şablon tek iplikli oligo nükleotidi (ssODN) tasarladık. Ancak hücreler tek hücre olarak elde edilmeye çalışıldığında elde edilemediler ve öldüler. Sonuç olarak, bu çalışma *MTHFR* C677T SNP'sinin KİMKH'lerin farklılaşma potansiyellerini etkilediğini gösterdi ve altında yatan nedenlerin ortaya çıkarılabilmesi için ileri çalışmaların gerekliliğini ortaya koydu.

Anahtar Kelimeler: İnsan mezenkimal kök hücreleri, CRISPR/Cas9, 5,10- Metilentetrahidrofolat redüktaz, MTHFR, SNP

1 AIM OF STUDY

When the function of the MTHFR enzyme and its related diseases are considered, it is concluded that it is important for normal cellular functions thus the tissue homeostasis. Accordingly as adult stem cells have important roles in providing tissue homeostasis, it was thought that *MTHFR* C677T polymorphism might be also interfering with the differentiation capacities of MSCs. However, there is no study investigating the effect of this polymorphism on the differentiation of MSCs associated with *MTHFR* C677T polymorphism. The aim of this thesis is to introduce *MTHFR* C677T polymorphism by using CRISPR/Cas9 technology to MSCs and to investigate the differentiating capacity, viability, morphological and physiological changes of MSCs bearing this polymorphism having the same genetic background with the wild type MSCs. Furthermore, there are not many studies including changes in the genome of the MSCs using the CRISPR/Cas9 system. This study aims to fill the technical deficits in the literature. Successful introduction of *MTHFR* C677T polymorphism into MSCs using CRISPR/Cas9 technology will also pave the way for the correction of a similar polymorphism by the same method and the use of gene-corrected autologous MSCs for control group. In addition, this technique will lead to the investigation of the effects of various polymorphisms on MSCs. The fact that this polymorphism can be introduced to MSCs by using CRISPR/Cas9 technology is important in terms of investigating the various disease models by filling the necessary information gap in order to study other polymorphisms which have not been studied in the literature.

2 INTRODUCTION

2.1 Stem Cells

Stem cells are cells, which have an ability to differentiate into multilineage and also have an ability to renew themselves. They form somatic cells by their differentiation abilities [1]. They undergo symmetric and also asymmetric cell divisions. When they enter symmetric cell division, they form two-daughter cells that have the same features and that are not differentiated yet but with the ability to differentiate into other somatic cells of different lineages. They can also undergo asymmetric cell division regulated by some intrinsic factors such as polarity formation and mitotic spindle orientation; as well as by extrinsic factors such as the niche of the stem cell. By this, they form progenitor cell and also non-differentiated version for maintaining the body's stem cell pool [2]. The categorization of the stem cells are done at their time of isolation. Embryonic stem cells (ESCs) are *in vitro* cells isolated from inner cell mass cells of the blastocysts, which are active in the early embryonic development time, however, the germ line cells are active in the later stages of the development, and the adult stem cells are active in post natal. Another type of categorization for the stem cells is done according to their potencies. In this type of categorization, ESCs are pluripotent cells which have an ability to form nearly all cells from all of the lineages except cells originating from trophoblast, however adult stem cells are categorized as multipotent, which can form multiple cell types.

2.1.1 Embryonic stem cells

Embryonic stem cells are cells isolated from the inner cell mass (ICM) of the embryo at blastula [3], [4]. They are pluripotent and can form all the cell types that arise from the inner cell mass. That is why they have the ability to generate cells of every three

germ layers -namely endoderm, ectoderm and mesoderm- through differentiation (**Figure 2.1**). Moreover, they keep their pluripotent ability during passages without losing their genetic integrities [5].

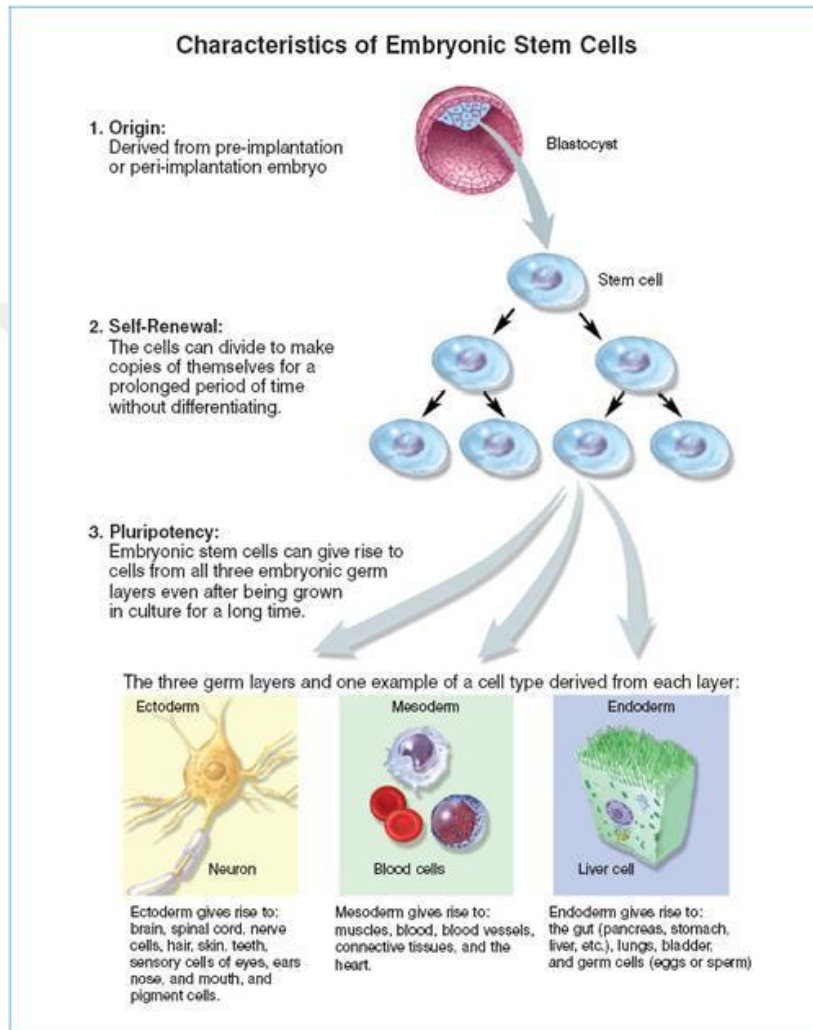


Figure 2.1 Characteristics of ESCs ©2006 Terese Winslow
(<http://stemcells.nih.gov/info/2006report/2006Chapter1.htm>)

In addition to normal embryonic development in health, ESCs are also associated with disease. Such that, teratomas are tumors that contain different cell types from all three germ layers and they are formed from undifferentiated ESCs *in vivo* [6].

Features of ESCs define their special requirements for laboratory handling. *In vitro* ESCs demand the presence of a feeder layer, which is basically usually irradiated mouse embryonic fibroblast cells (MEFs), which secrete growth factors for ESCs survival, or an extra cellular matrix, which increases ESCs' attachment [7]. Additionally, supplemented FGF2 is essential for prolonged ESCs' survival [7]. To maintain their pluripotency and undifferentiated state, endogenous expression of transcription factors like Oct4, Sox2, and Nanog are highly essential [8]. Besides these factors, SSEA 3 and SSEA 4 are expressed from human embryonic stem cells. All together, these endogenously expressed genes are regularly used as markers of pluripotency. ESC colonies, when they are cultured in suspension, form embryoid bodies (EBs), which offer extended possibilities for researchers in stem cell research.

Human ESCs can be obtained from *in vitro* fertilization clinics, however, their isolation comes with several ethical problems. In today's science, ESCs are highly important tools to investigate embryogenesis, cellular replacement therapies and the background of genetic diseases. On the contrary, they require the dissection of an embryo and also their uncontrolled usage has an increased risk of tumor formation, and possibility of immune rejection. In order to overcome these drawbacks, induced pluripotent cells (iPSCs) are invented.

2.1.2 Induced pluripotent stem cells

Because of the ethical and safety problems related with the usage of ESCs, scientists all around the World started to investigate new sources for stem cells with the same features of ESCs. In 2006, these investigations finally answered. Takahashi and Yamanaka, two scientists from Japan, published their study about creating stem cells, which are somatic cells made pluripotent by induction. In the corresponding study, it was shown that, when normal fibroblast cells isolated from mouse treated with a retroviral vector carrying cDNAs of *Oct4*, *Sox2*, *Klf4* and *c-myc* genes, cells gain

pluripotency. These cells are called as induced pluripotent stem cells and the factors mentioned are shortly named as Yamanaka factors. These newly created cells are capable of forming EBs, and teratomas just like ESCs are. In addition, they have the ability to contribute to the development of a mouse when they are injected into an ICM. When this study was revealed, a new era was opened and hopes for personalized medicine for the production of pluripotent stem cells specific for patient himself was raised. Shortly after the initial report, other studies to understand the iPSCs and their mechanisms started to be published worldwide. Although the first iPSCs were obtained by using fibroblast cells [9], [10] it was shown that other cell sources, such as keratinocytes, are also able to be used for obtaining iPSCs [11]. However, there are also some drawbacks using iPSCs. One of them is viral transfection system used in these studies, which can be mutagenic due to random integration of viral genetic material into the host cells' genome. Secondly, using c-myc can be dangerous since it can induce tumor formation. Such problems are highly important and should be solved before they are used in clinical applications such as personalized medicine and cellular therapies.

2.1.3 Adult stem cells

Adult stem cells (ASCs) are important to maintain the homeostasis of the body by locating the related tissues of organs. Their differentiation ability is more limited since they are multipotent rather than being pluripotent like ESCs. The adult stem cells are unique for the tissues they are located in and almost all tissue types have their own ASCs. Since they are tissue specific, they have special set of their own biomarkers, which can be used to identify and to categorize ASCs.

Adult stem cells are firstly discovered at 1950s during the studies after Hiroshima and Nagasaki atomic bombs related irradiation. In these studies, it was shown that, when bone marrow cells of mice were irradiated, their symptoms were highly similar with the patients surviving after atomic bombs. Whereas, when healthy bone

marrows were injected to them, their blood cells were started to proliferate again by regeneration [12], [13].

HSCs are ASCs. CD34, CD117, and Sca1 can be used as surface markers to identify them [14], [15]. They can form different cell types like cardiomyocytes, hepatocytes, muscle cells and also blood cells by differentiation [16], [17] (**Figure 2.2**). In the bone marrow transplantations, HSCs are transplanted and this treatment strategy is widely used for many diseases. In addition to their advantageous usages in clinics, HSCs transplantation has problems because of the increased possibility of immune rejection, called as graft versus host disease.

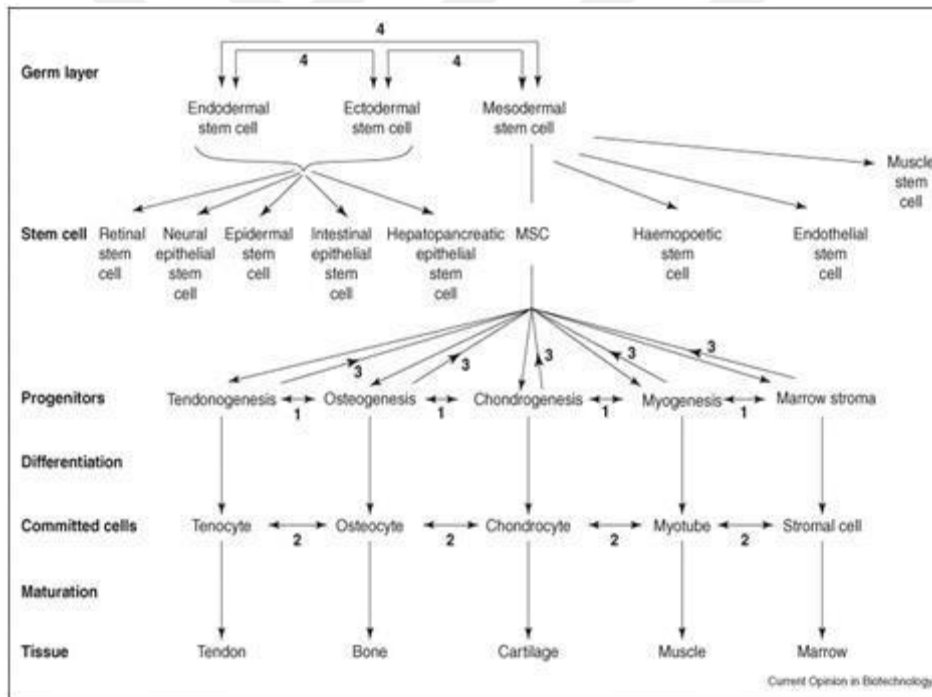


Figure 2.2 Adult Stem Cells © 2005 Elsevier Ltd. (<https://www.science-direct.com/science/article/pii/S0958166905001321>).

2.1.4 Mesenchymal stem cells

In bone marrow, besides HSCs, there are other adult stem cells, called mesenchymal stem cells (MSCs). MSCs are firstly discovered at 1968 by Friedenstein [19]. In the corresponding study, when the MSCs are cultured *in vitro*, it was seen that other than HSCs there were other type of cells that show fibroblastic morphology. They can attach to the culture plate surface and can form colonies. Furthermore, they can also form other cells like adipose cells, cartilage cells and also bone cells by directed differentiation (**Figure 2.3 and 2.4**). At 1988, these cells were firstly called as stromal stem cells, whereas in 1991, Caplan called them as MSCs [20]. In 1999, MSCs from bone marrow were firstly characterized by Pittenger et al. They separate bone marrow aspirates by their densities and plated them. The cells which attach to the plate was counted and checked for their colony forming abilities, which is called as colony forming unit fibroblasts (CFU-F). As a result, it was seen that only the 0.01% of the cells are able to form colonies. Also, it was seen that MSCs can specifically express CD 29, CD 90, CD 71, and CD 106 cell surface biomarkers, which can be used as surface markers for their identification. Beyond expressing specific surface markers, MSCs should lack CD 45, CD 14 and CD 34 surface expressions, which are indeed HSCs markers [21].

Different tissues can be used as a source for the isolation of MSCs. These include bone marrow -as mentioned earlier-, adipose tissue, dental pulp, umbilical cord blood and placenta. However, it was seen that the surface markers as well as the phenotypes of MSCs isolated from different tissue sources are different. For that reason, scientists defined solid criteria lists for their defined identification. According to International Society for Cellular Therapy, MSCs should express CD 73, CD 90, and CD 105; and they should not express CD 19, CD 34, CD 45, CD 11a, and HLA DR. Besides that, they should be able to attach to the surface and should be able to enter adipogenesis, osteogenesis and chondrogenesis *in vitro*. However, it also be checked the presence of tissue specific markers.

Homing capacity is the ability of the cells to migrate to injury sites. This is a highly important feature of MSCs. In the homing process, their surface receptors and also secreted chemokines and cytokines play important roles [22]. When there is an inflammation, chemokines and cytokines are secreted and MSCs start to migrate to the injury site [23]. It was seen that, between the surface receptors, CD 44 has an important role in the homing process [24]. MSCs are also anti-immunogenic cells and they have anti-apoptotic effects in the studies conducted on animal models. When there is a MSCs injection to the injured site, the apoptosis rate of the surrounding cells decrease. The reason for that anti apoptotic feature of MSCs comes from the secretion of important growth factors like VEGF, FGF 2, and TGF β , which are candidate survival signals for surrounding cells in the injured area. Additionally, it was seen that the secretion of these growth factors increase in hypoxia [25], [26].

MSCs have immunomodulatory effects as well. It was seen that when the T cells cultured with MSCs, their proliferation is inhibited [27, [28]. Besides cytotoxic and helper T cells, natural killer cells and other cells that have a role in immunity response are affected by MSCs too. However, still they have MHC receptors and may also be rejected [29]. For this reason, donor match is required for their use in therapies.

2.1.4.1 Differentiation pathways of MSCs

MSCs have differentiation ability into three lineages which are endoderm, ectoderm and mesoderm when they are cultured in specific conditions *in vitro* [30]. Differentiation of MSCs can also be controlled by transcription factors in such a way that, some genes regulate and induce the differentiation of progenitor cells to a specialized cell (**Figure 2.3 and 2.4**) [31].

2.1.4.1.1 Mesoderm differentiation

Differentiation of MSCs towards mesodermal lineage is easier when compared to differentiation into other two lineages as they share the same embryonic origin. For the induction of osteogenic differentiation, medium containing dexamethasone, ascorbic acid, and glycerophosphate is used. This type of differentiation is identified by the formation of calcium deposits, visualized by Alizarin Red staining [34].

In adipogenic differentiation, MSCs are cultured in a medium containing the chemicals insulin, dexamethasone, isobutylmethylxanthine, and indomethacin. The formation of adipocytes are detected by staining the lipid droplets with Oil Red O solution, [35], [36]. Whereas, in chondrocyte differentiation, growth factors TGF β 1 and TGF β 2 are widely administered in vitro to induce of chondrogenesis, and this is detected by toluidine blue staining.

2.1.4.1.2 Ectoderm differentiation

Notch 1 and Protein Kinase A (PKA) pathways are involved in that kind of differentiation. In order to differentiate MSCs into neurons the cells are cultured in a medium containing chemicals such as dimethyl sulfoxide, butylated hydroxyanisole and potassium chloride in addition to others. [37].

2.1.4.1.3 Endoderm differentiation

MSCs can be differentiated into pancreatic islet cells by culturing them in a medium containing nicotinamide and betamercaptaethanol like chemicals. When MSCs are differentiated into pancreatic islet cells, cells are started to secrete insulin and express nestin.[38].

In order to differentiate MSCs into liver cells, cells were cultured in a medium containing hepatocyte growth factors and oncostatin-M *in vitro* [39]. In the maturation of liver cells, mesodermal/endodermal phenotype was seen and some signaling pathways regulate this phenotype by using cytokines [40].

2.2 Genome Engineering Technologies

Genetic backgrounds and the phenotypic results have been linked by using stem cell models of diseases for years. Also, with the advent of sequencing technologies and molecular techniques, finding the links between genetic variants and diseases become possible for scientist. Furthermore, using genome engineering technologies on stem cells makes it possible to reveal the link between genetic background and phenotypic outcomes. In this, one manipulates the stem cells and reveals the effects of changes in genomic architecture on function. Thus combining of these two technologies opened new era for scientists in terms of personalized medicine.

There are various gene editing tools using artificial nucleases [41]. Firstly, there are protein based systems which bind the DNA at a specific location and create double strand breaks like meganucleases, transcription activator like effector nucleases (TALENs), and zinc finger nucleases (ZFNs) [42]. In meganucleases the systems are similar to restriction endonucleases as they have longer recognition sites on DNA [42]. TALEN and ZFN systems use engineered proteins for recognizing a desired sequence of DNA and carryinh a fused-*FokI* restriction enzyme to the target site in order to cut the DNA [42].

When ZFN technology and TALEN are compared, the DNA binding domain of TALEN consist of cys 2 his 2 sequence [43] and nearly 35 amino acid repeats, each

of which targets specific DNA nucleotide. For TALEN, when these amino acid motifs are engineered, specific DNA sequences can be targeted [30]. Such genome engineering technologies have been used to edit genomes of various organisms since their discovery. However there are also challenges of these technologies, which make them hard to use [42]. For meganucleases, their DNA binding-recognition sequence and cleavage site are intertwined [44], which makes the modification of its DNA binding sequence challenging. Whereas in TALEN and ZFN, they have separated DNA recognition sequence from their cleavage site (Fok I) [45], which makes the modification of their binding sites easier. When ZFNs and TALEN was compared, the zinc finger arrays were made to prevent unintended effects that make their creation more challenging for the laboratories. However in TALEN, despite the fact that its design is simpler than ZNF, since it has many TALE repeats, its construct cloning is more laborious and time consuming [42].

2.2.1 The CRISPR/Cas system

Because of the challenges presented by the above-mentioned genome engineering tools, a new gene editing system has been utilized in eukaryotes [46]. CRISPR/Cas system is a modified version of the natural defense mechanism in bacteria and archaea. [46] [47]. In this natural defense mechanism, foreign DNA is firstly cut into pieces and these short protospacer sequences were inserted into the bacterial genome, in the CRISPR locus exactly. This creates a cellular memory for the bacteria. If invasion of the same virus is repeated, the sequence specific CRISPR RNA (crRNA) will be transcribed and then will hybridize with the trans activating crRNA (tracrRNA) to the corresponding homology sequence of the viral genetic material. When this complex is formed, it guides a specific nuclease, Cas, to cut invading genetic material establishing a defense mechanism for the bacteria against the virus [41], [42], [48]. There are two classes of CRISPR/Cas systems using different Cas nucleases. Cas9 is the most widely used nuclease for research, which belongs to Class II, type II and it only needs one nuclease to cleave DNA[46]. This system is

firstly found in *Streptococcus pyogenes*. After nearly 20 years of its discovery, scientist started to think that this bacterial defense mechanism can be programmed to utilize for genome editing since it can induce double strand breaks in DNA and can be used for targeted genome editing. For that purpose, two components of this system should be introduced to the cells; Cas9 nuclease and a single guide RNA (sgRNA), which serves the role of crRNA and tracrRNA in a single transcript. [44].

The breaks that are created by CRISPR/Cas9 system are repaired by the DNA repair mechanisms of the host cell [44]. There are two different repair mechanisms for double strand breaks in mammalian systems, nonhomologous end joining (NHEJ) and homology directed repair (HDR). In NHEJ, the double strand break at the DNA is repaired by joining the broken ends together but during this process it introduces small insertions/deletions (indels). In case these indels are created in the reading frame of a protein-coding gene near its start codon, it is expected that they cause frame-shift mutations and create early stop codons. These mutated transcripts with early stop codons are usually destroyed by the nonsense mediated decay pathway or are sometimes translated into truncated, short and unfunctional proteins. As a result of these molecular cascades, CRISPR/Cas9 system can introduce knock-outs to the organism. In HDR, a DNA template is used to repair the DNA [41], [49]. That is why if a homology bearing sequence is introduced together with the CRISPR/Cas9 system, this repair template will be used while repairing the double strand breaks of the DNA, as a result custom made sequences can be inserted to the genome [41], [42]. Therefore, to introduce a single nucleotide polymorphism (SNP) to the genome requires the presence of three elements; Cas9 endonuclease, sgRNA and single stranded oligodeoxynucleotide (ssODN) as DNA repair template (**Figure 2.5**) [41], [42]. After these elements are delivered into the cell, sgRNA binds to the targeted DNA sequence, with a 20-nucleotide long homology, in the genome and brings about Cas9 protein, which will eventually incise both strands of the DNA at the 3bp upstream of the protospacer adjacent motif (PAM) site of the homology sequence [50] and forms a double stranded break. The host cell then will initiate its own repair mechanisms and the DNA will most likely be repaired using ssODN by HDR or in some cases without using ssODN by NHEJ.

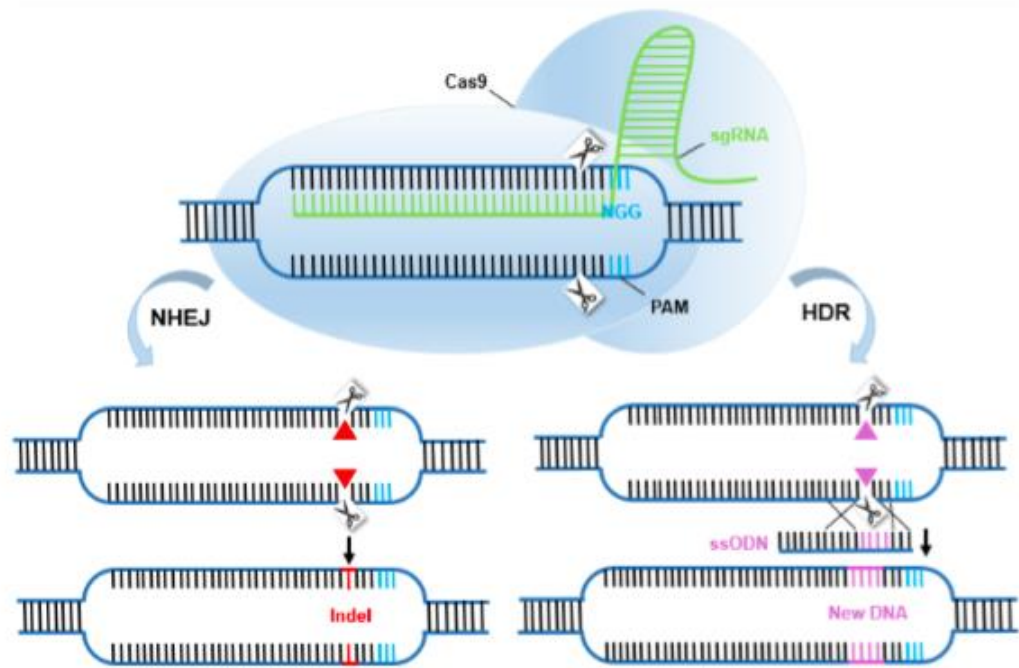


Figure 2.5 Schematic illustration of CRISPR/Cas9 mediated genome engineering © 2014, Springer Nature (<https://www.nature.com/articles/nbt.2842>)

CRISPR/Cas9 system led scientist to edit the genomes of various organisms including mammals, and it became the most widely used and studied genome engineering tool in the history of molecular biology [50], [51]. There are many new benefits of using this system. Multiple mutations can be introduced by using this editing tool to the same genome [52]. CRISPR/Cas9 is a promising tool for the treatment of genetic diseases. Furthermore, there are clinical trials using this genome editing system to treat human immunodeficiency virus (HIV) infections, various types of cancers and other diseases. Many scientists around the World are trying to understand and improve this system, as it will continue having impact in biomedical research [56-59].

There are some challenges to be solved before using this system on humans. The most important one is the off-target effects, which is the binding and cleavage of

unintended genomic loci by Cas9. This may lead to lethal problems. There are some strategies found to eliminate the possibility of off-target effects after the crystallization of Cas9-gRNA-DNA complex such as more improved bioinformatics tools to design sgRNAs. However, none of them actually prevents the problem to the full extent. Therefore novel strategies should be developed to improve CRISPR/Cas9 before being used for medical approaches [49].

2.3 Methylene tetrahydrofolate Reductase Gene

Methylene tetrahydrofolate Reductase (MTHFR) gene is located in p36.3 at chromosome 1 of human genome and encodes MTHFR enzyme which is highly important with its 656 amino acid structure. This enzyme plays role in folate metabolism [60]. Some mutations of *MTHFR* gene are considered to be risk factors for cardiovascular and cerebrovascular diseases by forming hyperhomocysteinemia and homocysteinuria [61-63]. *MTHFR* gene is conserved and present both in humans and mice. Moreover, the conserved genes have 11 exons and their exon sizes are similar bearing about 85% similarity at their coding sequences [64], [65]. The promoter region of *MTHFR* gene does not contain a TATA box, while it contains CpG islands and multiple potential specificity protein 1 (Sp1) binding sites [60]. There is alternative splicing on *MTHFR* gene generating different *MTHFR* transcripts in different tissues [65], [66], [67].

According to the studies conducted on both human and mice, it was seen that there were 15 different mutations on *MTHFR* gene [64], [68]. However, two of them were highly important since they can be seen frequently and are related with serious diseases. One of them is C677T polymorphism, affecting the catalytic domain of the enzyme and related with various diseases like vascular diseases, neural tube defects, and various cancers. The other one is A1298C polymorphism, affecting the regulator site of the enzyme and is mostly related with neural tube defects [66], [68], [69-72].

2.3.1 MHTFR enzyme

5,10-methylenetetrahydrofolate reductase enzyme is a flavoprotein and synthesized by *MTHFR* gene [60], [73], [74]. This enzyme is a cytoplasmic and it has two subunits creating a homodimer structure [75]. The studies conducted on humans showed that, it has 2 isoforms [60], [65]. One of the isoforms is 70 kDa, which is isolated from liver and the other one is 77kDa, which is isolated from other tissues [60], [65].

MTHFR enzyme is an important enzyme for folate metabolism. It has a role in the conversion of homocysteine for remethylation by using homocysteine, transsulphuration and remediation pathways [60]. MTHFR enzyme convert 5,10 methylenetetrahydrofolate (5,10-methylen THF) to 5-methyl tetrahydrofolate (5-methyl THF) [60], [61]. This formed 5-methyl THF becomes a methyl donor for DNA methylation and methionine synthesis. For this purpose, 5-methyl THF gives methyl group for the conversion of homocysteine.

There are some frequently seen mutations especially C677T mutation on *MTHFR* gene causing decrease in enzyme activity [77]. Because of this decrease in MTHFR activity, 5-methyl THF levels decrease and 5-10 methylene THF and plasma homocysteine levels increase [77]. Functional defects in MTHFR enzyme have been related with various health problems [68], [78]. In severe MTHFR deficiency in which hyperhomocysteinemia and homocysteinuria occur, clinical features such as peripheral neuropathy, growth retardation, stroke, and thrombosis are observed [68], [78]. In cases where MTHFR deficiency is mild, which is quite common throughout the population, it can be a risk factor in the occurrence of arterial diseases [68], [78].

2.3.2 C677T polymorphism

MTHFR C677T polymorphism occurs at the 4th exon at *MTHFR* gene effecting N-terminal catalytic domain of the enzyme [78], [79]. In that polymorphism, there is a point mutation at gene of *MTHFR* enzyme and causing the conversion of cytosine to thymine [68], [74], [80], [81]. This mutation, causes conversion of alanine in the protein to a valine [81], [82], [83] decreasing the enzyme activity [81], [82], [83]. Because of this decrease, 5-methyl tetrahydrofolate levels also decrease which blocks the conversion of homocysteine to methionine. These events as a result cause an increase in the homocysteine levels [71], [80-83]. There are three genotypes on *MTHFR* C677T polymorphism; CC(Alanine/Alanine) refers homozygous normal, CT(Alanine/Valine) refer heterozygous and TT (Valine/Valine) refers homozygous mutants genotypes [63], [70].

It has been revealed by metaanalysis that, the C677T polymorphism on *MTHFR* gene is a risk factor for cardiovascular diseases, neural tube defects, strokes, Down syndrome and various cancer types [71], [73]. It has also been shown that, the risks of acute leukemia, colorectal cancer and lung cancer are decreasing however the risk of endometrial cancer is increasing with the presence of the SNP [73], [84], [85].

MTHFR activity in homozygous mutants is less than heterozygous mutants and homozygous normal genotypes, with increased blood homocysteine levels [69], [86]. *MTHFR* deficiency exposes the organism to both the reduction of methionine (and S-adenosylmethionine) and the toxic effects of homocysteine accumulation [69], [71], [86]. Moreover, C677T polymorphism reduces the thermo stability and activity of the *MTHFR* enzyme at 37⁰C or higher. It has been seen that the activity of the enzyme in homozygous mutants are 60 % lower at 37⁰C and 65 % lower at 46⁰C compared to wild type controls [87], [88].

2.3.2.1 *MTHFR* C677T and cerebrovascular diseases

Studies have been shown that, in approximately 25-50% of patients with stroke, moderate hyperhomocysteinemia may occur [73]. According to the results of a metaanalysis approach performed with 24 studies, that have been conducted since 1994 with 900 patients having stroke, has showed that patients having stroke had elevated levels of homocysteine compared to control groups [73]. And also the results coming from other study done with 256 patients having stroke and 325 healthy controls, it was shown that homozygous mutant (TT) genotype and stroke is highly related [89]. In this study, the plasma homocysteine levels are higher in the patients with T/T or C/T genotype compared to patients having C/C genotype [89].

2.3.2.2 *MTHFR* C677T and venous thrombosis

It was already have been shown that, because of the sulfhydryl group of homocysteine, and its hypomethylation and acylation effects, homocysteine has dangerous effects on vein endothelium [73]. Because of that damage caused by homocysteine on veins, it increases the platelet production causing thrombosis [90]. However, there were also studies claiming T/T genotype and Venous Thrombosis are not related [73]. The mutation of *MTHFR* C677T may be an important risk factor for thromboembolism among individuals who carry another risk factor such as cystathionine beta-synthase, homozygous deficiency, which is a transsulfuration enzyme [73].

2.3.2.3 *MTHFR* C677T and neural tube defects

There are some studies claiming that, mutant T allele is a risk factor for neural tube defects [61]. Furthermore, it is well established that, decreased levels of blood folate

is a risk factor for the occurrence of neural tube defects [91]. *MTHFR* polymorphism and folate deficiency together, effect neural development and increase the risk of neural tube defects [61], [71], [91], [92].

2.3.2.4 *MTHFR* and cancer

Decreased level of enzyme activity caused by *MTHFR* polymorphism affects the tumor suppressor gene stability and also hypermethylation [71]. Studies conducted with patients having lung cancer, C677T allele is related with the elevated levels of p16 gene expression which is a tumor suppressor gene [71]. In another study, it was shown that, the decreased levels of MTHFR activity on the lymphocyte of patients having TT genotype caused the elevated levels of 5,10-methylenhydrofolate's concentration required for thymine synthesis [93]. This decreases the DNA damage by blocking the uracil formation caused by cytosine deamination [94]. In another study conducted with patients having cervical cancer, it was shown that TT and CT genotypes are strongly related with cervical cancer [95].

2.3.2.5 *MTHFR* C677T polymorphism and bone related diseases

The *MTHFR* C677T polymorphism results in increased homocysteine levels. High levels of homocysteine are thought to be an indicator of bone diseases and at the same time cause a decrease in bone density by triggering osteoclast formation [96]. In another study, high concentrations of homocysteine have been shown to induce apoptosis in BMMSCs [97].

Behcet's disease is also associated with *MTHFR* C677T polymorphism. In a study, autologous MSCs were injected into patients for treatment of Behcet's disease

vasculitis [98]. However, in this study, three patients had no improvement in their visions, and stem cell therapy was found to be unsuccessful. In another Behcet's disease study, when allogeneic MSCs were given to a patient with central nervous system damage, the damage was significantly reduced [96].

2.4 Aim of this thesis study

When the function of the MTHFR enzyme and its related diseases are considered, it is concluded that MTHFR is important for normal cellular functions thus the tissue homeostasis. Accordingly, as adult stem cells have important roles in providing tissue homeostasis, it was thought that *MTHFR* C677T polymorphism might be also interfering with the differentiation capacities of MSCs. However, there is no study investigating the effect of this polymorphism on the differentiation of MSCs associated with *MTHFR* C677T polymorphism. The aim of this thesis is to introduce *MTHFR* C677T polymorphism by using CRISPR/Cas9 technology to MSCs and to investigate the differentiating capacity, viability, morphological and physiological changes of MSCs bearing this polymorphism having the same genetic background with the wild type MSCs. Furthermore, there are not many studies including changes in the genome of the MSCs using the CRISPR/Cas9 system. This study aims to fill the technical deficits in the literature. Successful introduction of *MTHFR* C677T polymorphism into MSCs using CRISPR/Cas9 technology will also pave the way for the correction of an SNP by the same approach and the use of gene-corrected autologous MSCs for damage repair. In addition, this technique will lead to the investigation of the effects of various polymorphisms on MSCs. The fact that this polymorphism can be introduced to MSCs by using CRISPR/Cas9 technology is important in order to investigate the various disease models by filling the necessary information gap in order to study other polymorphisms which have not been studied in the literature.

3 Materials and Methods

3.1 Cell Culture

3.1.1 Maintenance of human embryonic kidney 293T cells

Human embryonic kidney 293T (HEK293T) cells (ATCC® CRL-3216™) were maintained at Dulbecco's Modified Eagle Medium (DMEM), high glucose (Gibco, 41965039) containing 10% qualified, heat inactivated fetal bovine serum (FBS) (Gibco, 10500064) in tissue culture plates in an Forma Steri-Cycle CO₂ incubator (Thermo Scientific, 51030301) set to 37⁰C and 5% CO₂. When the confluency of the cells reached 80%, cells were splitted mechanically into pre-warmed fresh DMEM (10%FBS) in a ratio of 1:10. Cells were splitted in every three days.

3.1.2 Cryopreservation of HEK293T cells

HEK293T cells were frozen for later use when they reached exponential growth phase. For freezing, cells were counted by 0.4%, liquid, sterile-filtered Trypan blue solution (Sigma-Aldrich, T8154) and approximately 1.000.000-1.500.000 cells were resuspended in ice-cold freezing medium containing 10% DMSO (Biomatik, A2424) in FBS and transferred to cryovials. Cryovials were stored at -80⁰C for 24 hours and transferred to liquid nitrogen tank for long term storage. When the cells were thawed, they were centrifuged at 300g, 3 min. and pellet was washed with pre-warmed fresh DMEM (10% FBS) to remove residual DMSO.

3.1.3 Maintenance of BMMSCs

BMMSCs were cultured in MSC medium by mixing MSC NutriStem® XF medium (Biological Industries, 05-200-1A) and MSC NutriStem® XF Supplement Mix (Biological Industries, 05-201-1U), in tissue culture plates covered with 0.1% Gelatin (Sigma, G9391) in a 5% CO₂ incubator at 37⁰C. The media of the cells were changed with pre-warmed fresh MSC medium every 2 days. When the confluency of the cells reached 80%, cells were trypsinized at 37⁰C for 3 min. with Trypsin 0.05% (1X) with EDTA (Gibco, 25300054). Trypsinization was ended by adding DMEM(10% FBS). Cell were collected to a 15mL falcon tubes and centrifuged at 300 g, 10 min. Pellet was washed with 1X Dulbecco's Phosphate Buffered Saline (DPBS)(Biological Industries, 02-023-1A) than, re-centrifuged at 300g, 5 min and resuspended at pre-warmed fresh MSC medium in a ratio of 1:2 .

3.1.4 Cryopreservation of BMMSCs

BMMSCs were frozen for later use when they reached exponential growth phase. For freezing, they were counted by trypan blue solution and approximately 1.000.000 cells were re-suspended in their culture medium containing 8% DMSO and 12% Dextran40 (Polifleks, Polifarma, PPC-1802140) and transferred to cryovials. Cryovials were stored at -80⁰C for 24 hours and transferred to liquid nitrogen tank for long term storage. When the cells were thawed, they were centrifuged at 300 g, 10 min. Pellet was washed with 1X DPBS, re-centrifuged at 300g, 5 min and re-suspended at pre-warmed fresh MSC medium to remove residual DMSO.

3.2 Differentiation of BMMSCs

3.2.1 Differentiation of BMMSCs into adipocytes

In order to differentiate BMMSCs into adipocytes, cells were counted by trypan blue and seeded into 12 well tissue culture plates to be 1×10^4 cells/cm². Cells were incubated in pre-warmed fresh MSC medium in 5% CO₂ incubator at 37⁰C until the cells were reached 90% confluency. Complete adipogenesis differentiation medium was prepared by mixing StemPro® Adipogenesis Differentiation Basal Medium (Gibco, A10410-01) and StemPro® Adipogenesis Supplement (Gibco, A10065-01). When the cells reached to desired confluency, medium was changed with pre-warmed complete adipogenesis differentiation medium. Cells were cultured for 21 days and medium was changed with pre-warmed prepared complete adipogenesis differentiation medium every 3 days. After 21 days, cells were fixed with 4% paraformaldehyde for 30 min. Fixative was washed with 1X PBS twice and 3 times with ddH₂O and the cells were covered with oil red O solution and incubated for 50 min at RT. The cells then were washed with ddH₂O 3 times. The cells were kept in ddH₂O to prevent from drying for observation. Pictures were taken on Zeiss AX10 microscope (Carl Zeiss, USA) with bright filter.

3.2.2 Differentiation of BMMSCs into osteocytes

In order to differentiate BMMSCs into osteocytes, cells were counted by trypan blue and seeded into 12 well plates to be 5×10^3 cells/cm². Cells were incubated in pre-warmed fresh MSC medium in 5% CO₂ incubator at 37⁰C until the cells were reached 90% confluency. Complete osteogenesis differentiation medium was prepared by mixing StemPro® Osteocyte/Chondrocyte Differentiation Basal Medium (Gibco, A10069-01) and StemPro® Osteogenesis Supplement (Gibco,

A10066-01). When the cells reached desired confluency, medium was changed with pre-warmed prepared complete osteogenesis differentiation medium. Cells were cultured for 21 days and medium was changed with pre-warmed complete osteogenesis differentiation medium every 3 days. After 21 days, the cells were fixed with 70% ethanol for 1h at RT and rinsed twice with ddH₂O and stained with alizarin red-s solution for 30 min at RT. The cells were washed with ddH₂O for 3 times and kept in ddH₂O to prevent from drying for observation. Pictures were taken on Zeiss AX10 microscope (Carl Zeiss, USA) with bright filter.

3.2.3 Differentiation of BMMSCs into chondrocytes

In order to differentiate BMMSCs into chondrocytes, cells were counted by typhan blue and resuspended to generate a cell suspension of 1.6×10^7 viable cells/mL in MSC medium. Micromasses were generated by seeding the cells as 5 μ L droplets in the center of each well in 12 well plates. Cells were incubated in pre-warmed fresh MSC medium in 5% CO₂ incubator at 37⁰C for 2 hours. Complete chondrogenesis differentiation medium was prepared by mixing StemPro[®] Osteocyte/Chondrocyte Differentiation Basal Medium (Gibco, A10069-01) and StemPro[®] Chondrogenesis Supplement (Gibco, A10064-01). After 2 hours, medium was changed with pre-warmed complete chondrogenesis differentiation medium. Cells were cultured for 21 days and medium was changed with pre-warmed complete chondrogenesis differentiation medium every 3 days. After 21 days, the cells were washed with 1X PBS twice and were fixed with 4% paraformaldehyde for 1 hour. After fixation, cells were washed twice and stained with freshly prepared toluidine blue solution for 30 min at RT. The cells were washed with ddH₂O for 3 times (5 min once) until the water became clean and kept in ddH₂O to prevent from drying for observation. Pictures were taken on Zeiss AX10 microscope (Carl Zeiss, USA) with bright filter.

3.3 CRISPR/Cas9 vector design for the HDR-mediated genome editing of cells to introduce C677T SNP in *MTHFR* gene

3.3.1 Bioinformatic design of the sgRNAs

In order to introduce desired SNP to *MTHFR*, firstly the suitable transcript of that gene was selected. According to literature; there were 9 transcripts of *MTHFR* [ensembl.org]. However just MTHFR-202 and MTHFR-204 transcripts had RefSeq accession numbers. That is why they were considered as suitable transcripts (**Figure 3.1**).

Name	Transcript ID	bp	Protein	Biotype	CCDS	UniProt	RefSeq	Flags
MTHFR-201	ENST00000376486.2	1135	29aa	Protein coding	-	A0A1B0GXD9	-	CDS 3' incomplete TSL:1
MTHFR-202	ENST00000376583.7	7044	697aa	Protein coding	CCDS81262	P42898	NM_001330358 NP_001317287	TSL:5 GENCODE basic APPRIS ALT1
MTHFR-203	ENST00000376585.5	5532	697aa	Protein coding	CCDS81262	P42898	-	TSL:5 GENCODE basic APPRIS ALT1
MTHFR-204	ENST00000376590.7	6232	656aa	Protein coding	CCDS137	P42898	NM_005957 NP_005948	TSL:1 GENCODE basic APPRIS P3
MTHFR-205	ENST00000376592.5	7057	656aa	Protein coding	CCDS137	P42898	-	TSL:1 GENCODE basic APPRIS P3
MTHFR-206	ENST00000413656.5	398	29aa	Protein coding	-	A0A1B0GXD9	-	CDS 3' incomplete TSL:1
MTHFR-207	ENST00000418034.1	1034	143aa	Protein coding	-	Q5SNW5	-	CDS 3' incomplete TSL:3
MTHFR-208	ENST00000423400.5	1539	52aa	Protein coding	-	Q5SNW7	-	CDS 3' incomplete TSL:1
MTHFR-209	ENST00000431243.5	870	29aa	Protein coding	-	A0A1B0GXD9	-	CDS 3' incomplete TSL:1

Figure 3.1 Transcripts of MTHFR according to databases on 03.08.2017, (ensembl.org).

Although in the literature, the SNP is called as C677T (Rs number: rs1801133), it is actually found to be at C1711T and C788T of MTHFR-204 and of 202 cDNAs respectively (NM_001330358.1:c.788C>T, NM_005957.4:c.665C>T according to databases on 03.08.2017). When MTHFR-204 and 202 transcripts were considered, the C677T SNP with the Rs number rs1801133 -causing the conversion of Alanine to Valine- is located at chromosome 1, exon 5 instead of exon 4 as cited in the literature according to databases released on 03.08.2017 (**Figure 3.2**) (ensemble.org)

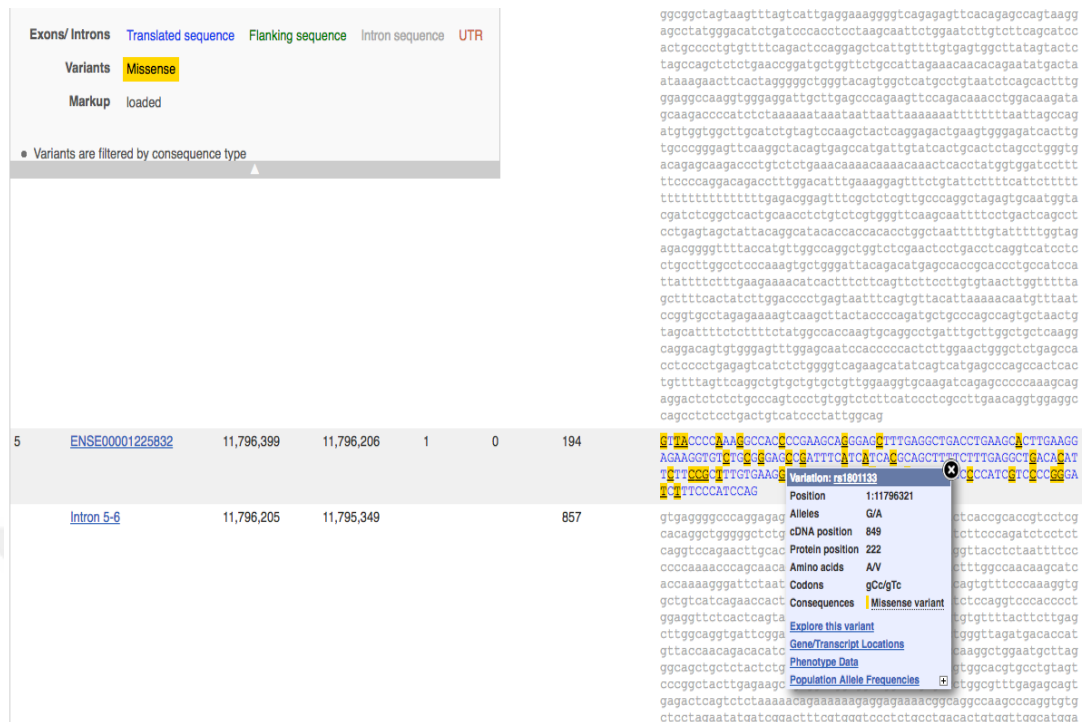


Figure 3.2 Location of the SNP(ensemble.org) (taken on 03.08.2017)

After determining the actual location of the C677T SNP, gRNAs and ssODN was designed *in silico* using crispor.tefor as an online tool. (Figure 3.3). First gRNA listed in the Figure 3.3 was selected because its location was at the targeted area.

Excel tables: Guides Off-targets Saturation-mutagenesis

Position/ Strand	Guide Sequence + PAM + Restriction Enzymes + Variants <input type="checkbox"/> Only G- <input type="checkbox"/> Only A-	Specificity Score	Predicted Efficiency Show all scores		Out-of-Frame score	Off-targets for 0-1-2-3-4 mismatches + next to PAM	Genome Browser links to matches sorted by CFD off-target score <input type="checkbox"/> exons only <input type="checkbox"/> chr1 only
			Doench '16	Mor-Mateos	Click on score to show micro- homology		
22 / rev	AAGCTGCGTGAATGAAAT CGG A- Enzymes: LmnI, TspDTI, NlaIV Cloning / PCR primers	73	57	77	72	0 - 0 - 1 - 18 - 159 0 - 0 - 0 - 1 - 4 178 off-targets	4:intron:RCAN1 4:intron:RP11-797M17.1 4:intergenic:AP000797.4-AP001891.1 show all...
52 / fw	CATCACGCAGCTTTCTTTG AGG Cloning / PCR primers	69	33	28	56	0 - 0 - 2 - 13 - 141 0 - 0 - 2 - 1 - 6	4:intergenic:RP1-309H15.2-RP1-209A6.1 4:intergenic:TRHR-NUJDC1 4:intergenic:RP11-567P19.1-XYLT1 show all...

Figure 3.3 Predicted gRNA sequences (crispor.tefor)

Table 3.1 gRNA sequences

Top oligo	caccgAAGCTGCGTGATGATGAAAT
Bottom oligo	caaaATTTTCATCATCACGCAGCTTc

3.3.1.1 ssODN design

MTHFR gene is at the reverse strand of the gDNA. For that reason, PAM sequence should be located at the forward strand and ssODN should be at the reverse strand since the enzyme will locate to the region where PAM sequence is and mediate the digestion of the other strand at the first order. For that reason, ssODN that would supposed to be used for the homologous recombination was designed as 120 bp by replacing the nucleotide to be changed at the center of the sequence, G to A (complementary to C to T).(**Table 3.2**). Moreover, the conversion of cytosine into thymine, also disturbs the NGG of the PAM sequence. This will prevent re-binding and possible re-cutting of Cas9 enzyme to the corresponding genomic locus after homologous recombination.

Table 3.2 Sequence of ssODN repair template

CCGAAGCAGGGAGCTTTGAGGCTGACCTGAAGCACTTGAAGGAGA AGGTGTCTGCGGGAGTCGATTTTCATCATCACGCAGCTTTTCTTTGA GGCTGACACATTCTTCCGCTTTGTGAAGG

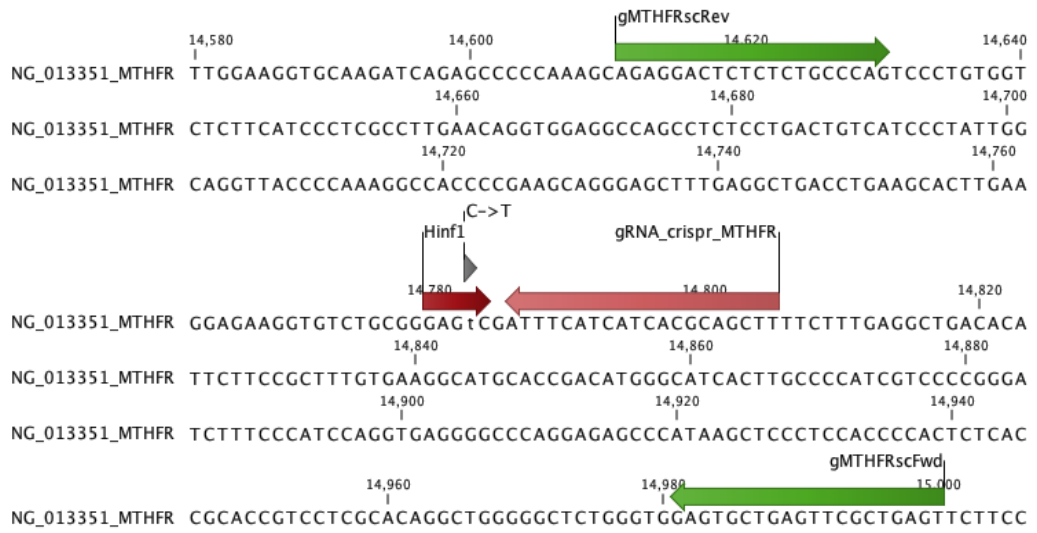


Figure 3.4 Schematic presentation of CRISPR design with gRNAs and screening primers used for genotyping

3.3.2 Construction of CRISPR/Cas9 vector

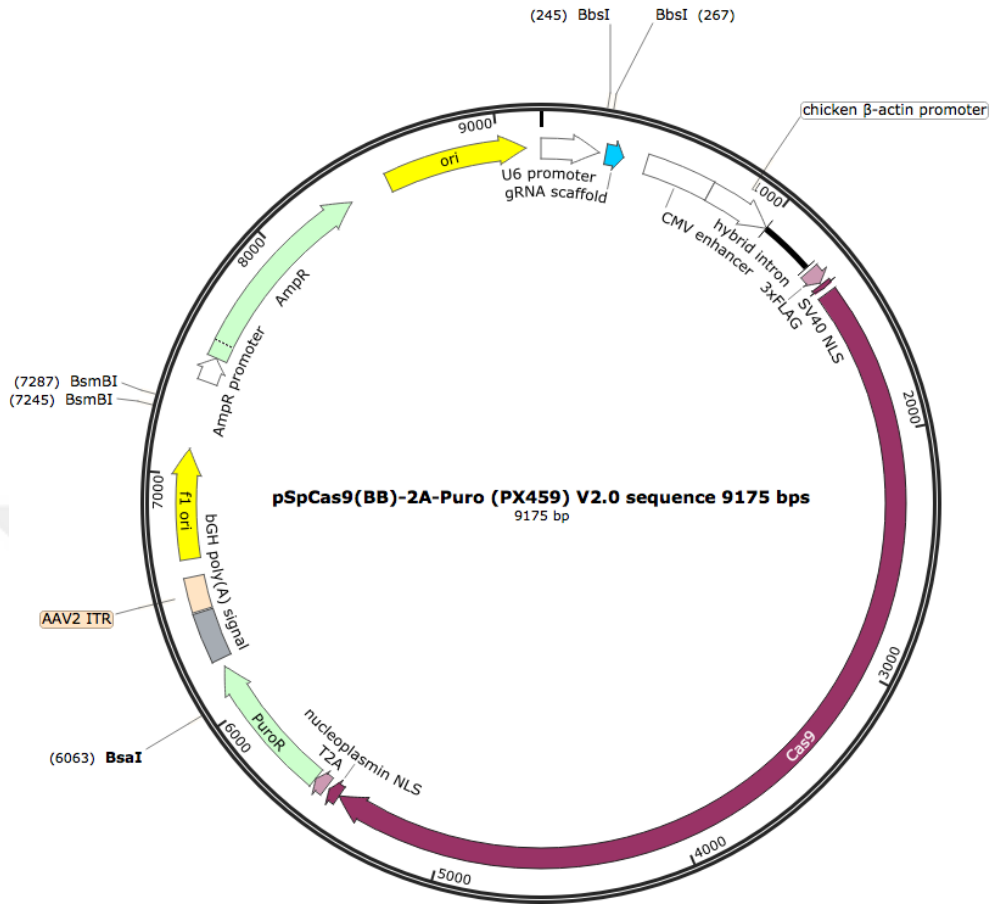


Figure 3.5 Representative image of of pSpCas9(BB)-2A-Puro (PX459) vector (addgene.org)

The designed sgRNAs were single stranded and in order to clone them into expression plasmid vector, complementary strands of sgRNAs were firstly annealed together (**Figure 3.6**) and then ligated into pSpCas9(BB)-2A-Puro vector, which is also cut with *Bbs* I enzyme simultaneously. (**Figure 3.7**).

3.3.2.1 Annealing of the sgRNAs

For the annealing of the sgRNAs following reaction indicated in **Table 3.3** were prepared in PCR tubes. PCR reactions were performed on T100™ Thermal Cycler (BioRad,1861096) with the thermal cyler conditions indicated in **Table 3.4 (Figure 3.6)**

Table 3.3 Annealing of sgRNA

Sg Top oligo (100 µM)	1 µL
Sg Bottom oligo (100 µM)	1 µL
T4 ligation buffer	1 µL
T4 PNK	1 µL
ddH ₂ O	6 µL

Table 3.4 Annealing reaction

37°C	30 min
95°C	5 min
95°C	14 min (Ramp down 0.1°C/s)

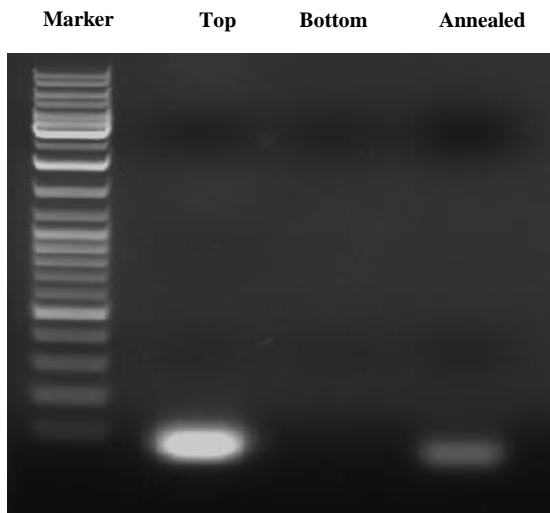


Figure 3.6 Agarose gel electrophoresis image of the sgRNA oligonucleotides. sgRNA targeting top strand was indicated as Top, sgRNA targeting bottom strand was indicated as bottom, and annealed sgRNAs were indicated as annealed.

3.3.2.2 Ligation of pspCas9-2a-Puro plasmid

For the ligation of plasmid with sgRNAs, following reaction indicated in **Table 3.5** were prepared in PCR tubes. Ligation reactions were performed on T100™ Thermal Cycler (BioRad,1861096) with the thermal cyler conditions indicated in **Table 3.6** (**Figure 3.7**)

Table 3.5 Ligation reaction of sgRNA into the plasmid

pspCas9-2a-Puro (100 ng/ μ L)	1 μ L
Diluted oligo (1:200)	2 μ L
T4 ligase buffer	2 μ L
DTT (Freshly diluted to 10 mM)	1 μ L
ATP (10 mM)	1 μ L
Bbs I	1 μ L
T4 DNA ligase	0.5 μ L
ddH2O	11.5 μ L

Table 3.6 Ligation reaction condition

37°C	5 min
21°C	x6 cycles 5 min
95°C	14 min (Ramp down 0.1°C/s)

Marker **Cut** **Uncut** **Ligated**
 plasmid **plasmid** **plasmid**

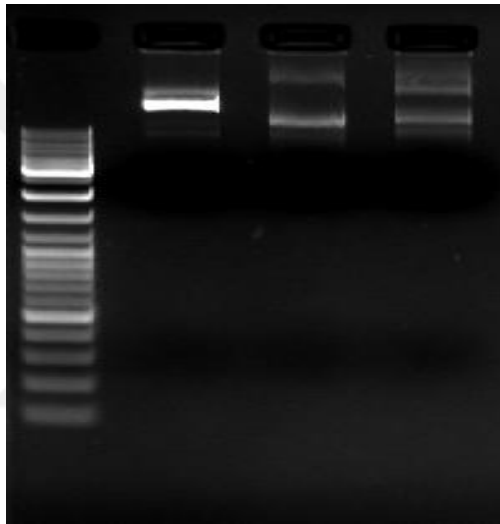


Figure 3.7 Confirmation digest for the cloning of annealed sgRNAs intoPX459 vector.

It can be seen from the agarose gel that, two sgRNAs were annealed together (**Figure 3.6**) and pSpCas9(BB)-2A-Puro vector cut with *Bbs* I enzyme ligated with annealed sgRNAs correctly (**Figure 3.7**)

3.3.2.3 Colony PCR

After the CRISPR/Cas9 vector was constructed, it was transformed into chemically competent DH5 α strain of *E.coli* cells and colony PCR was performed as described before by using a primer which can bind PX459 vector as a reverse primer and designed sgRNA targeting top strand as a forward primer so that if the vector inside the bacteria ligated with sgRNA, as a result of the PCR an approximately 120 bp sized band will be observed in the gel (**Figure 3.8**)

For the colony PCR, following reactions indicated in **Table 3.7** were prepared in PCR tubes. Transformed and grown colonies were picked by using sterile micropipette tips and firstly spread onto a replica plate than, immersed into the prepared reaction mixtures in PCR tubes. PCR reactions were performed on T100™ Thermal Cycler (BioRad,1861096) with the thermal cyler conditions indicated in **Table 3.8** Replica plate was stored at 4⁰C for later use.

Table 3.7 Colony PCR reaction

Component	10 μ l reaction
10X Standard <i>Taq</i> (Mg-free) Reaction Buffer	1.25 μ l
25 mM MgCl ₂	0.65 μ l
10 mM dNTPs	0.20 μ l
10 μ M Forward Primer	1 μ l
10 μ M Reverse Primer	1 μ l
<i>Taq</i> DNA Polymerase	0.125 μ l
ddH ₂ O	Up to 10 μ l

Table 3.8 Colony PCR reaction conditions

95 ⁰ C	3 min
95 ⁰ C	30 sec

60°C	30 sec	x28 cycles
68°C	30 sec	
68°C	5 min	

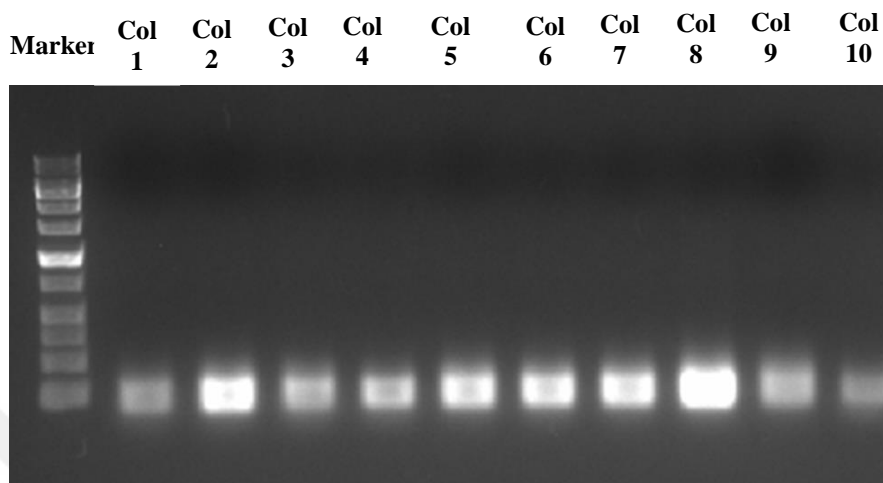


Figure 3.8 Colony PCR result

According to colony PCR, colony-2 and colony-8 were selected since their PCR bands were denser than others (**Figure 3.8**) and they were sent to sanger sequencing (MedsanTek Co.) to prove that they contained the designed sgRNAs.

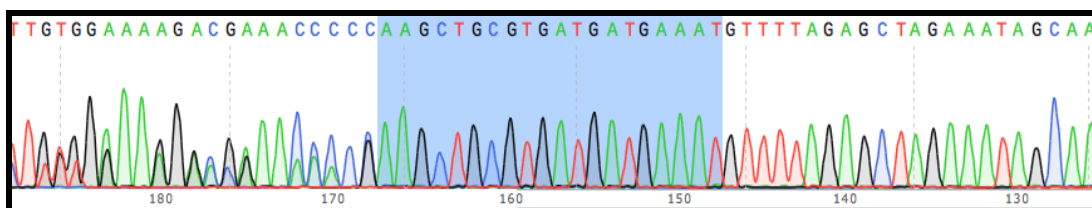


Figure 3.9 Sequencing result of Colony-2. Highlighted blue regions show the sgRNA sequence

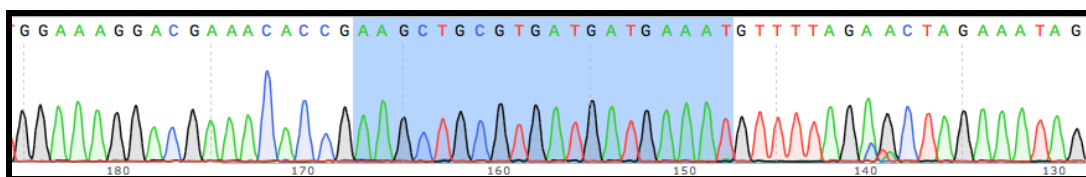


Figure 3.10 Sequencing result of Colony-8. Highlighted blue regions show the sgRNA sequence

According to the sequencing result (**Figure 3.9** and **Figure 3.10**), both the colonies contained desired sgRNAs, colony-8 was selected for further use. The plasmid isolated from this colony was pSpCas9(BB)-2A-Puro (PX459) ligated with sgRNA vector and decided to be used as a CRISPR/Cas9 vector to introduce *MTHFR* gene C677T polymorphism into HEK293T cells first and then primary human BMMSCs in later experiments will be discussed in following sections.

3.3.2.4 Bacterial culture

Escherichia coli (*E. coli*) DH5 α and HB101 strains were used for desired applications. Bacteria were cultured in LB broth (Sigma, L7659) containing Ampicillin(Neofroxx, 1728GR010) at a final concentration of 100 μ g/ml overnight at 37 $^{\circ}$ C with vigorous shaking at 180 rpm (shaker info ver). For long term storage; glycerol stocks were prepared by adding 87% glycerol to bacterial culture until final volume of glycerol was reached to 10% by mixing 115 μ l of 87% glycerol with 885 μ l of bacterial culture for 1 ml bacteria stock. Glycerol stocks of bacteria were stored at -80 $^{\circ}$ C. For single colonies, bacteria were cultured on LB agar containing final concentration of 100 μ g/ml ampicillin in petri dishes for 24 hours at 37 $^{\circ}$ C HeraTherm incubator (Thermo Scientific, 1GS60)

3.3.2.5 Transformation

For the transformation; plasmid DNA (1 μ L for ligation reaction) was mixed with competent cells taken from -80°C and incubated on ice for 30 min. After the incubation, cells were heat shocked at 42°C by using heat block for 90 sec followed by incubation on ice for 1 min. 800 μ L of LB was added on the cells and this culture was incubated at 37°C heat block for 45 min. After 45 min, cells were centrifuged at 13 000 rpm for 30 sec and pellet was resuspended with 100 μ L of LB. Cells were spread on LB agar petri dishes containing final concentration of 100 $\mu\text{g}/\text{ml}$ ampicillin by using glass beads. Petri dishes was incubated overnight at 37°C HeraTherm incubator (Thermo Scientific, 1GS60).

3.3.2.6 Plasmid DNA isolation

Plasmid DNA isolation was performed using PureLink™ HiPure Plasmid DNA Purification Kits (Invitrogen, K2100-04). For plasmid DNA isolation, bacteria were taken either from glycerol stock (-80°C) or as single colony on LB agar plate, and cultured overnight in 100 mL LB Broth containing 100 $\mu\text{g}/\text{ml}$ Ampicillin at 37°C with vigorous shaking at 180 rpm. After 24 hours, bacteria cultures were centrifuged at 4000 g for 10 min. Pellets were resuspended with resuspension buffer and lysed for 5 min with lysis buffers at RT. For the precipitation, precipitation buffer was added and samples were centrifuged at 4000 g for 30min than supernatants were loaded on equilibrated columns. After the solution in the column drained by gravity flow, columns were washed and eluted with Elution buffer. DNA was recovered with isopropanol and samples were centrifuges at 12 000g for 45 min at 4°C . Pellets were washed with 70% ethanol and after 10 min of air drying, pellets were resuspended in ddH₂O containing RNase (Macherey-Nagel, 740505). The concentration and purity of the DNA isolated were determined by using Microplate reader Varioscan Flash (Thermo Scientific, MIB#5250030)

3.4 DNA Isolation

DNA isolation was performed by using a DNA isolation from Tails-Proteinase K method by Jacks Lab, Koch Institute for Integrative Cancer Research at MIT, 2017. Tail lysis buffer (Appendix A) containing Proteinase K (Macherey-Nagel, 740506) was added to the samples. Samples were incubated in digital heating shaking drybath (ThermoFisher Scientific,88880028) adjusted to 55⁰C for 1.5 hours, then 5 M NaCl solution was added on them. Tubes were shaken and incubated on ice for 10 min. Samples were centrifuged (Thermo Scientific, MicroCl 21R) at 3000 rpm for 30 min at 4⁰C, isopropanol was added onto them and incubated on RT. DNA was recovered by centrifuge at max speed for 10 min at RT. Pellets were resuspended with 70% Ethanol, samples were re-centrifuged at max speed for 10 min at RT. Tubes were inverted on bench and air dried, pellets were resuspended with ddH₂O containing RNase The concentration and purity of the DNA isolated were determined by using Microplate reader Varioscan Flash (Thermo Scientific, MIB#5250030)

3.5 Primer Design

Primers for all the genes amplified were listed in **Table 3.9** were designed by using Primer Blast (NCBI). Ensemble and NCBI databases were used to check the specificity of the primers and product sizes they would amplify. Primers were ordered from Sentegen Biotech,Turkey.

Table 3.9 Primer sequences used in screening

Primer Name	Primer Sequence (5' - 3')
<i>MTHFR-Forward</i>	ACTCAGCGAACTCAGCACTC
<i>MTHFR-Reverse</i>	AGAGGACTCTCTCTGCCAG
<i>BNP-Forward</i>	CAGCCTCGGACTTGGAAC
<i>BNP-Reverse</i>	CTCCAGACACCTGTGGGAC

3.6 Polymerase Chain Reaction (PCR)

For amplifications of *MTHFR* and *BNP*, PCR was applied by using optimized PCR conditions indicated in **Table 3.10** and **Table 3.11** on T100™ Thermal Cycler (BioRad,1861096) with the thermal cycler conditions indicated in **Table 3.12**.

Table 3.10 PCR conditions for *BNP* amplification

Component	25 µl reaction
10X Standard <i>Taq</i> (Mg-free) Reaction Buffer	2.5 µl
25 mM MgCl ₂	1.5 µl
10 mM dNTPs	0.5 µl
10 µM Forward Primer	1 µl
10 µM Reverse Primer	1 µl
Template DNA	100 ng
<i>Taq</i> DNA Polymerase	0.125 µl
ddH ₂ O	Up to 25 µl

Table 3.11 PCR conditions for *MTHFR* amplification

Component	25 µl reaction
10X Standard <i>Taq</i> (Mg-free) Reaction Buffer	2.5 µl
25 mM MgCl ₂	1 µl
10 mM dNTPs	0.5 µl
10 µM Forward Primer	1 µl
10 µM Reverse Primer	1 µl
Template DNA	100 ng
<i>Taq</i> DNA Polymerase	0.125 µl
ddH ₂ O	Up to 25 µl

Table 3.12 Thermal cyler conditions

	<i>BNP</i>	<i>MTHFR</i>
Initial denaturation	95 ⁰ C, 4 min	95 ⁰ C, 4 min
Denaturation	95 ⁰ C, 30 sec.	95 ⁰ C, 30 sec.
Annealing	60 ⁰ C, 30 sec.	60 ⁰ C, 30 sec.
Extension	68 ⁰ C,30 sec.	68 ⁰ C,30 sec.
Cycles	35	35
Final Extension	68 ⁰ C, 5 min.	68 ⁰ C, 5 min.

3.7 Restriction Fragment Length Polymorphism (RFLP) Assay

RFLP assay was performed by incubating the amplified PCR samples with *HinfI* (New England Biolabs, R0155S) enzyme and CutSmart (New England Biolabs, R0155S) buffer for 1 hour at 37⁰C in T100™ Thermal Cycler (BioRad,1861096). For 25 µl of PCR sample; conditions indicated below was applied (**Table 3.13**)

Table 3.13 RFLP conditions. Cut indicates samples cut with *HinfI* enzyme, uncut indicates samples do not cut with enzyme. Uncut samples were used as a control

	Uncut	Cut
CutSmart Buffer	2.5 µl	2.5 µl
<i>HinfI</i> enzyme	-	0.5 µl (5 units)
ddH₂O	2.5 µl	2 µl

3.8 Agarose Gel Electrophoresis

Gels were prepared by dissolving the required amount of PegGOLD universal agarose (Peqlab, HD00020) (ranging from 0.5 g to 3 g) in 50 ml-150 ml (depending on the sizes of the DNA fragments in the samples) 1X TAE. 1% agarose gel was used for all experiments (PCR analysis, control of annealing and ligation of the sgRNAs etc.) except RFLP analysis. For RFLP analysis, 2% agarose gel was used. For fully dissolving the agarose, microwave oven was used. 1.5 µl ethidium bromide stock (10 mg/ml)(Sigma, E1510) per 100 ml gel solution for a final concentration of 0.15 µg/ml DNA samples were mixed with 6X DNA Loading dye (R0611, Thermo Scientific) stock solution for final concentration of loading dye in solution 1X and loaded on gel. Gels were run at 80 V, 60 min for RFLP and T7E1 assays and 100 V 60 min for PCR. The bands were visualized under UV light by using ChemiDoc Imaging System (BioRad, 1708265). Generuler DNA ladder (Thermo Prizma,LSG-SM0331)

3.9 Transient Transfection of Human Cell Lines

3.9.1 Transient transfection of cell lines using polyethylenimine (PEI)

The day before the transfection, cells were split as previously described in section 2.1.1 and 2.1.3 into 10 cm tissue culture plates. Transfection mixtures were prepared by mixing totaly 10 µg DNA (plasmid DNA and ssODN) in 1 mL serum free DMEM with (1µg/µL) PEI MAX -Transfection Grade Linear Polyethylenimine Hydrochloride (MW 40,000) (Polysciences, 24765-1) at a desired ratio. Mixture was immediately vortexed and incubated at RT for 15 min, then mixture was added onto the cells drop by drop.

3.9.2 Transient transfection of BMMSCs with electroporation

For the electroporation, 1×10^6 cells were transferred into the 2 mm electroporation cuvettes and pulsed at the following conditions **Table 3.14**. GenePulser Xcell (Biorad, 1652660) was used for the electroporation.

Table 3.14 Electroporation conditions for BMMSCs

Amount of DNA used in the transfection (μg)	Conditions
60 μg DNA	350 V, 950 μF 200 Ω
50 μg DNA	150 V, 1050 μF , 200 Ω
10 μg DNA	90 V, 5.5 to 5.7 msec duration
50 μg DNA	200 V, 0.500 μF

3.9.3 Transient transfection of cell lines with lipofectamine

The day before the transfection, cells were split as previously described in section 2.1.1 and 2.1.3 into 10 cm tissue culture plates. Transfection mixtures were prepared by mixing totally 10 μg DNA (plasmid DNA and ssODN) in 1 mL serum free DMEM with Lipofectamine™ 3000 Transfection Reagent (Invitrogen, L3000015) at a desired ratio. Mixture was immediately vortexed and incubated at RT for 15 min, then mixture was added onto the cells drop by drop.

4 RESULTS

4.1 Characterization of BMMSCs by Stem Cell Marker Expressions

BMMSCs previously were isolated from human donors' bone marrow and were characterized for their MSCs marker expressions using flow cytometry by Labcell (Acibadem Health Group Co.). MSCs marker expressions and validation reports of the cells were shown below (**Table 4.1, Figure 4.1**). Figure 4.1. given below is a representative flow analysis result showing the gates and the quadrans. All the donor cells were analyzed accordingly and their specific quantitated results were given at the Table 4.1 As can be seen from the table, all the BMMSCs are expressing universal MSC markers validated by ISCT including CD73, CD90 and CD 105 and excluding the hematopoietic markers (CD 34, CD45 and HLA DR) [99] (**Figure 4.1**) (**Table 4.1**). The actual names of the donors were hidden for their privacy and for the ethical reasons and in this study they were simply referred as donor1, donor2, and donor3.

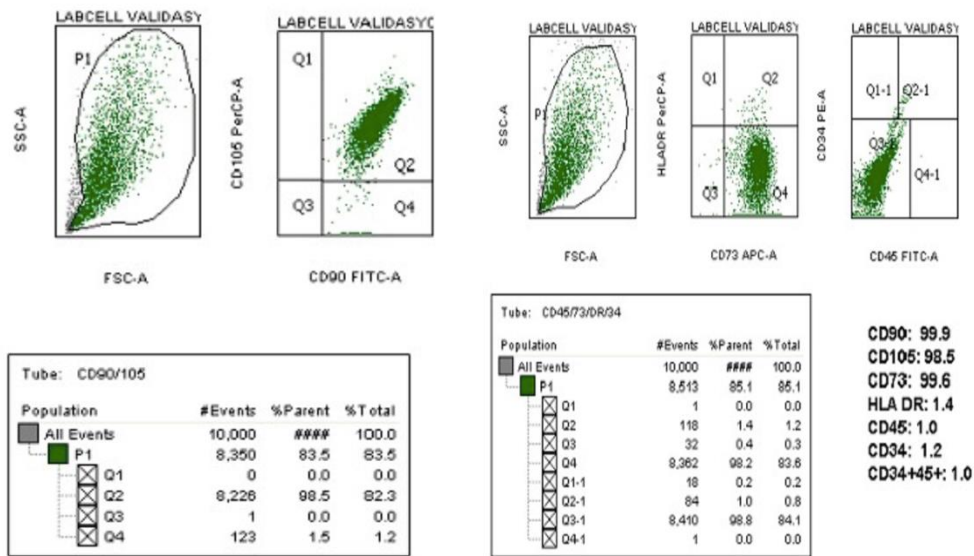


Figure 4.1 Representative flow cytometry analysis of BMMSC marker expressions of Donor 1

Table 4.1 Flow cytometry analysis of BMMSC marker expressions of Donors

	CD90	CD105	CD73	HLA-DR	CD34	CD45
Donor1	99,9	98,5	99,6	1,4	1,2	1,0
Donor2	99,8	99,5	99,3	0,1	0,7	0,1
Donor3	99,9	99,9	99,3	0,2	0,4	0,1

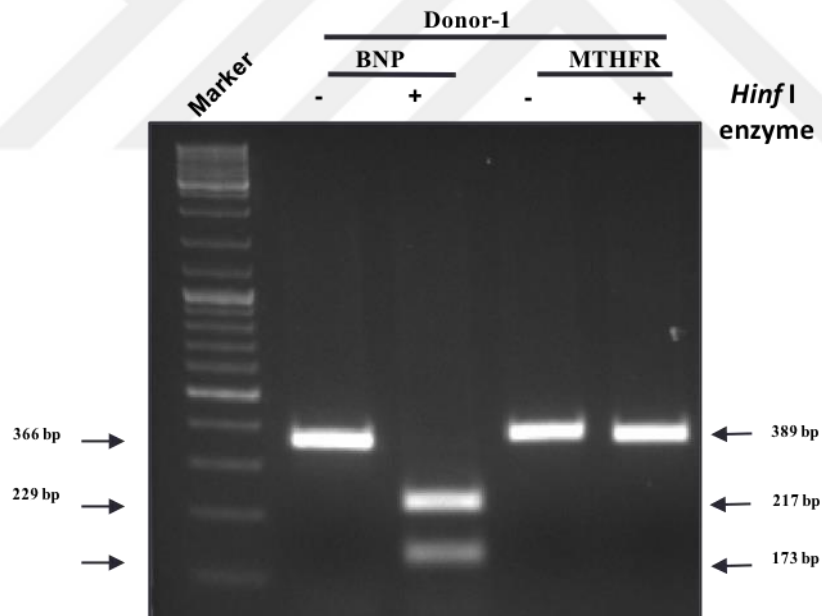
4.2 Evaluating the Effect of C677T Polymorphism on Mesenchymal Stem Cell Properties

4.2.1 Genotyping of the BMMSCs

In order to determine the genotypes of the BMMSCs, restriction fragment length polymorphism (RFLP) assay was applied to the cells. The C677T mutation in *MTHFR* gene, generates a restriction site for *Hinf*I restriction enzyme (5'- GANTC-

3'). That is why the SNP region was first amplified by PCR and then digested with *Hinf* I to identify homozygous (T/T) , heterozygous(C/T) and wild type (C/C) donors. The expected PCR product size for the amplified *MTHFR* gene region is 389 base pairs and *Hinf* I digests this product into two fragments having the size of 173 bp and 217 bp if C677T SNP is present. For this reason, after the enzyme treatment the expected band sizes for wild type is 1 band sized 389bp, for homozygous 2 bands sized 173 bp and 217 bp and for heterozygous 3 bands sized 173 bp, 217 bp and 389bp. Also in this assay, *BNP* gene PCR amplicon (366 base pairs) was used as a control since this region has a *Hinf* I digest site and is suitable to use in RFLP assay to test the efficiency of the enzyme. *BNP* PCR product is 366 bp and when treated with *Hinf* I, two fragments are observed at the size of 137 base pairs and 229 base pairs.

A



B

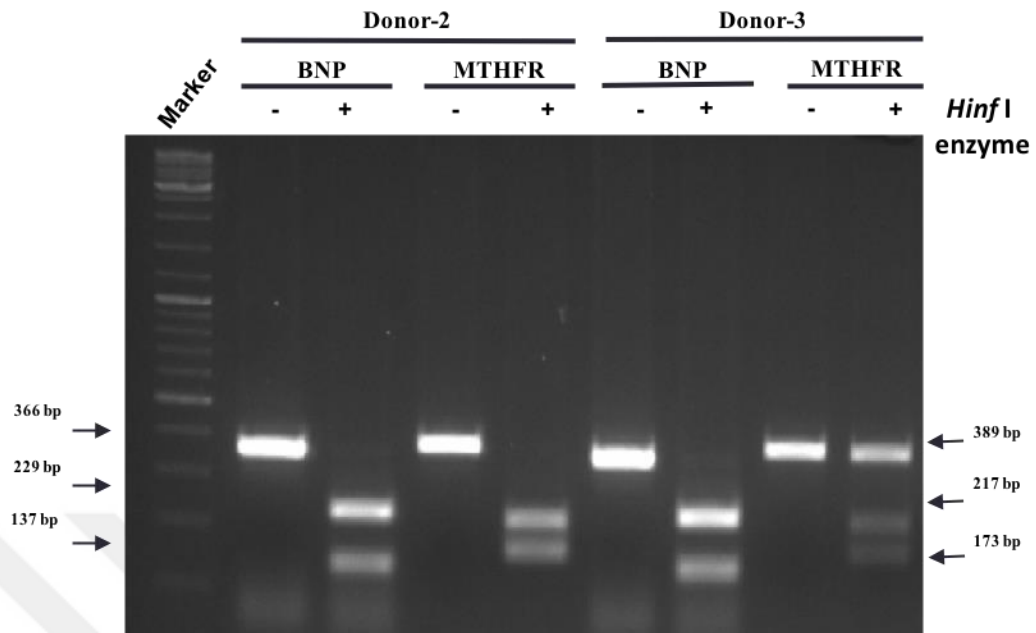


Figure 4.2 RFLP assays of hBM-MSCs **A**) isolated from Donor 1, **B**) isolated from Donor 2 and Donor 3, respectively

As a result of these assays (**Figure 4.2**), the BMMSCs taken from Donor-1 (**Figure 4.2 A**) was identified as wild type (C/C), BMMSCs taken from Donor-2 (**Figure 4.2 B**) was identified as homozygous (T/T) and BMMSCs taken from Donor-3 (**Figure 4.2 B**) was selected as heterozygous (C/T) to be used in the studies conducted to evaluate the effect of C677T polymorphism on MSC properties.

4.2.2 The effect of *MTHFR* C677T polymorphism on BMMSC morphology

After genotyping, the BMMSCs were seeded in to 10 cm tissue culture plates covered with gelatin to investigate their morphological properties *in vitro* and cultured in a humidified incubator as described before. 3 population doublings (PD) were performed with these cells and each passage was performed at the same time for all three donors' BMMSCs. Our results revealed that *MTHFR* C677T polymorphism did not have any observable effects on the morphology of the cells under these conditions (**Figure 4.3**).

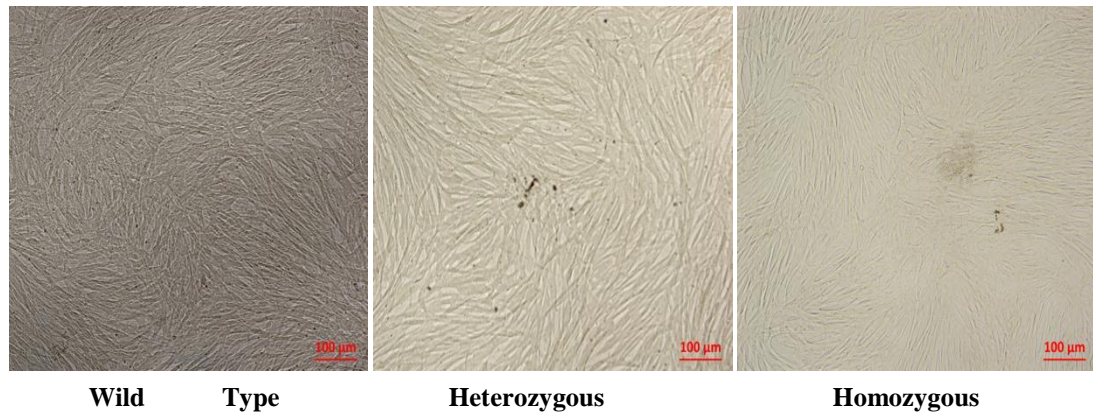


Figure 4.3 Bright field microscopy images of first passage A) wild type, B) heterozygous and C) homozygous BMMSCs

4.2.3 The effect of *MTHFR* C677T polymorphism on differentiation of BMMSCs

Multipotency is a very important feature for MSC regenerative capacities. For this reason, the effect of *MTHFR* C677T polymorphism on BMMSC differentiation potential was investigated by performing adipogenic, osteogenic and chondrogenic differentiation protocols.

4.2.3.1 Adipogenic differentiation

The cells were treated with Stem Pro Adipogenic differentiation medium to induce adipocyte differentiation for 21 days and stained with Oil Red O to visualize the lipid droplets. Lipid droplets were observed (**Figure 4.4 A, B and C**) at all BMMSCs regardless of their genotypes.

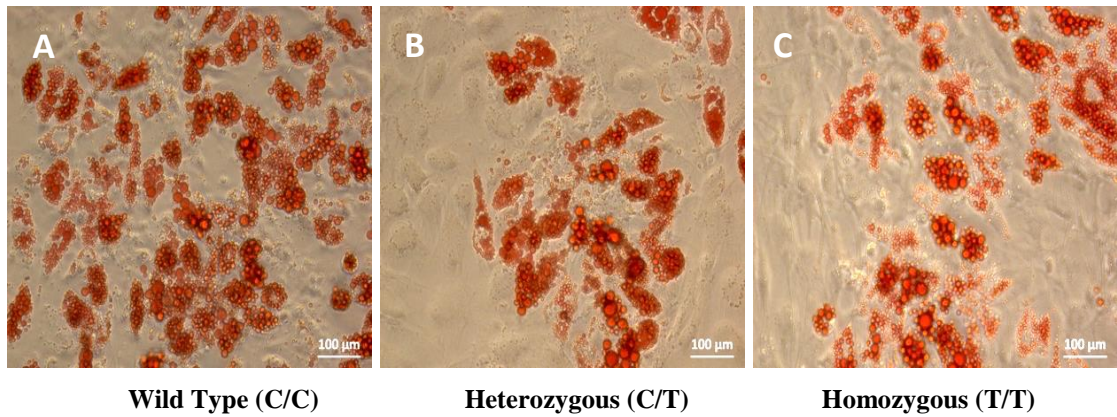


Figure 4.4 Lipid droplets observed after Oil Red O staining of A) wild type, B) heterozygous, C) homozygous differentiated cells, respectively

However, the differentiation potential of each genotype was different. The adipocytic differentiation capacity of the BMMSCs were seem to decrease with the presence of the SNP (Figure 4.5 and 4.6) So that when compared with the wild type heterozygous and homozygous BMMSCs had lower differentiation capacity. These results can be interpreted as, C677T SNP on MTHFR gene may have an effect on adipogenic differentiation capacity of BM-MSCs.

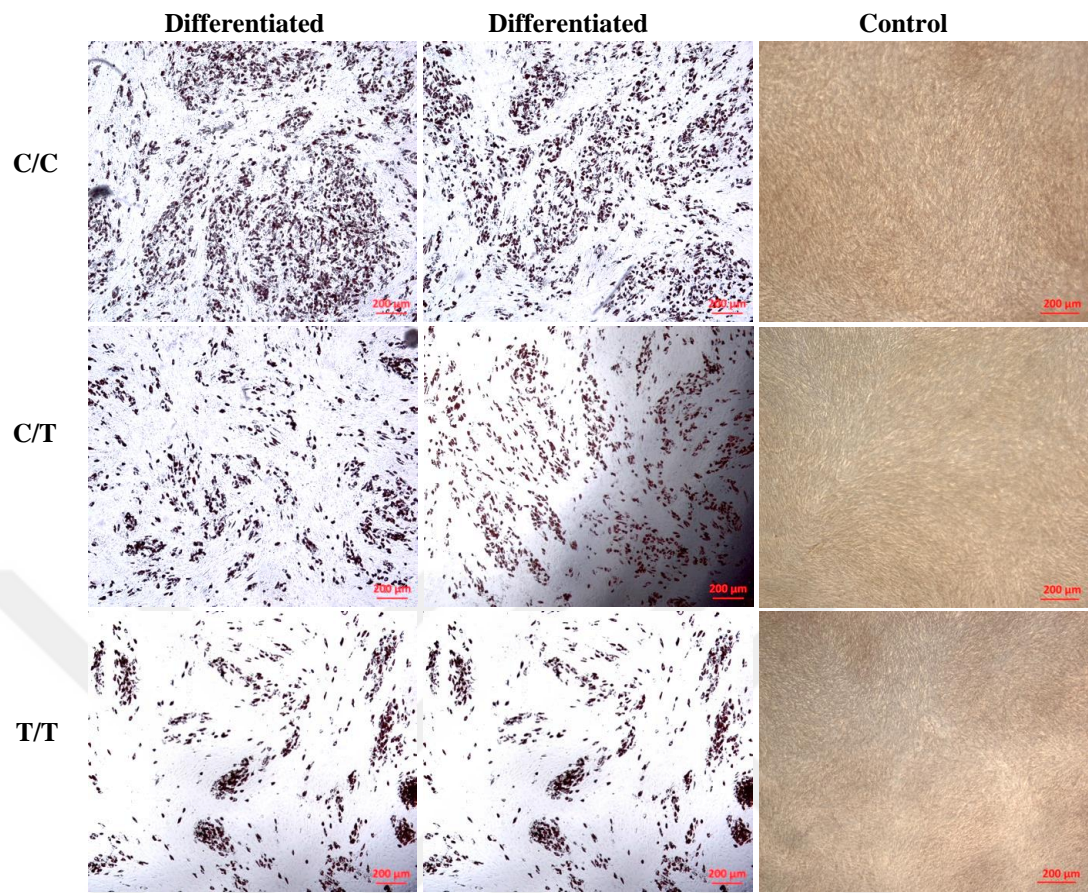


Figure 4.5 Adipogenic differentiation of BMMSCs from all genotypes determined by Oil Red O staining. Undifferentiated BMMSCs were stained and used as a control.

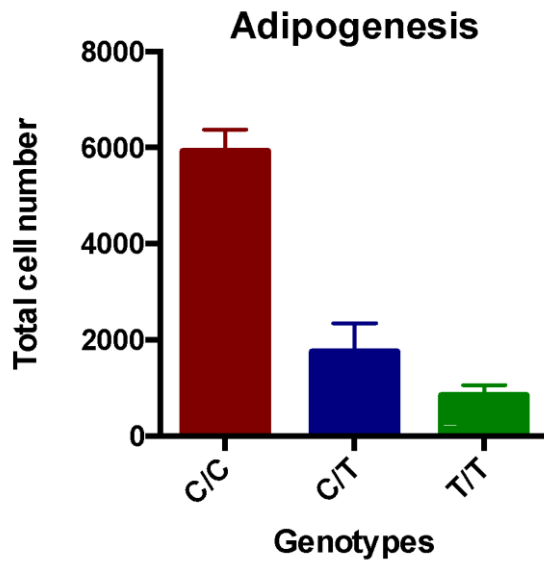


Figure 4.6 Comparison of adipogenic differentiation capabilities between three genotypes. According to ordinary one-way ANOVA test, differences among means statistically significant ($P < 0.05$) ($P < 0.0001$) (****)

4.2.3.2 Osteogenic differentiation

The cells were treated with Stem Pro Osteogenic differentiation medium to induce osteocyte differentiation for 21 days and stained with Alizarin Red to visualize the calcium deposits. Calcium deposits were observed (**Figure 4.7 A, B and C**) in all BMSCs regardless of their genotypes although at different levels.

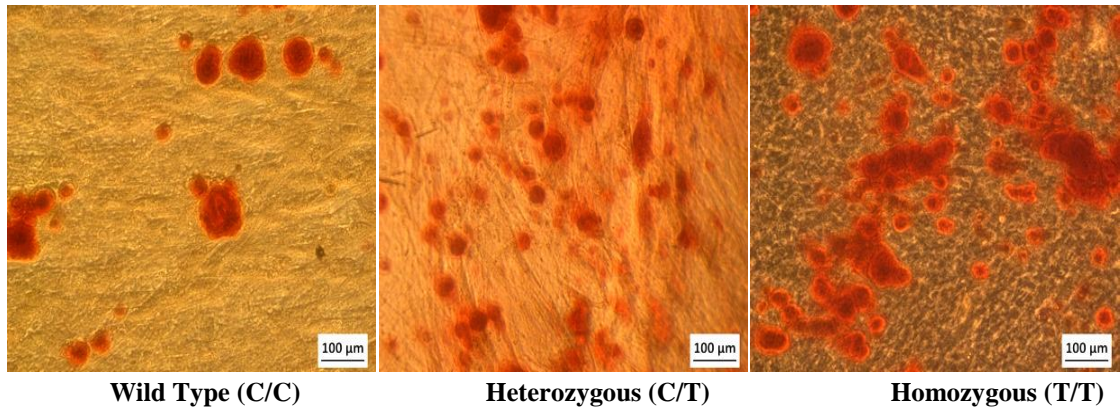


Figure 4.7 Calcium deposits observed after Alizarin red staining of A) wild type, B) heterozygous, C) homozygous differentiated cells, respectively

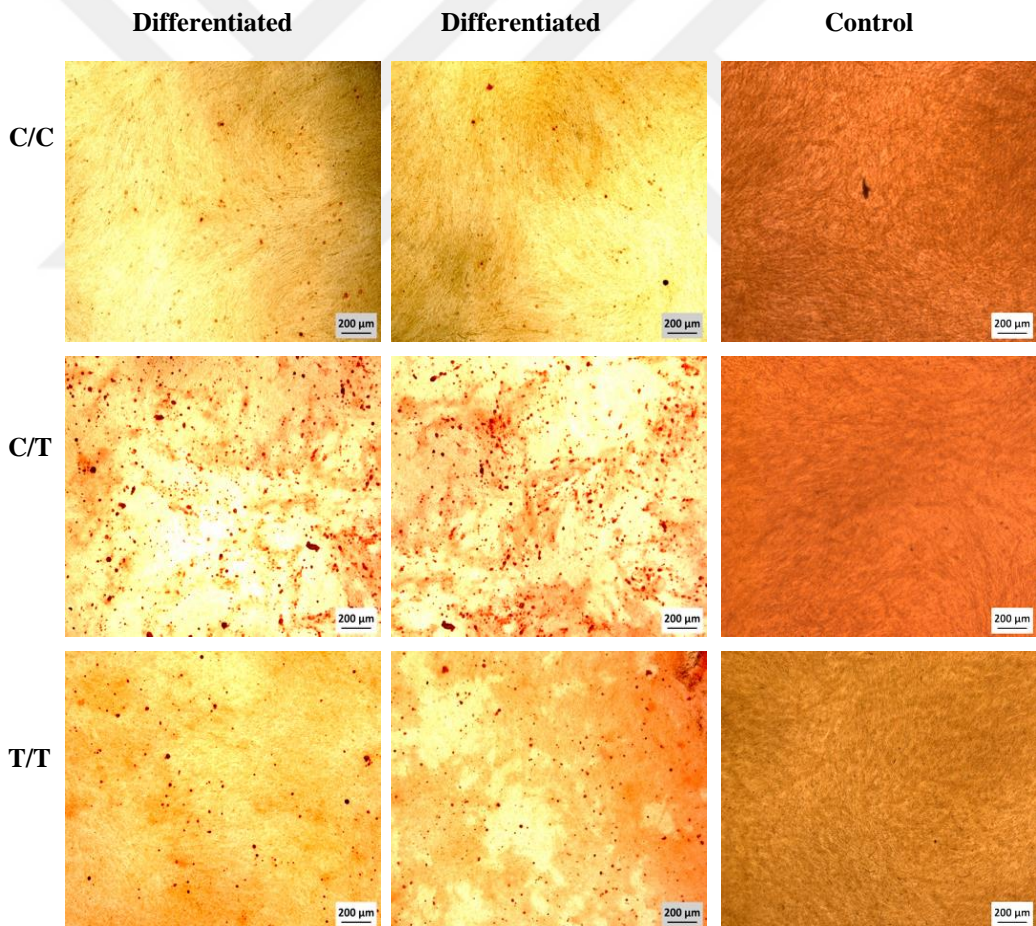


Figure 4.8 Osteogenic differentiation of BMMSCs from all genotypes determined by Alizarin Red staining. Undifferentiated BMMSCs were stained and used as a control.

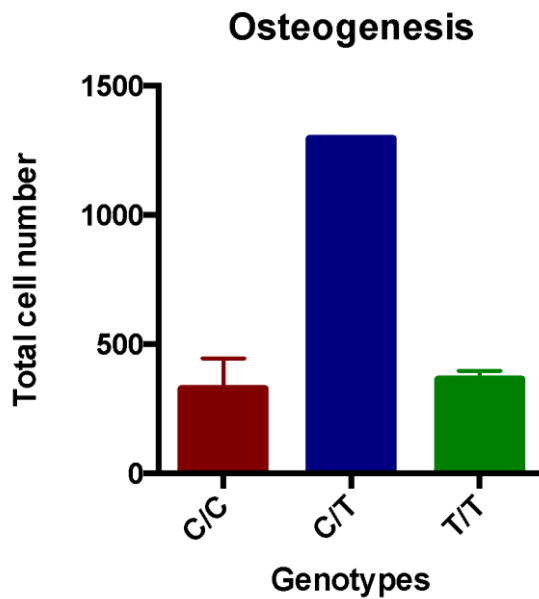


Figure 4.9 Comparison of osteogenic differentiation capabilities between three genotypes. According to ordinary one-way ANOVA test, differences among means statistically significant ($P < 0.05$) ($P = 0.0001$)(***)

The differentiation potential of each genotype was different in terms of their efficiency to form osteocytes, heterozygous BMMSCs have the highest differentiation capacity (**Figure 4.8 and 4.9**) among all genotypes. These results can be interpreted that, C677T SNP on *MTHFR* gene may have an affect on osteogenic differentiation capacity of BMMSCs.

4.2.3.3 Chondrogenic differentiation

For chondrogenesis, cells were cultured as micro masses and differentiation was induced by using chondrogenic differentiation medium(Stem Pro). Firstly, cells were seeded on non-coated tissue culture plates, and, after 24 hours, they formed 3D aggregates floating in medium in homozygous and wild type cells. However the cells needed to attach to the surface for differentiation. For that reason, aggregates were

transferred into plates coated with gelatin and induced to become chondrocytes for 21 days. After 21 days of differentiation, it was seen that, there were no viable cell in heterozygous and control (undifferentiated BMMSCs) plates. Aggregates were observed only with the wild type and the homozygous BMMSC samples. (**Figure 4.10 B**) (**Figure 4.10 A**)

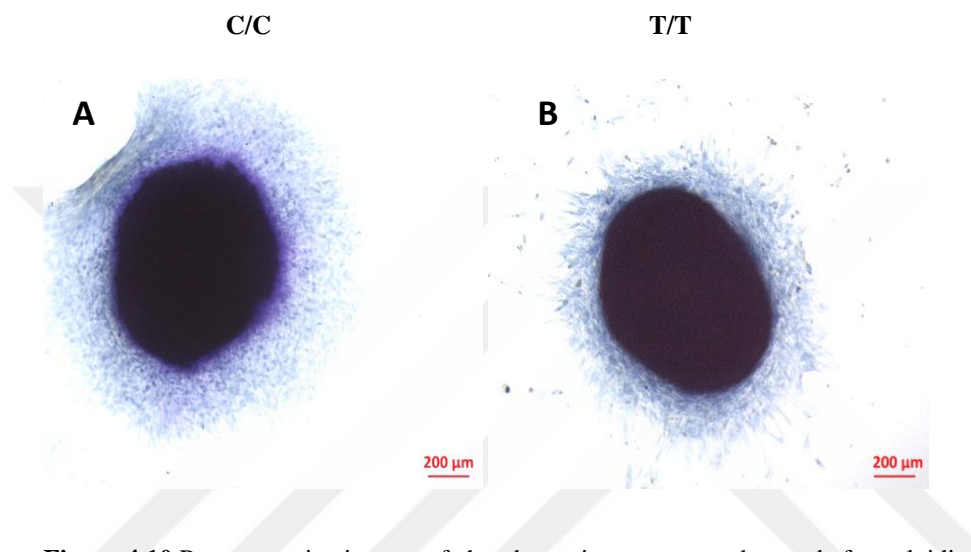


Figure 4.10 Representative images of chondrogenic aggregates observed after toluidine blue staining of A) differentiated wild type cells, B) differentiated homozygous cells, respectively

According to our observations the chondrogenic differentiation potential of BMMSCs does not change with the presence of the homozygous mutation. However as the heterozygous (C/T) cells died and the differentiation potential of each genotype can be different (**Figure 4.10**).

4.3 Introducing the *MTHFR* gene C677T polymorphism to HEK293T cells with CRISPR/Cas9 gene editing system

4.3.1 Transient transfection of HEK293T cells

Since the introduced SNP to *MTHFR* gene will affect the MTHFR enzyme activity, and betaine is a methyl donor for the conversion of homocysteine to methionine in the homocysteine pathway. For this reason, betaine supplement should be added to medium to rescue T/T mutant cells. Because, Firstly, because the growth medium contained betaine, it was highly important to evaluate the effect of betaine on transfection efficiency. In order to evaluate that, HEK293T cells were transfected with pSpCas9(BB)-2A-GFP (PX458) vector, which carries a GFP marker cDNA, by using PEI reagent in a ratio of 1:3 (DNA:PEI ratio in weight) in two conditions: with or without 10mM betaine (final concentration). After the transfection, GFP expression of HEK293T cells were investigated under fluorescent microscope using appropriate filters (**Figure 4.11**).

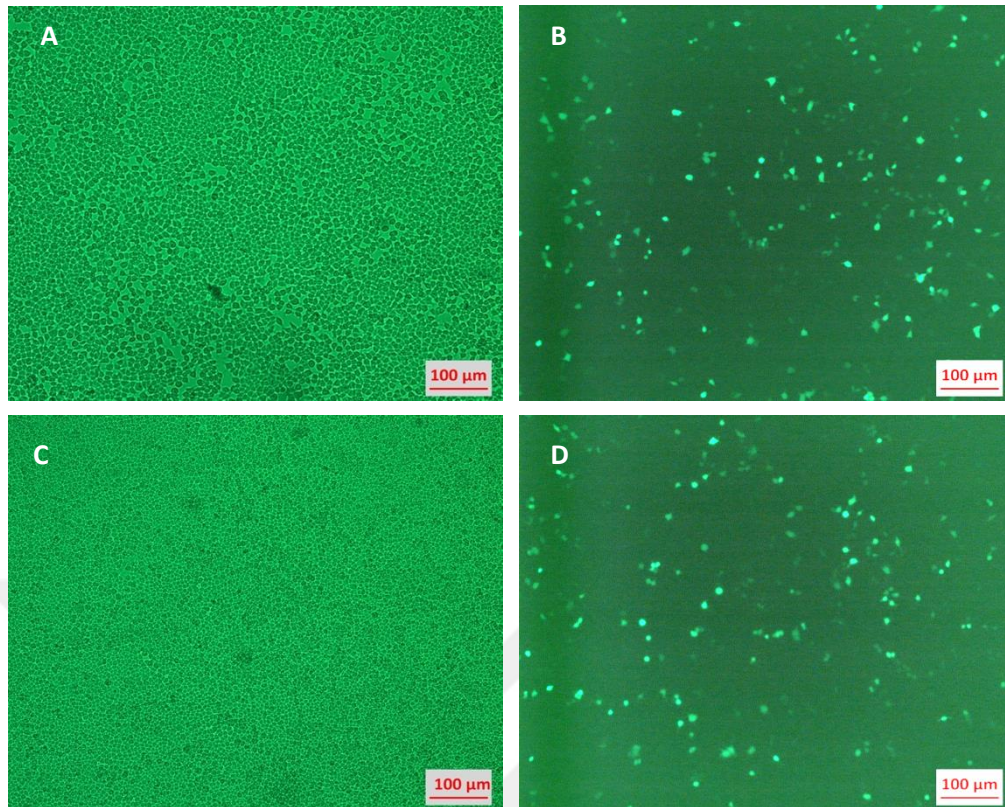


Figure 4.11 Fluorescent microscopy images of HEK293T cells transfected by using PEI 1:3 with PX458 vector A) and B) incubated in DMEM (with 10%FBS) (bright field), C) and D) incubated in DMEM(with 10% FBS) containing 10 mM betain.

Since the transfection of the cells were done simultaneously, GFP⁺ cells also indicates the transfection efficiency and not much difference was observed among samples having different media contents. However, the efficiency of the transfection in two conditions were still not as high as expected

Introducing ssODN mediated *MTHFR* targeted modification requires co-transfection of the designed ssODN together with with pSpCas9(BB)-2A-PURO (PX459) carrying the designed sgRNA sequence into the corresponding cells.. In that purpose, HEK293T cells were transfected with pSpCas9(BB)-2A-GFP (PX458) vector and ssODN by using PEIMAX in a ratio of 1:4 (DNA:PEI ratio in weight) (**Figure 4.11 A and B**). GFP positive cells were observed after 24h with fluorescent microscopy. (**Figure 4.12**)

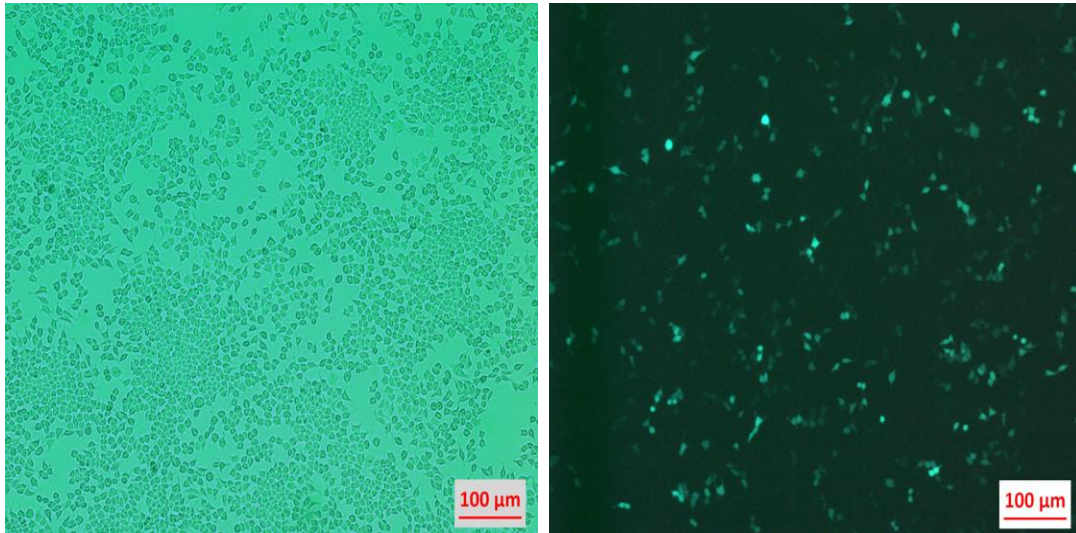


Figure 4.12 Fluorescent microscopy images of A) bright field, B)transfected HEK293T cells transfected with PX458 vector and 1.85 µg of ssODN by using PEIMax in a ratio of 1:4

As higher number of GFP expressing cells were obtained after transfection with pSpCas9(BB)-2A-GFP (PX458) vector by using PEIMAX with a ratio of 1:4 (**Figure 4.12 B**) than PEI with a ratio of 1:3 (**Figure 4.11 B**), using PEIMAX in 1:4 ratio was selected to be continued for transfection of HEK293T cells.

After necessary optimization studies mentioned above, HEK293T cells were seeded into two plates in DMEM (10% FBS) containing 10 mM betain and the cells in one of the plate were transfected with the vector pSpCas9(BB)-2A-PURO (PX459) carrying *MTHFR* sgRNA and 1.85 µg ssODN in 10 cm cell plate. In order to evaluate the transfection efficiency, a separate plate was transfected with pSpCas9(BB)-2A-GFP (PX458) vector. Both transfections were performed at optimized conditions with PEIMax 1:4, simultaneously. GFP positive cells were observed after 24h with fluorescent microscopy (**Figure 4.13 B**).

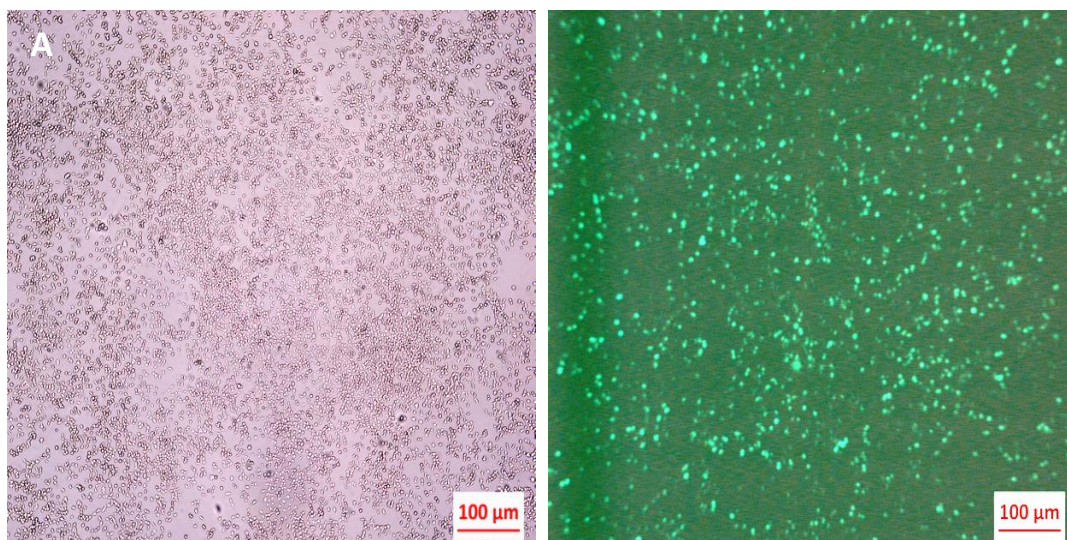


Figure 4.13 Fluorescent microscopy images of A) bright field, B)transfected HEK293T cells transfected with pSpCas9(BB)-2A-GFP (PX458) vector by using PEI_{Max} 1:4.

Florescent microscopy images of GFP positive cells indicate that approximately 80% of the cells were transfected with pSpCas9(BB)-2A-GFP (PX458) vector (**Figure 4.13**). It was assumed that approximately the same percent of the cells were transfected with pSpCas9(BB)-2A-PURO (PX459) -*MTHFR* sgRNA vector. In order to select transfected cells puromycin selection was applied to both plates until all the cells transfected with pSpCas9(BB)-2A-GFP (PX458) vector were death. pSpCas9(BB)-2A-PURO (PX459) vector contains puromycin resistance gene while pSpCas9(BB)-2A-GFP (PX458) vector does not. That is was gfp expressing cells are expected to die under puromycin selection. This serves as a control for the success of the selection. After the puromycin selection, remaining cells were accepted as cells carrying the pSpCas9(BB)-2A-PURO (PX459).

4.3.2 Genotyping of the mutant HEK 293T colonies with RFLP

When the CRISPR/Cas9 plasmids are transfected into the cells, a heterogeneous population is created, in which there might be cells that do the desired genomic

modification or cells that do unexpected genomic modifications or cells that do not do any genomic modifications. Therefore, in the aforementioned transection, HEK293T cells had to be seeded as single cells to select the cell clones that had the desired genomic modification. Single cells were grown as colonies approximately for 3 weeks in the wells of 96-well plate. During this period, betain supplement was always available for the cells. 20 colonies were survived. Genotyping of these colonies were performed by RFLP assay to separate them as wild type (C/C), homozygous (T/T) and heterozygous (C/T) colonies. The gene editing system transfected to the HEK293T cells was designed to create a DNA break at the specific point of the *MTHFR* gene region and it was expected that this DNA break will be repaired using by ssODN as the template DNA, cotransfected to the cells. If this break will repaired in both alleles, homozygous alleles (T/T) will be obtained, however if one of the alleles is repaired by HDR, heterozygous cells (C/T) will be obtained and unaffected colonies will appear as wild type. In addition to that, some colonies might present a genotype having random mutations (insertions/deletions - indels) due to NHEJ. The C677T mutation on *MTHFR* gene generates a restriction site for *Hinf* I. That is why the genomic locus surrounding the targeted SNP region was first amplified by PCR and then the PCR product was digested with *Hinf* I. The expected PCR product size for the amplified *MTHFR* gene region is 389 base pairs and *Hinf* I digests this product into two fragments having the size of 173 bp and 217 bp if C677T SNP is present. For this reason, after the enzyme treatment the expected band sizes for homozygous 2 bands sized 173 bp and 217 bp and for heterozygous 3 bands sized 173 bp, 217 bp and 389bp. Also in this assay, *BNP* gene PCR amplicon (366 base pairs) was used as a control since this region has a *Hinf* I digest site and is suitable to use in RFLP assay to test the cutting efficiency of the enzyme. *BNP* PCR product is 366 bp and when digested with *Hinf* I, two fragments are observed at the size of 137 base pairs and 229 base pairs. (Figure 4.14)

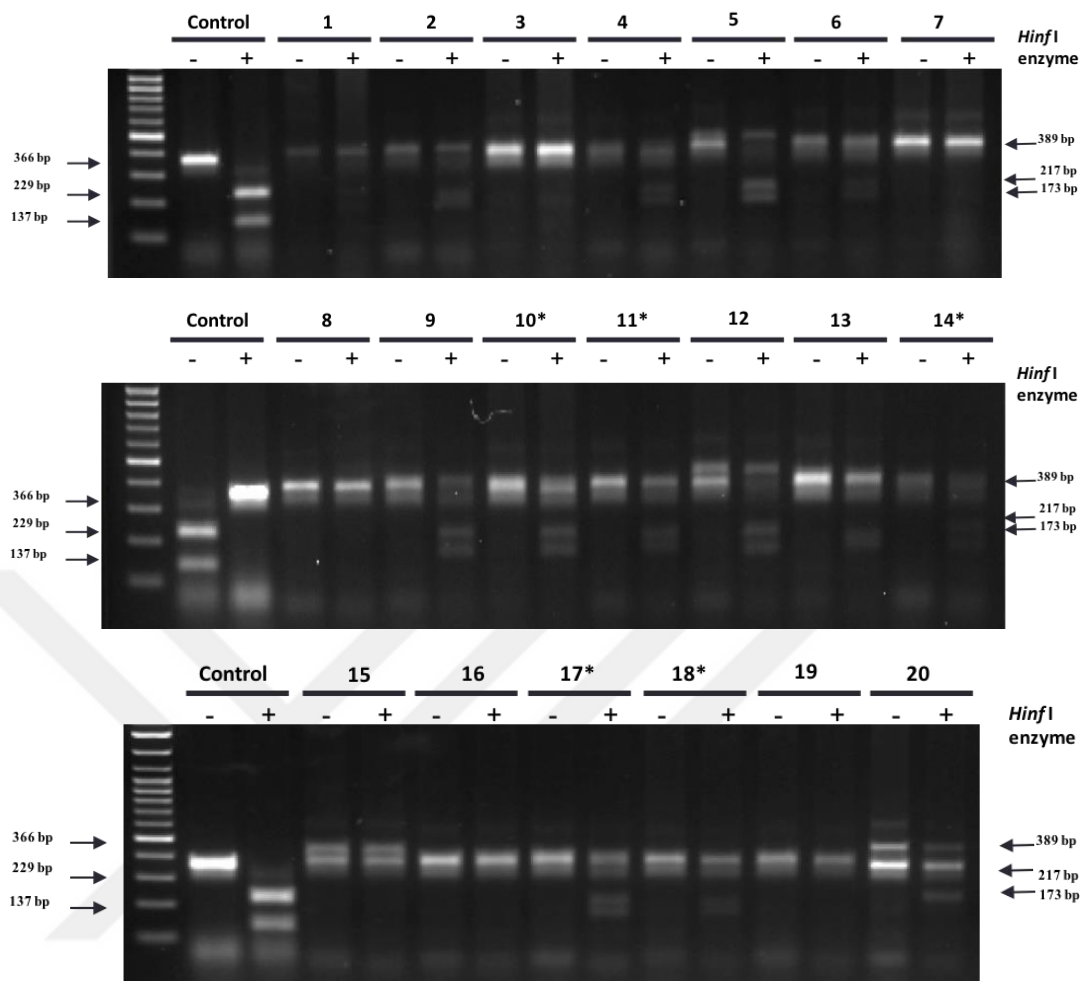


Figure 4.14 Genotyping results of mutant HEK293T colonies by RFLP assay. Possible heterozygous colonies (C/T) were indicated by the star(*). Control indicates *BNP* gene PCR amplicon.

The genotyping results of transfected colonies indicated that, in the group of 20 colonies, only five of them (colony number 10, 11, 14, 17 and 18) were chosen as possible heterozygous colonies (C/T) according to their RFLP assay results as one of their alleles was repaired by HDR and the other allele stayed as the same (**Figure 4.14**). Regarding the band numbers and sizes, some of the colonies (Colony number 5, 9 and 20), represented both HDR and NHEJ upon CRISPR/Cas9 engineering.

The transfection of HEK293T cells yielded with only heterozygous mutants rather than homozygous mutants. Furthermore, after the transfection, only 20 colonies were survived, grown and screened. This indicates that the survival capacity of the colonies was highly decreased after the transfection. Moreover, the growing rates of the colonies were highly slow compared to wild type HEK293T cells.

4.3.3 Genotyping of the mutant HEK 293T colonies with T7 endonuclease1 assay

After the genotyping, successfully transfected colonies were chosen and possibly heterozygous colonies were seeded and grown for further investigations. However before going further, *MTHFR* region was amplified by PCR and T7E1 assay was applied to two possibly heterozygous mutants (colony number 10 and 17) and also the pool of the cells obtained after transfection. This assay was applied in order to be sure that the chosen colonies were heterozygous and also, SpCas9 of the PX459 vector used in the transfection works fully (**Figure 4.15**).

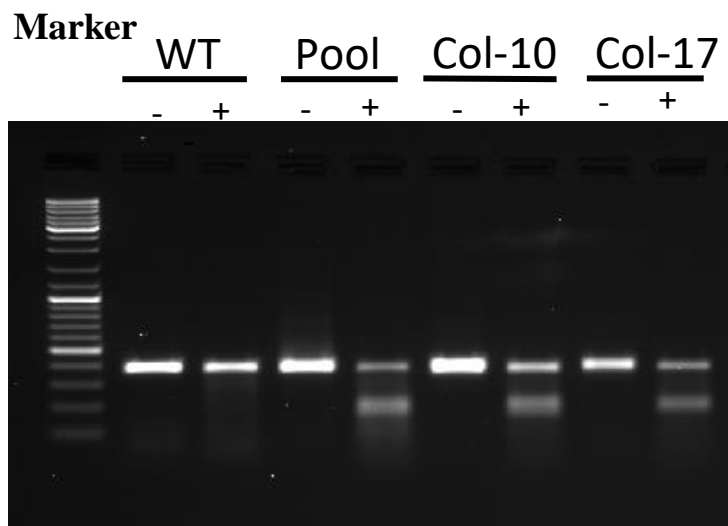


Figure 4.15 T7E1 assay of pool of transfected cell and two heterozygous (C/T) colonies (Colony 10 and 17). Untransfected Hek293T cells were used as a control (WT).

In T7E1 assay, T7 endonuclease recognizes and cleaves non perfectly annealed DNA complementary strands. When the *MTHFR* PCR product was incubated with T7 endonuclease, it cleaved from the positions mismatches/indels from NHEJ repair. It was seen that, there was mismatches for pool and heterozygous colonies compared to wild type (**Figure 4.15**). Thus, the cleavage was effective proved that, chosen colonies were heterozygous and also, SpCas9 of the PX459 vector used in the transfection works fully.

4.4 Introducing the *MTHFR* C677T polymorphism to BMMSCs by using CRISPR/Cas9 gene editing system

4.4.1 Optimization of transfection of BMMSCs

It was seen that C677T mutation in *MTHFR* can change the differentiation capacities and multipotency of BMMSCs isolated from different donors (**Figure 4.5, 4.8, 4.10**). On the other hand the cells bear different genetic backgrounds and it can be an important factor affecting the differentiation potentials of the cells. In order to eliminate the effect of genetic background and better understand the effect of the SNP on the differentiation potentials of BMMSCs, the designed CRISPR/Cas9 gene editing system, which was shown to work on HEK293T cells, was also used for BMMSCs (**Figure 4.13**). Moreover, although previous experiments showed that, PEI_{Max} in a ratio of 1:4 is the best transfection agent for HEK293T cells (**Figure 4.13**), MSCs and HEK293T cells have different cell properties. That is why different transfection methods were investigated on BMMSCs

Firstly, electroporation with different conditions was used to transfect the vector and ssODN to the BMMSCs however, cells were death right after transfection. So, it was decided that electroporation was not a suitable way to transfect primary BMMSCs

isolated from adults. Moreover, BMMSCs were transfected with pSpCas9(BB)-2A-GFP (PX458) vector by using Lipofectamine with different DNA:Lipofectamine ratios (in weight) in order to find the optimum transfection efficiency with the lowest number of dead cells possible. 24 h and 48 h after the transfection, GFP expression of BMMSCs were investigated under fluorescent microscope to assess the transfection efficiency (**Figure 4.16**).

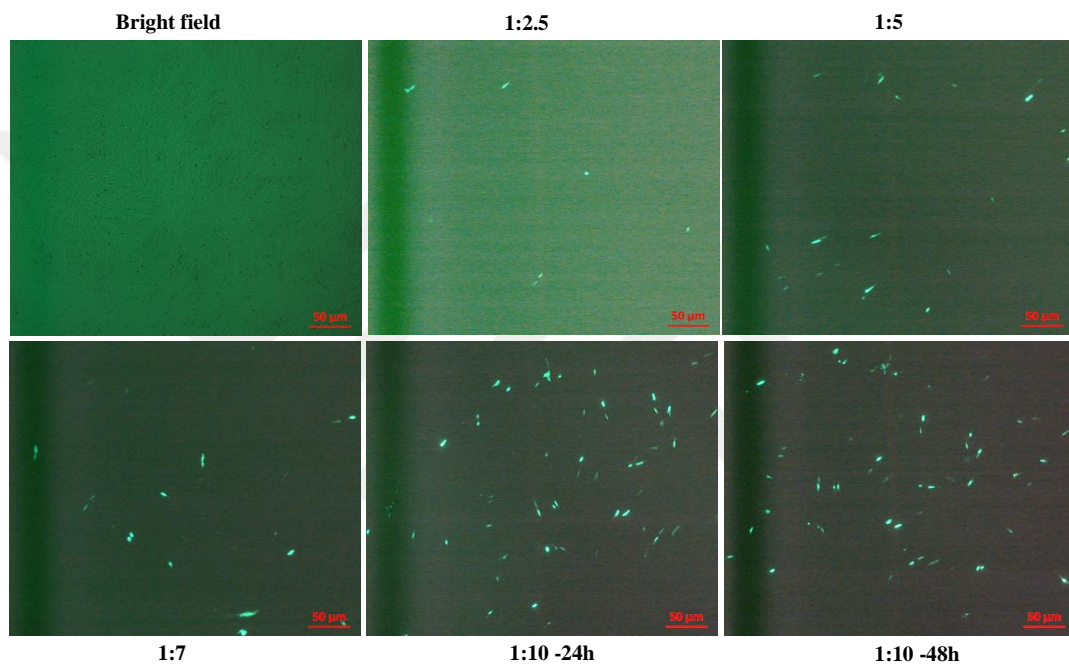


Figure 4.16 Fluorescent microscopy images of BMMSCs transfected with PX458 vector by using Lipofectamine with different lipofectamine:DNA amount ratio; A) bright field image of the cells, B) the GFP expression of the GFP⁺ cells 24 hours after transfected with Lipofectamine by using ratio of 1:2.5 C) the GFP expression of the GFP⁺ cells 24 hours after transfected with Lipofectamine, 1:5, D) the GFP expression of the GFP⁺ cells 24 hours after transfected with Lipofectamine, 1:7, E) the GFP expression of the GFP⁺ cells 24 hours after transfected with Lipofectamine, 1:10, F) the GFP expression of the GFP⁺ cells 48 hours after transfected with Lipofectamine by using ratio of 1:10 as DNA:Lipofectamine.

Highest number of GFP expressing cells were observed 48 hours after transfection with Lipofectamine at a ratio of 1:10 (**Figure 4.16 F**) when compared with the other ratios (1:2.5, 1:5, 1:7). However, Lipofectamine was toxic to BMMSCs and most of the cells died after the transfection.

BMMSCs were then transfected with pSpCas9(BB)-2A-GFP (PX458) vector by different PEI_{Max} ratios (**Figure 4.17 A and B**) Moreover Chloroquine addition to transfection medium was also investigated (**Figure 4.17 C and D**), since it was shown to increase the transfection efficiency up to 20 folds for Chinese hamster ovary (CHO) cells [100].

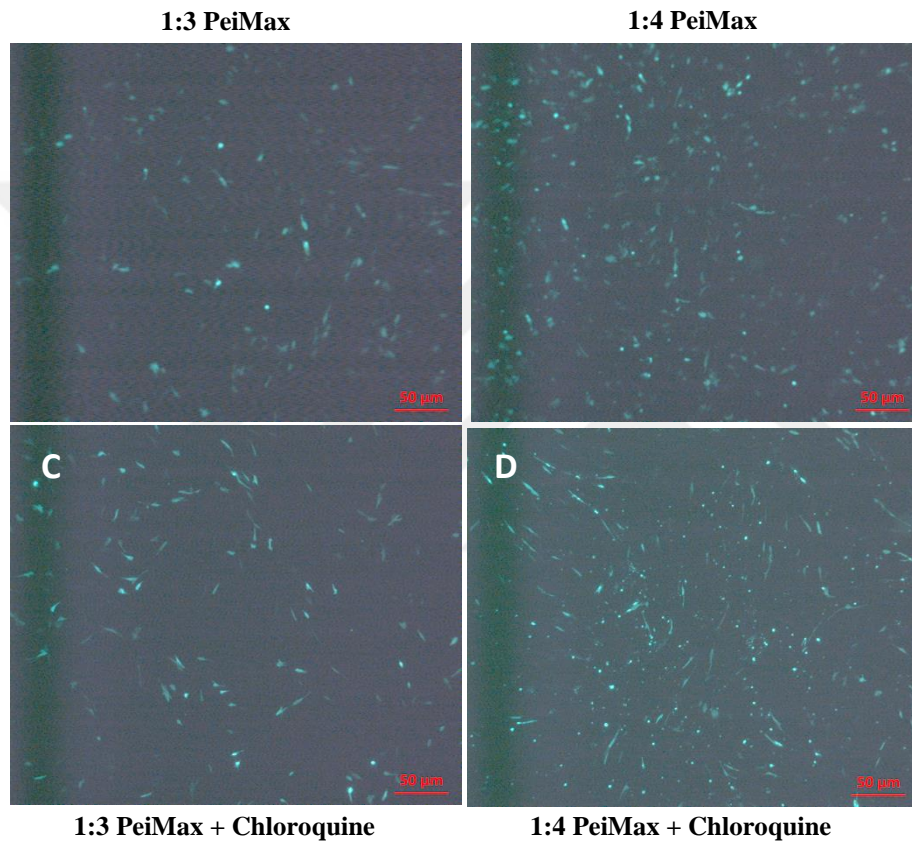


Figure 4.17 Fluorescent microscopy images of BMMSCs transfected with PX458 vector by using; A) PEI_{Max} with the ratio of 1:3, B) PEI_{Max} with the ratio of 1:4, C) PEI_{Max} with the ratio of 1:3 in a medium containing chloroquine D) PEI_{Max} with the ratio of 1:4 in a medium containing chloroquine

Higher number of GFP positive cells were obtained after transfection with pSpCas9(BB)-2A-GFP (PX458) vector by using PEI_{Max} in a ratio of 1:4 (in weight) (**Figure 4.17 B**) with lowest number dead cells. In addition, contrary to the information in the literature [100], using chloroquine in the transfection medium did not increase transfection efficiency on BMMSCs (**Figure 4.17 D**) according to our

observations. It may be because of the unique characteristics of BMMSCs or the concentration of chloroquine was not optimal.

The pSpCas9(BB)-2A-PURO (PX459) vector contains puromycin resistance gene. For this, optimum concentration and application time range of puromycin for the selection of the transfected colonies are highly important. Excess amount of puromycin in the medium can be toxic by causing stress and leading apoptosis. On the other hand, less amount of puromycin will not be enough to identify and select the mutant colonies after transient transfection. Because of these reasons, BMMSCs were treated with different puromycin concentrations for a period of time until nearly all cells died. Medium was changed with fresh medium containing puromycin and cells were observed under light microscope (**Figure 4.18**) and a death curve for puromycin was plotted (**Figure 4.19**).

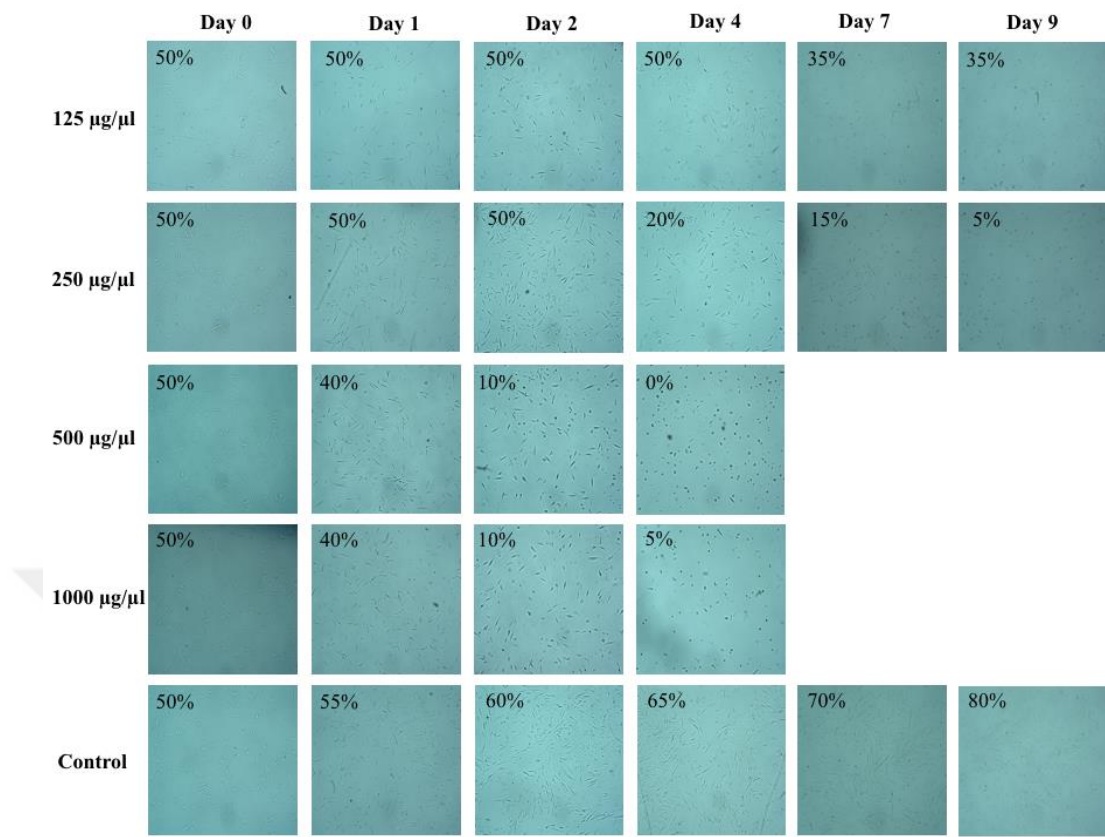


Figure 4.18 Bright field images of BMMSCs treated with different puromycin concentrations. Concentration of the puromycin used in the selection medium, the time range of the application and confluences of the cells were indicated.

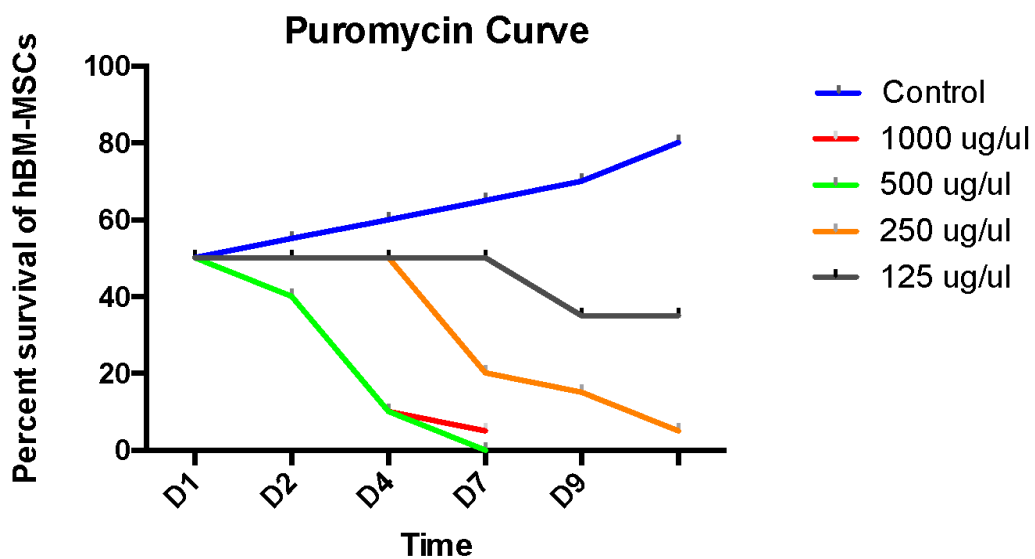


Figure 4.19 Puromycin resistance death curve of BMMSCs

It was seen from the puromycin death curve (**Figure 4.19**) that using 500 $\mu\text{g}/\mu\text{l}$ puromycin for the selection of mutant colonies for 2 days was enough for BMMSCs when it compared to 100 $\mu\text{g}/\mu\text{l}$, excess amount of that concentration can be toxic for these cells.

4.4.2 Transient transfection of BMMSCs with the CRISPR/Cas9 system

After all the necessary optimization studies were performed, BMMSCs were seeded into two plates and the cells in one of the plates were transfected with pSpCas9(BB)-2A-PURO (PX459) -MTHFRsgRNA vector and ssODN. The cells in second plate were transfected with pSpCas9(BB)-2A-GFP (PX458) vector. Both transfections were performed with PEIMax 1:4, simultaneously and GFP positive cells were observed after 24h with fluorescent microscopy (**Figure 4.20 B**).

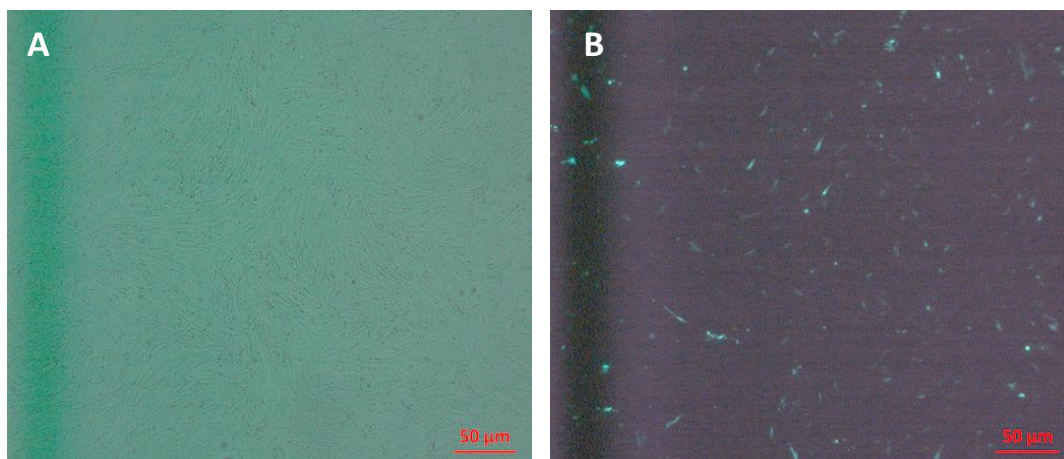


Figure 4.20 Fluorescent microscopy images of A) bright field, B)transfected BMMSCs transfected with PX458 vector by using PEIMax 1:4

Florescent microscopy images of the GFP positive cells indicated that approximately 50% of the cells were transfected with pSpCas9(BB)-2A-GFP (PX458) vector (**Figure 4.20 B**). That can be interpreted that, approximately same percent of the cells were transfected with pSpCas9(BB)-2A-PURO (PX459) carrying the sgRNA for MTHFR SNP region. Afterwards, transfected cells were selected with 500 µg/µl puromycin for 4 days. After the puromycin selection, the confluency of the pSpCas9(BB)-2A-PURO (PX459) MTHFR sgRNA transfected plate was approximately 40%. The selected cells were trypsinized and some of the cells were separated for T7 endonuclease assay (T7E1) and the rest of the cells were seeded to 96 well plates for single colonies.

The result of the BMMSC T7 endonuclease assay is presented at (**Figure 4.21 A, B**). Previously created CRISPR/Cas9 MTHFR sgRNA transfected HEK293T pool gDNA was used as a positive control of T7E1. Another control of the assay was PCR derived from C/T BMMSCs gDNA, however, T7E1 did not work as efficiently for this sample. For this reason, we compared our T7E1 results of all BMMSC samples among each other but not with HEK293T. When wild type BMMSC T7E1 digested bands were observed, a very clean neat undigested MTHFR band at the expected size was seen. However, when CRISPR/Cas9 transfected BMMSC T7E1 band is compared with untransfected wild type band, there a smear was observed underneath

the main band. Furthermore, this smear is also present at the T7E1 digested bands of C/T and T/T samples. Observing such a smear was not expected at T/T samples however our interpretation is the presence of other SNPs at the same region of the amplified PCR product.

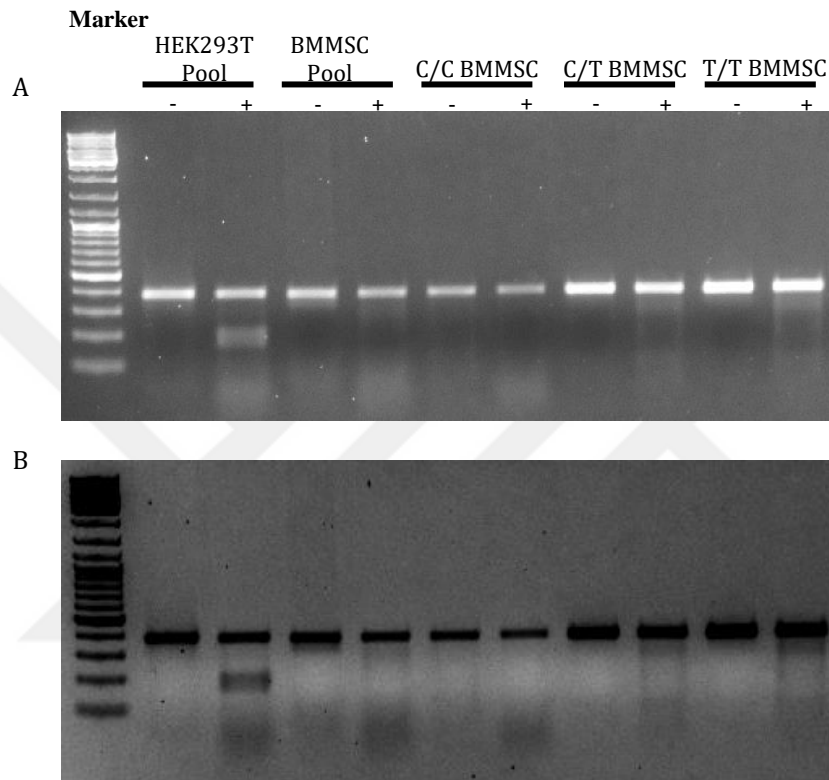


Figure 4.21 T7E1 assay of BMMSCs A) T7E1 assay of pool of transfected HEK293T cells, pool of transfected BMMSCs, wild type, heterozygous and homozygous BMMSCs, respectively. B) contrast enhanced image of (A)

In order to obtain single cell clones, remaining cells were seeded into 96 well plates and monitored for 2-3 weeks. However, none of them started proliferating, because they did not survived. Because these cells require survival signals coming from other cells, transfection was repeated, and this time cells were cultured with medium containing 10 μ M Y-27632 which is required for survival. However none of the cells were able to survive out of the single cell cloning.

5 DISCUSSION AND CONCLUSION

When the function of the MTHFR enzyme and its related diseases are considered, it is concluded that, MTHFR is highly important for normal cellular functions for the tissue homeostasis. Accordingly, as adult stem cells have important roles in providing tissue homeostasis, we thought that *MTHFR C677T* polymorphism might be also interfering with the differentiation capacities of BMMSCs. To this end, there is no study investigating the effect of this polymorphism on the differentiation capacities of BMMSCs. For this reason, in this study the effect of *MTHFR C677T* on BMMSCs was investigated.

There are important parameters of MSCs in order to maintain tissue homeostasis. The ability to form colonies *in vitro* that supports hematopoiesis is one of the main features that define MSCs. According to Kuznetsov et al. colony forming efficiency (CFE) values may provide useful insights into bone and bone marrow pathophysiology and CFE was significantly altered in patients with several skeletal and metabolic disorders. Since *MTHFR C677T* has been associated with several skeletal and metabolic dysfunctions, we investigated the morphologic properties of the three genotypes. Our results revealed that *MTHFR C677T* polymorphism did not have any observable effects on the colony forming abilities of the cells and we were able to observe colonies under light microscope. Also, their growth rates were highly similar and all the cells were passaged and treated for all experiments at the same time. That's why it was concluded that, *C677T* SNP on *MTHFR* do not affect growth and phenotypic characters of BMMSCs. However for further experiments and quantitative assays could be performed to better identify these properties.

Moreover, multipotency is a very important feature for MSC regenerative capacities. For this reason, the effect of *MTHFR C677T* polymorphism on BMMSC differentiation potential was also investigated by performing adipogenic, osteogenic

and chondrogenic differentiation protocols. Firstly, all BMMSCs regardless of their genotypes were successfully differentiated into adipocytes, osteocytes and chondrocytes. However, the differentiation potential of each genotype was different.

Adipose tissue is an active endocrine organ, which plays a central role in lipid and glucose metabolisms. Dysfunctions in adipogenesis lead to dysfunctioning adipose tissue which produces a large number of hormones and cytokines that both play important roles in the development of metabolic syndrome, diabetes mellitus, and vascular diseases. According to our results, the adipocytic differentiation capacity of the BMMSCs were seem to decrease with the presence of the SNP, which directs us to think that, C677T *MTHFR* may have an effect on adipogenesis. Furthermore this defect can be linked with the increasing risk of diabetes mellitus and frequently seen cancers in patients having this SNP. According to Yang et al. there is an increased risk seen in the Caucasian populations with type 2 Diabetes having *MTHFR* C677T, also in another study it was demonstrated that C677T significantly associated with diabetes in Arabic population according to Al-Rubeaan et al. and might be a risk genetic factor of Type 2 diabetes mellitus in the Chinese Han population. The association of this polymorphism and diabetes mellitus and its complications were also reported in two studies conducted by Settin et al. and Zhong et al. In addition, adipokines are cytokines (cell signaling proteins) secreted by adipose tissue and dysregulated production or secretion of these adipokines leading to adipose tissue dysfunctions can lead to the pathogenesis of obesity linked complications. Thereby, adipokines produced by the placenta regulate the maternal metabolic adaptation to pregnancy and dysfunction in the production of adipokines. These dysfunctions in the production of adipokines can be the main reason behind the meta-analysis indicating that C677T *MTHFR* is associated with recurrent pregnancy loss (Yang et al.). Furthermore, *MTHFR* C677T is also significantly associated with many psychiatric disorders like Schizophrenia, Bipolar Disorder and Unipolar Depressive Disorder (Gilbody et al. and Peerbooms et al.) There is another study revealing that, *MTHFR* C677T had a significant association with the risk of Parkinson's disease according to Wu et al. And it was also revealed that disturbances in adipokine

secretion are important in the pathogenesis, clinical presentation and outcome of mental disorders. It can be hypothesized that, dysfunctions in adipogenesis causing form C677T can cause these complications, however, further investigations should be done in order to understand the mechanism and prove that hypothesis. Moreover although we have performed three technical replicates for each biological sample our results must be repeated with a higher number of donor cells.

Additionally, the differentiation potential of each genotype was different in terms of their efficiency to form osteocytes and chondrocytes. There are many studies related to bone fracture risks and dysregulated bone mineral density with *MTHFR* C677T. The main reason of this correlation can be related with the altering osteogenesis and chondrogenesis related with the existence of the SNP. Also, altering osteogenic and chondrogenic differentiation capacity of BMMSCs can be the reason behind the improved central nervous system damage of the patients having Behcet's disease transplanted with allogeneic mesenchymal stem cells instead of autologous mesenchymal stem cells [96,98].

Our results demonstrated that, C677T SNP on *MTHFR* affects differentiation capacity of BMMSCs. On the other hand, these cells were isolated from different donors so the cells bear different genetic backgrounds. Also, diseases related with *MTHFR* C677T are complex diseases meaning that, the occurring of the diseases are not only caused by the mutation on a single gene, it can be due to multigene interactions or environmental factors as well. Our results have enough technical replicas, however they are not supported by the presence of biological replicas. For that reason, in order to correlate the C677T mutation and the altered differentiation ability of BMMSCs with a greater confidence, our study should be repeated multiple times with cells isolated from different donors. Increasing the sample size may help normalizing and generalizing our findings but still it will not be enough to eliminate the background differences to the fullest extent. For that reason, in order to eliminate the effect of genetic background and better understand the effect of the SNP on the

differentiation potentials of BMMSCs, CRISPR/Cas9 genome editing system was designed *in silico* in order to introduce C677T SNP on BMMSCs.

We chose CRISPR/Cas9 system since it is less time consuming and its design is simpler than the other genome editing systems. However, there are some challenges to be solved before using this system on humans. The most important one is the off-target effect, which is the binding and cleavage of untargeted sites by Cas9 that can lead to lethal problems. In order to reduce the possibility of off-target cleavage and recombination, we choose gRNAs having slightly less off target effects compared to others while performing the *in silico* design of our genome editing system. Successful introduction of *MTHFR* C677T into BMMSCs using CRISPR/Cas9 technology will also pave the way for the correction of a similar polymorphism by the same method and the use of gene-corrected autologous MSCs for damage repair. The fact that this polymorphism can be introduced to MSCs by using CRISPR/Cas9 technology is important in order to investigate the various disease models by filling the necessary information gap in order to study other polymorphisms which have not been studied in the literature. Many of the studies related with MSCs do not include gene editing. The few studies that used CRISPR/Cas9 system on MSCs employed viruses to transfect the cells. However, this kind of transfection system can not be used in this study since the result can be used as a guideline in personalized medicine in the future and viral transfection systems are not suitable to be used in humans. Also, technically, it is impossible to deliver the donor DNA template through viral infections in the case of a desired HDR modification such as in this study. Because of all these factors, this study serves as a guide for employing CRISPR/Cas9 genome editing of BMMSCs by transient transfection methods. One of the main challenges in this study was the limited availability of BMMSCs isolated from donors. Therefore, we first used HEK293T cells to prove that our design works. After that we continued with BMMSC transfection experiments.

We investigated the efficiency of different transfection reagents. From the pool of cells we indirectly demonstrated that, BMMSCs could be transfected with a chemical agent, PEI_{max} instead of viral transfection systems. According to our T7E1 results we expected to see a band at low intensity at the C/T BMMSC lane corresponding to the *MTHFR* PCR digest sizes however instead of that we observed a smear underneath the main band. These results were not comparable with our HEK293T CRISPR/Cas9 *MTHFR*sgrNA treated pool. The reason for this discrepancy is most probably because of the very low transfection efficiency and large cell size of BMMSCs. In a confluent 10cm tissue culture plate we could obtain $5 \cdot 10^6$ BMMSCs. The transfection efficiency was 40% in our experiments that means approximately $2 \cdot 10^6$ BMMSCs were transfected. The modification efficacy is approximately 1/100 with ssODNs, which gives us a yield of 20000 cells that could possibly carry the correct mutation. The other reason is the presence of high number of indel bearing HEK293T cells within the pool after CRISPR/Cas9 modification due to high transfection efficiency with a higher population size that is approximately $8 \cdot 10^6$ cells. CRISPR/Cas9 *MTHFR*sgrNA treated pool of BMMSCs gave similar results with C/T and T/T primary BMMSCs. Furthermore the C/C wild type was clearly negative according to our results. The presence of the smear at T/T could be explained by the presence of other mutations at the PCR amplicon as exon 5 of *MTHFR* gene bears many other mutations reported in the literature that could be followed via ENSEMBLE genome browser. Due to the very clear difference between the wild type BMMSCs and the CRISPR/Cas9 *MTHFR*sgrNA treated wild type BMMSCs we expected that our modification system successfully but not efficiently worked in BMMSCs.

However still, the major challenge after the transfection was that, BMMSCs should be seeded as single cells in order to obtain the clones harboring the specific C677T mutation. When cells were seeded as single cells and grown at very low numbers, unfortunately none of the cells were survived. The possible reason for that could be anoikis which is a type of programmed cell death induced when anchorage-dependent cells like BMMSCs detach from their surrounding ECM. According to Fujii et al. BMMSCs need essential growth factors and survival signals provided by

neighboring cells and the ECM. Several methods have been tested, including seeding them as 10-cell-subpopulations or culturing them in the presence of Y-27632, a ROCK inhibitor. The role of Y-27632 is not yet fully known but it improves the survival of certain cells in the cell culture when they are seeded as single cells like human ESCs. Unfortunately none of the tested methods were successful in our hands. These results indicated that further optimization is required to obtain single cell colonies out of BMMSC transient transfection experiments.

To conclude, our study demonstrated that C677T SNP on *MTHFR* may have an important effect on differentiation ability of BMMSCs into adipocytes, osteocytes and chondrocytes. However in order to prove this, either sample size should be increased or BMMSCs with the same genetic background should be used. For the gene editing of these cells, chemical agents can be used for the transfection however in order to select transfected cells, techniques should be improved.

6 REFERENCES

1. Morrison SJ, Shah NM, Anderson DJ. Regulatory mechanisms in stem cell biology. *Cell* 1997; 88(3):287-98.
2. Venkei, ZG and Yamashita, YM. Emerging mechanisms of asymmetric stem cell division *Journal of Cell Biology* 2018; 7(3): 72-80
3. Evans MJ, Kaufman MH. Establishment in culture of pluripotential cells from mouse embryos. *Nature* 1981; 292(5819):154-6
4. Reubinoff BE, Pera MF, Fong CY, Trounson A, Bongso A. Embryonic stem cell lines from human blastocysts: somatic differentiation in vitro. *Nat Biotechnol* 2000; 18(4):399-404
5. Keller G. Embryonic stem cell differentiation: emergence of a new era in biology and medicine. *Genes Dev* 2005; 19(10):1129-55
6. Wobus AM, Boheler KR. Embryonic stem cells: prospects for developmental biology and cell therapy. *Physiol Rev* 2005; 85(2):635-78
7. Amit M, Margulets V, Segev H, Shariki K, Laevsky I, Coleman R, Itskovitz-Eldor J. Human feeder layers for human embryonic stem cells. *Biol Reprod* 2003; 68(6):2150-6
8. Mitsui K, Tokuzawa Y, Itoh H, Segawa K, Murakami M, Takahashi K, Maruyama M, Maeda M, Yamanaka S. The homeoprotein Nanog is required for maintenance of pluripotency in mouse epiblast and ES cells. *Cell* 2003; 113(5):631-42.
9. Park IH, Zhao R, West JA, Yabuuchi A, Huo H, Ince TA, Lerou PH, Lensch MW, Daley GQ. Reprogramming of human somatic cells to pluripotency with defined factors. *Nature* 2008; 451(7175):141-6
10. Takahashi K, Yamanaka S. Induction of pluripotent stem cells from mouse embryonic and adult fibroblast cultures by defined factors. *Cell* 2006; 126(4):663-76
11. Aasen T, Raya A, Barrero MJ, Garreta E, Consiglio A, Gonzalez F, Vassena R, Bilić J, Pekarik V, Tiscornia G, Edel M, Boué S, Izpisua Belmonte JC. Efficient and rapid generation of induced pluripotent stem cells from human keratinocytes. *Nat Biotechnol* 2008; 26(11):1276-84
12. Nowell PC, Cole LJ, Habermeyer JG, Roan PL. Growth and continued function of rat marrow cells in x-irradiated mice. *Cancer Res* 1956; 16(3):258-61.
13. Gengozian N, Urso IS, Congdon CC, Conger AD, Makinodan T. Thymus specificity in lethally irradiated mice treated with rat bone marrow. *Proc Soc Exp Biol Med* 1957;96(3):714-20.
14. Kim M, Cooper DD, Hayes SF, Spangrude GJ. Rhodamine-123 staining in hematopoietic stem cells of young mice indicates mitochondrial activation rather than dye efflux. *Blood* 1998; 91(11):4106-17
15. Negrin RS, Atkinson K, Leemhuis T, Hanania E, Juttner C, Tierney K, Hu WW, Johnston

- LJ, Shizurn JA, Stockerl-Goldstein KE, Blume KG, Weissman IL, Bower S, Baynes R, Dansey R, Karanes C, Peters W, Klein J. Transplantation of highly purified CD34+Thy-1+ hematopoietic stem cells in patients with metastatic breast cancer. *Biol Blood Marrow Transplant* 2000; 6(3):262-71.
16. Ferrari G, Cusella-De Angelis G, Coletta M, Paolucci E, Stornaiuolo A, Cossu G, Mavilio F. Muscle regeneration by bone marrow-derived myogenic progenitors. *Science* 1998; 279(5356):1528-30
 17. Jackson KA, Majka SM, Wang H, Pocius J, Hartley CJ, Majesky MW, Entman ML, Michael LH, Hirschi KK, Goodell MA. Regeneration of ischemic cardiac muscle and vascular endothelium by adult stem cells. *J Clin Invest* 2001; 107(11):1395-402
 18. Raghunath J, Salacinski HJ, Sales KM, Butler PE, Seifalian AM. Advancing cartilage tissue engineering: the application of stem cell technology. *Curr Opin Biotechnol* 2005; 16(5):503-9.
 19. Friedenstein AJ, Petrakova KV, Kurolesova AI, Frolova GP. Heterotopic of bone marrow. Analysis of precursor cells for osteogenic and hematopoietic tissues. *Transplantation* 1968; 6(2):230-47
 20. Caplan AI. Mesenchymal stem cells. *J Orthop Res* 1991; 9(5):641-50
 21. Pittenger MF, Mackay AM, Beck SC, Jaiswal RK, Douglas R, Mosca JD, Moorman MA, Simonetti DW, Craig S, Marshak DR. Multilineage potential of adult human mesenchymal stem cells. *Science* 1999; 284(5411):143-7.
 22. da Silva Meirelles L, Caplan AI, Nardi NB. In search of the in vivo identity of mesenchymal stem cells. *Stem Cells* 2008; 26(9):2287-99.
 23. Salem HK, Thiemermann C. Mesenchymal stromal cells: current understanding and clinical status. *Stem Cells* 2010; 28(3):585-96
 24. Sackstein R, Merzaban JS, Cain DW, Dagia NM, Spencer JA, Lin CP, Wohlgemuth R. Ex vivo glycan engineering of CD44 programs human multipotent mesenchymal stromal cell trafficking to bone. *Nat Med* 2008; 14(2):181-7.
 25. Tögel F, Weiss K, Yang Y, Hu Z, Zhang P, Westenfelder C. Vasculotropic, paracrine actions of infused mesenchymal stem cells are important to the recovery from acute kidney injury. *Am J Physiol Renal Physiol* 2007; 292(5):F1626-35.
 26. Block GJ, Ohkouchi S, Fung F, Frenkel J, Gregory C, Pochampally R, DiMattia G, Sullivan DE, Prockop DJ. Multipotent stromal cells are activated to reduce apoptosis in part by upregulation and secretion of stanniocalcin-1. *Stem Cells* 2009; 27(3):670-81.
 27. Di Nicola M, Carlo-Stella C, Magni M, Milanese M, Longoni PD, Matteucci P, Grisanti S, Gianni AM. Human bone marrow stromal cells suppress T-lymphocyte proliferation induced by cellular or nonspecific mitogenic stimuli. *Blood* 2002; 99(10):3838-43.
 28. Krampera M, Glennie S, Dyson J, Scott D, Laylor R, Simpson E, Dazzi F. Bone marrow mesenchymal stem cells inhibit the response of naive and memory antigen-specific T cells to their cognate peptide. *Blood* 2003; 101(9):3722-9.

29. Berglund AK, Schnabe LV. Allogeneic major histocompatibility complex-mismatched equine bone marrow-derived mesenchymal stem cells are targeted for death by cytotoxic anti-major histocompatibility complex antibodies. *Equine Vet. J* 2017; 49:4,539-544.
30. Oishi K, Noguchi H, Yukawa H, Hayashi S. Differential ability of somatic stem cells. *Cell Transplant* 2009;18(5): 581–589.
31. Dennis JE, Carbillet JP, Caplan AI, Charbord P, The STRO-1⁺marrow cell population is multipotential. *Cells Tissues Organs* 2002; 170(2–3):73–82.
32. Ding DC, Shyu WC, Lin SZ. Mesenchymal Stem Cells. *Cell Transplantation* 2011; 20, 5–14.
33. Uccelli A, Moretta L, Pistoria V. Mesenchymal stem cells in health and disease. *Nature Reviews Immunology* 2008; 8, 726–736.
34. Ouyang HW, Goh, JC, Thambyah, A, Teoh SH, Lee EH. Knitted polylactide-co-glycolide scaffold loaded with bone marrow stromal cells in repair and regeneration of rabbit Achilles tendon. *Tissue Eng* 2003; 9(3): 431–439.
35. Hung SC, Chang CF, Ma HL, Chen TH, Lowtone Ho, L. Gene expression profiles of early adipogenesis in human mesenchymal stem cells. *Gene* 2004; 340(1):141– 150.
36. Sekiya I, Larson BL, Smith JR, Pochampally R, Cui JG, Prockop DJ. Expansion of human adult stem cells from bone marrow stroma: Conditions that maximize the yields of early progenitors and evaluate their quality. *Stem Cells* 2002; 20(6):530–541.
37. Qian L, Saltzman WM. Improving the expansion and neuronal differentiation of mesenchymal stem cells through culture surface modification. *Biomaterials* 2004; 25(7–8):1331– 1337.
38. Chen, LB., Jiang, XB., Yang, L. Differentiation of rat marrow mesenchymal stem cells into pancreatic islet beta- cells. *World J. Gastroenterol* 2004; 10(20):3016–3020.
39. Lee KD, Kuo TK, Whang-Peng J, Chung YF, Lin CT, Chou SH, Chen JR, Chen YP, Lee OK. In vitro hepatic differentiation of human mesenchymal stem cells. *Hepatology* 2004; 40(6):1275–1284.
40. Inada M, Follenzi A, Cheng K, Surana M, Joseph B, Benten D, Bandi S, Qian H, Gupta S. Phenotype reversion in fetal human liver epithelial cells identifies the role of an intermediate mesoendodermal stage before hepatic maturation. *J. Cell Sci* 2008; 121(7):1002–1013.
41. Zhang F, Wen Y, Guo X. CRISPR/Cas9 for genome editing: Progress, implications and challenges. *Hum Mol Genet* 2014; 23,40–46.
42. Sander JD, Joung JK. CRISPR-Cas systems for genome editing, regulation and targeting. *Nat Biotechnol* 2014; 32, 4,347–355.
43. Kim YG, Cha J, Chandrasegaran S. Hybrid restriction enzymes: zinc finger fusions to Fok I cleavage domain, *Proc. Natl. Acad. Sci.* 1996; 93, 1156–1160.
44. Silva G. Meganucleases and other tools for targeted genome engineering: perspectives and challenges for gene therapy. *Curr Gene Ther* 2011;11, 11–27.
45. Urnov FD, Rebar EJ, Holmes MC, Zhang HS, Gregory PD. Genome editing with engineered

- zinc finger nucleases. *Nat Rev Genet* 2010; 11, 636– 646.
46. Jinek M, Chylinski K, Fonfara I, Hauer M, Doudna JA, Charpentier E. A programmable dual-RNA-guided DNA endonuclease in adaptive bacterial immunity. *Science* 2012; 80, 337, 816–821.
 47. Fineran PC., Charpentier, E. Memory of viral infections by CRISPR-Cas adaptive immune systems: Acquisition of new information. *Virology* 2012; 434, 202–209.
 48. Deltcheva, E. CRISPR RNA maturation by trans-encoded small RNA and host factor RNase III. *Nature* 2011; 471, 602–607
 49. Zhang, JH, Adikaram, P., Pandey, M., Genis, A., Simonds, WF. Optimization of genome editing through CRISPR-Cas9 engineering. *Bioengineered* 2016; 7, 3,166–174.
 50. Weninger A, Hatzl AM, Schmid C, Vogl T, Glieder A. Combinatorial optimization of CRISPR/Cas9 expression enables precision genome engineering in the methylotrophic yeast *Pichia pastoris*. *J. Biotechnol* 2016; 7(3): 72-80.
 51. Calarco J, Friedland A. Creating genome modifications in *C. elegans* using the CRISPR/Cas9 system. *Methods Mol. Biol* 2015; 1327, 59–74.
 52. Cong L. Multiplex genome engineering using CRISPR/Cas systems, *Science* 2013; 80, 819–823
 53. Vojta A. Repurposing the CRISPR-Cas9 system for targeted DNA methylation, *Nucleic Acids Res* 2016; 8(5): 96-110
 54. Dominguez AA, Lim WA, Qi LS. Beyond editing: repurposing CRISPR- Cas9 for precision genome regulation and interrogation. *Nat. Rev. Mol Cell Biol* 2015; 17, 5–15.
 55. Xue HY, Ji LJ, Gao AM, Liu P, He JD, Lu XJ. CRISPR-Cas9 for medical genetic screens: applications and future perspectives, *J. Med. Gene* 2015; 0, 1– 7.
 56. Savic N, Schwank G. Advances in therapeutic CRISPR/Cas9 genome editing, *Transl. Res.* 2015; 967.
 57. Müller M. *Streptococcus thermophilus* CRISPR-Cas9 systems enable specific editing of the human genome. *Mol. Ther*; 2015.
 58. Wojtal D. Spell checking nature: Versatility of CRISPR/Cas9 for developing treatments for inherited disorders, *Am. J. Hum. Genet* 2016; 98, 1–12
 59. White MK, Khalili K. CRISPR/Cas9 and cancer targets: future possibilities and present challenges, *Oncotarget* 2016; (7)11, 12305–12317.
 60. Homberger G, Linnebank M, Winter C, Genomic structure and transcript variants of the human methylenetetrahydrofolate reductase gene. *Eur J Hum Genet* 2000; 8:725-729.
 61. Weisberg I, Tran P, Christensen, B, A second genetic polymorphism in methylenetetrahydrofolate reductase (MTHFR) associated with decreased enzyme activity. *Mol Genet Metab* 1998; 64: 169- 172
 62. Daly SF, Molloy AM, Mills JL. The influence of 5,10 methylenetetrahydrofolate reductase

- genotypes on enzyme activity in placental tissue. *Brit J Obstet Gynae* 1999; 106:1214-1218.
63. Stern LL, Bagley PJ, Rosenberg IH. Conversion of 5-formyltetrahydrofolic acid is unimpaired in folate-adequate persons homozygous for the C677T mutation in the methylenetetrahydrofolate reductase gene. *J Nutr* 2000; 130: 2238-2242.
 64. Goyette P, Pai A, Milos R. Gene structure of human mouse methylenetetrahydrofolate reductase (MTHFR). *Mammalian Genome* 1998; 9:652-656.
 65. Rozen R. Methylenetetrahydrofolate reductase in vascular disease, neural tube defects and colon cancer; 1998.
 66. Botto LD, Yang Q. 5,10-Methylenetetrahydrofolate reductase gene variants and congenital anomalies: *Am J Epidemiol* 2000; 151, 862-77
 67. Tonetti C, Burtscher A, Bories D. Methylenetetrahydrofolate reductase deficiency in four siblings: A clinical, biochemical, and molecular study of the family. *Am J Med Genet* 2000; 91:363-367.
 68. Goyette P, Pai A, Milos R. Gene structure of human mouse methylenetetrahydrofolate reductase (MTHFR). *Mammalian Genome* 1998; 9:652-656
 69. Bagley PJ, Jacob S. A common mutation in the methylenetetrahydrofolate reductase gene is associated with an accumulation of formylated tetrahydrofolates in red blood cells. *Med Sci* 1998;95:13217-13220.
 70. Molloy AM, Daly S, Mills JL. Thermolabile variant of 5,10-methylenetetrahydrofolate reductase associated with low red-cell folates: Implications for folate intake recommendations. *The Lancet* 1997; 49: 1591-1593.
 71. Schmitz C, Lindpainter K, Verhoef P. Genetic polymorphism of methylenetetrahydrofolate reductase and myocardial infarction. *Circulation* 1996; 94: 1812-1814.
 72. Shpichinetsky V, Raz I, Friedlander Y, et al. The association between two common mutations C677T and A1298C in human methylenetetrahydrofolate reductase gene and the risk for diabetic nephropathy in type II diabetic patients. *J Nutr* 2000; 130: 2493-2497.
 73. Fodinger M, Horl WH, Sunder-Plassman G. Molecular biology of 5,10-methylenetetrahydrofolate reductase. *J Nephrol* 2000; 13(1):20-33.
 74. Goyette P, Rozen R. The thermolabile variant 677CT can further reduce activity when expressed in cis with severe mutations for human methylenetetrahydrofolate reductase. *Hum Mutat* 2000; 16:132-138.
 75. Sibani S, Christensen B, O'Ferrall E, et al. Characterization of six novel mutations in the methylenetetrahydrofolate reductase (MTHFR) gene in patients with homocystinuria. *Hum Mutat* 2000; 15: 280-287.
 76. Liew SC, Gupta ED. Methylenetetrahydrofolate reductase (MTHFR) C677T polymorphism: Epidemiology, metabolism and the associated diseases. *European Journal of Medical Genetics* 2014; 1-10.
 77. Peng F, Labelle LA, Rainey B, et al. Single nucleotide polymorphisms in the

- methylenetetrahydrofolate reductase gene are common in US Caucasian and Hispanic American populations. *Int J Mol Med* 2001; 8: 509-511.
78. Rady PL, Tying SK, Hundnall SD, Methylenetetrahydrofolate reductase (MTHFR): The incidence of mutations C677T and A1298C in the Ashkenazi Jewish population. *Am J Med Genet* 1999; 86:380-384.
 79. Tonetti C, Burtscher A, Bories D. Methylenetetrahydrofolate reductase deficiency in four siblings: A clinical, biochemical, and molecular study of the family. *Am J Med Genet* 2000; 91:363- 367.
 80. Schneider JA, Rees DC, Liu YT. Worldwide distribution of a common methylenetetrahydrofolate reductase mutation. *Am J Hum Genet* 1998; 62: 1258-1260.
 81. Sell SM, Lagemwa PR. Development of a highly accurate, rapid PCR-RFLP genotyping assay for the methylenetetrahydrofolate reductase gene. *Genet Test* 1999; 3:287-289.
 82. Demuth K, Moatti N, Hanon O,. Opposite effects of plasma homocysteine and the methylenetetrahydrofolate reductase C677T mutation on carotid artery geometry in asymptomatic adults. *Thromb Vasc Biol* 1998; 18:1838-1843.
 83. Lee H, Choi J, Ha K,. Influence of 5,10- methylenetetrahydrofolate reductase gene polymorphism on plasma homocysteine concentration in patients with end-stage renal disease. *Am J Kidney Dis* 1999; 34: 259-263.
 84. Bova I, Chapman J, Sylantiev C,. The A677C methylenetetrahydrofolate reductase gene polymorphism and carotid atherosclerosis . *Stroke* 1999; 30: 2180-2182.
 85. Kang S, Wong PWK, Susmano A. Thermolabile methylenetetrahydrofolate reductase: An inherited risk factor for coronary artery disease. *J Hum Genet* 1991; 48: 536-545.
 86. Lievers KJA, Boers GHJ, Verhoef V, et al. A second common variant in methylenetetrahydrofolate reductase (MTHFR) gene and its relationship to MTHFR enzyme activity, homocysteine and cardiovascular disease risk. *Journal of Molecular Medicine* 2011; 73-87.
 87. Kang S, Zhou J, Wong P, Kowalisyn J, Strokosch G. Intermediate homocysteinaemia: a thermolabile variant of methylenetetrahydrofolate reductase. *Am J Hum Genet* 1998; 43:414-21.
 88. Rozen R. Genetic predisposition to hyperhomocysteinaemia: deficiency of methylenetetrahydrofolate reductase (MTHFR). *Thromb Haemost* 1997; 78:523-6.
 89. Morita H, Kurihara H, Tsubaki S,. Methylenetetrahydrofolate reductase gene polymorphism and ischemic stroke in Japanese. *Arterioscler Thromb Vasc Biol* 1998; 18:1465-1469.
 90. Donnelly JG, Rock GA. Genetic determinants of heritable venous thrombosis: Genotyping methods for factor V_{LEIDEN} A1691G, methylenetetrahydrofolate reductase C677T, prothrombin G20210A mutation, and algorithms for venous thrombosis investigations. *Clin Biochem* 1999; 32: 223-228.
 91. van der Put NM, Gabreels F, Stevens EMB. A second common mutation in the

- methylenetetrahydrofolate reductase gene: An additional risk factor for neural-tube defects. *Am J Hum Genet* 1998; 62:1044-1051.
92. Dean JCS, Moore SJ, Osborne A, Fetal anticonvulsant syndrome and mutation in the maternal MTHFR gene. *Clin Genet* 1999; 56: 216- 220.
 93. Crott JW, Mashiyama ST, Ames BN, The effect of folic acid deficiency and MTHFR C677T polymorphism on chromosome damage in human lymphocytes in vitro. *Cancer Epidem Biomar* 2001;10(10):1089-1096.
 94. Güneş HV. *Moleküler Hücre Biyolojisi* 2003; 1,223-224.
 95. Piyathilake CJ, Macaluso M, Johanning GL, et al. Methylenetetrahydrofolate reductase (MTHFR) polymorphisim increases the risk of cervical intraepithelial neoplasia. *Anticancer Res* 2000; 20:1751-1757.
 96. Behera J, Bala J, Nuru M, Tyagi SC, Tyagi N, Homocysteine as a Pathological Biomarker for Bone Disease, *Journal of Cellular Physiology* 2016; 17: 23-35.
 97. Cai B, Li X, Wang Y, Liu Y, Yang F, Chen H. Apoptosis of Bone Marrow Mesenchymal Stem Cells Caused by Homocysteine via Activating JNK Signal. *PLoS ONE* 2013; 8(5): 63561.
 98. Davatchi F, Nikbin B, Shams H, Sadeghi Abdollahi B, Mohyeddin M, Shahram F, Mesenchymal stem cell therapy unable to rescue the vision from advanced Behcet's disease retinal vasculitis: report of three patients, *International Journal of Rheumatic Diseases* 2013; 16: 139–147.
 99. Horwitz E, Le BK, Dominici M. Clarification of the nomenclature for MSC: the International Society for Cellular Therapy position statement. *Cytotherapy* 2013; 7:393 5.
 100. Chang TY, Subbaroyan R, Hasan MT. High-efficiency stable gene transfection using chloroquine-treated Chinese hamster ovary cells. *Somat. Cell Mol Genet* 1991; 17, 5,513-7.

7 CURRICULUM VITAE

Personal Information

Name	Burcu	Surname	Taluğ
Birth of place	İstanbul	Date of birth	18.03.1992
Nationality	T.C.	Telephone number	
E-mail	burcutalug@gmail.com		

Educational Level

	Institution Name	Graduate Year
Master	Mehmet Ali Aydınlar Acibadem University	2019
Undergraduate	Yeditepe University	2016
High-School	Kadir Has Anadolu Lisesi	2010

Work Experience

	Position	Enterprise	Duration
1.	Long Term R&D Internship (Project based)	TAYF Biotechnology	4/2014 – 8/2014
8	Yeditepe University	Assistant student in Regenerative Biology laboratory	9/2015 – 6/2016
3.	NCMM Center for Molecular Medicine Norway, University of Oslo	Internship	06/2018- 09/2018

Foreign Languages	Reading*	Speaking*	Writing*
English	Very good	Very Good	Very Good

Foreign Languages Exams•

YÖK- DİL	UDS	IELTS	TOEFL IBT	TOEFL PBT	TOEFL CBT	FCE	CAE	CPE
92/100		6.5/9						

	Quantitative	Equally Weighted	Verbal
ALES Exam	77,66	80,74	73,65

Projects				
	Granted Program	Active Years	Position	Project Name
1.	TÜBİTAK 1003 (216S404)	2017-2019	Burslu	Genome-Wide Screening With CRISPR/Cas9 and Modeling of Resistance Mechanisms Developed Against Cytotoxic Drugs in Cancer Treatment

Presentations & Awards			
	Organization	Presentation Type	Title of the Presentation
1.	5th International Congress of Molecular Biology Association of Turkey, Bogazici University	Poster	Investigating The Effects Of 5,10-Methylenetetrahydrofolate Reductase C677t Polymorphism On Mesenchymal Stem Cells By Using Crispr/Cas9 System As A Gene Editing Tool
2.	5th International Congress of Molecular Biology Association of Turkey, Bogazici University	Poster	The Role Of Long Noncoding Rna Dancr In The Dna Damage Response
3.	Adv Exp Med Biol	Publication	Induced Pluripotent Stem Cells in Disease Modeling and Regeneration



REPUBLIC OF TURKEY
ACIBADEM MEHMET ALİ AYDINLAR UNIVERSITY
INSTITUTE OF HEALTH SCIENCES

**INVESTIGATING THE EFFECTS OF *5,10-*
METHYLENETETRAHYDROFOLATE REDUCTASE C677T
POLYMORPHISM ON HUMAN MESENCHYMAL STEM
CELLS BY USING CRISPR/CAS9 SYSTEM AS A GENE
EDITING TOOL**

BURCU TALUĞ

MASTER THESIS

DEPARTMENT OF MEDICAL BIOTECHNOLOGY

SUPERVISOR

Assist. Prof. Dr. Zeynep Tokcaer Keskin

SECOND SUPERVISOR

Assist. Prof. Dr. Emre Deniz

ISTANBUL-2019



REPUBLIC OF TURKEY
ACIBADEM MEHMET ALİ AYDINLAR UNIVERSITY
INSTITUTE OF HEALTH SCIENCES

**INVESTIGATING THE EFFECTS OF *5,10-*
METHYLENETETRAHYDROFOLATE REDUCTASE C677T
POLYMORPHISM ON HUMAN MESENCHYMAL STEM
CELLS BY USING CRISPR/CAS9 SYSTEM AS A GENE
EDITING TOOL**

BURCU TALUĞ

MASTER THESIS

DEPARTMENT OF MEDICAL BIOTECHNOLOGY

SUPERVISOR

Assist. Prof. Dr. Zeynep Tokcaer Keskin

SECOND SUPERVISOR

Assist. Prof. Dr. Emre Deniz

ISTANBUL-2019

Department: Institute of Health Sciences
Program: Medical Biotechnology
Thesis title: Investigating the Effects of 5,10-
Methylenetetrahydrofolate Reductase
Polymorphism on Human Mesenchymal Stem Cells
Using CRISPR/Cas9 System as a Gene Editing Tool
Students' name and surname: Burcu Taluğ
Date of defence: 10 / 05 / 2019

This is to certify that I have examined this copy of master thesis. I have found that she prepared after fulfilling requirements specified in the associated legislations before the final examining committee whose signatures are below.

Jury president	Prof. Dr. H. Uygur Tazebay Gebze Technical University
Supervisor of the thesis	Assist. Prof. Dr. Zeynep Tokcaer Keskin Acıbadem Mehmet Ali Aydınlar University
Second Supervisor of the thesis	Assist. Prof. Dr. Emre Deniz Acıbadem Mehmet Ali Aydınlar University
Jury member	Assist. Prof. Dr. Beste Kınıkoğlu Erol Acıbadem Mehmet Ali Aydınlar University
Jury member	Assist. Prof. Dr. Hande Koçak Demiroglu Bilim University

This thesis has been approved by the above jury and it has been accepted by decision of Health Sciences Board of Directors.


Prof. Dr. Uğur Özbek

Director of the Institute

Acıbadem Mehmet Ali Aydınlar University

DECLARATION

I hereby declare that, this thesis has been written by me based on the data obtained in line with the scientific rules and ethical principles of responsible conduct of research. All information, data, comments, analyses have been collected and processed through scientific, academic writing style, and literature used have been duly shown by giving reference to the original sources in accordance with the publication ethics. I also announce and emphasize that I have not violated any rules secured by patent and copyrights whilst the conduct and writing of this research.



10.04.2019

Burcu Taluğ

ACKNOWLEDGEMENT

Firstly, I would like to express my deep gratitude to my supervisor Assist. Prof. Dr. Zeynep TOKCAER KESKİN, for her patient guidance, enthusiastic encouragement and useful critiques of this research work. She is more than just a good advisor and supervisor to me, she became also my mentor though life besides science. I am very lucky meet her and say that she was my supervisor. I would also like to thank my co-supervisor Assist. Prof. Dr. Emre DENİZ, all kinds of support, especially throughout the laboratory experiences and troubleshooting.

I would like to offer my special thanks to my colleagues Ömer Faruk TAŞTAN, Hazal YILMAZ, Fatma PINAR, Süleyman BOZKURT, Ayşegül EKMEKÇİOĞLU and especially Gülin BARAN for their help during my master studies and for giving me joy and strength to overcome the hard times. I was very lucky to have especially Gülin as a lab partner with helpful discussions on every single experiment and idea and as a friend with constant support.

Finally, I would like to thank my lovely dad, Mustafa TALUĞ and beloved mum, Şenay TALUĞ. I could not make it without their support and unconditional love. And I would like to thank Ömer Faruk TAŞTAN who has always been with me throughout the thesis, and who has always supported me. I am grateful for their support.

This thesis project was supported by Acıbadem Mehmet Ali Aydınlar University Scientific Research Fund ABAPKO 2017/01/12. Burcu Taluğ was supported by TÜBİTAK 1003 project entitled "Genome-Wide Screening With CRISPR/Cas9 and Modeling of Resistance Mechanisms Developed Against Cytotoxic Drugs in Cancer Treatment" with Grant Number: 216S404.

LIST OF CONTENTS

Page No

ACKNOWLEDGEMENT	iv
LIST OF CONTENTS	v
LIST OF ABBREVIATIONS	viii
LIST OF TABLES	xii
SUMMARY	xiii
ÖZET.....	xiv
1 AIM OF STUDY	1
2 INTRODUCTION	2
2.1 Stem Cells	2
2.1.1 Embryonic stem cells	2
2.1.2 Induced pluripotent stem cells	4
2.1.3 Adult stem cells.....	5
2.1.4 Mesenchymal stem cells	7
2.2 Genome Engineering Technologies	11
2.2.1 The CRISPR/Cas system	12
2.3 Metylenetetrahydrofolate Reductase Gene	15
2.3.1 MHTFR enzyme	16
2.3.2 C677T polymorphism	17
2.4 Aim of this thesis study.....	20
3 Materials and Methods	21
3.1 Cell Culture	21
3.1.1 Maintenance of human embriyonic kidney 293T cells	21
3.1.2 Cryopreservation of HEK293T cells.....	21
3.1.3 Maintenance of BMMSCs	22

3.1.4	Cryopreservation of BMMSCs	22
3.2	Differentiation of BMMSCs	23
3.2.1	Differentiation of BMMSCs into adipocytes	23
3.2.2	Differentiation of BMMSCs into osteocytes.....	23
3.2.3	Differentiation of BMMSCs into chondrocytes.....	24
3.3	CRISPR/Cas9 vector design for the HDR-mediated genome editing of cells to introduce C677T SNP in <i>MTHFR</i> gene	25
3.3.1	Bioinformatic design of the sgRNAs	25
3.3.2	Construction of CRISPR/Cas9 vector	29
3.4	DNA Isolation	37
3.5	Primer Design	37
3.6	Polymerase Chain Reaction (PCR)	38
3.7	Restriction Fragment Length Polymorphism (RFLP) Assay	39
3.8	Agarose Gel Electrophoresis.....	40
3.9	Transient Transfection of Human Cell Lines.....	40
3.9.1	Transient transfection of cell lines using polyethylenimine (PEI).....	40
3.9.2	Transient transfection of BMMSCs with electroporation.....	41
3.9.3	Transient transfection of cell lines with lipofectamine	41
4	RESULTS	42
4.1	Characterization of BMMSCs by Stem Cell Marker Expressions.....	42
4.2	Evaluating the Effect of C677T Polymorphisim on Mesencyhmal Stem Cell Properties.....	43
4.2.1	Genotyping of the BMMSCs	43
4.2.2	The effect of <i>MTHFR</i> C677T polymorphism on BMMSC morphology	45
4.2.3	The effect of <i>MTHFR</i> C677T polymorphism on differentiation of BMMSCs	46

4.3	Introducing the <i>MTHFR</i> gene C677T polymorphism to HEK293T cells with CRISPR/Cas9 gene editing system.....	53
4.3.1	Transient transfection of HEK293T cells	53
4.3.2	Genotyping of the mutant HEK 293T colonies with RFLP.....	56
4.3.3	Genotyping of the mutant HEK 293T colonies with T7 endonuclease1 assay	59
4.4	Introducing the <i>MTHFR</i> C677T polymorphism to BMMSCs by using CRISPR/Cas9 gene editing system	60
4.4.1	Optimization of transfection of BMMSCs.....	60
4.4.2	Transient transfection of BMMSCs with the CRISPR/Cas9 system ...	65
5	DISCUSSION AND CONCLUSION.....	68
6	REFERENCES.....	74
7	CURRICULUM VITAE	81

LIST OF ABBREVIATIONS

ASC	Adult Stem Cells
BMMSC	Bone Marrow Derived Mesenchymal Stem Cells
BNP	Brain Natriuretic Peptide
bp	Base Pairs
CD	Cluster Of Differentiation
CFU-F	Colony Forming Unit Fibroblasts
CRISPR	Clustered Regularly Interspaced Short Palindromic Repeats
crRNA	CRISPR RNA
DMEM	Dulbecco's Modified Eagle Medium
DMSO	Dimethyl Sulfoxide
dNTP	Deoxyribonucleotide Triphosphate
DPBS	Dulbecco's Phosphate Buffered Saline
EB	Embryoid Bodies
EDTA	Ethylenediaminetetraacetic Acid
ESCs	Embryonic Stem Cells
FBS	Fetal Bovine Serum
FGF	Fibroblast Growth Factor
GFP	Green Fluorescence Protein
HDR	Homology Directed Repair
HEK	Human Embryonic Kidney
HSC	Hematopoietic Stem Cells
ICM	Inner Cell Mass
ISCT	International Society for Cellular Therapy
iPSC	Induced Pluripotent Cells
LB	Lysogeny Broth
MEF	Mouse Embryonic Fibroblast Cells
MSC	Mesenchymal Stem Cells
<i>MTHFR</i>	Methylenetetrahydrofolate Reductase
NHEJ	Non-homologous End Joining
PAM	Protospacer Adjacent Motif

PBS	Phosphate Buffered Saline
PCR	Polymerase Chain Reaction
PD	Population Doublings
PEI	Polyethylenimine
PKA	Protein Kinase A
RFLP	Restriction Fragment Length Polymorphism
RT	Room Temperature
sgRNA	Single Guide RNA
SNP	Single Nucleotide Polymorphism
Sp1	Specificity Protein 1
ssODN	Single Stranded Oligodeoxynucleotide
T7E1	T7 Endonuclease1
TALEN	Transcription Activator Like Effector Nucleases
TGF	Transforming Growth Factor
THF	Tetrahydrofolate
tracrRNA	Trans Activating CRISPR RNA
UV	Ultra Violet
VEGF	Vascular Endothelial Growth Factor
ZFN	Zinc Finger Nucleases

LIST OF FIGURES

Page No

Figure 2.1 Characteristics of ESCs	3
Figure 2.2 Adult Stem Cells	6
Figure 2.3 Pathways involved in MSC differentiation.....	9
Figure 2.4 MSC differentiation	9
Figure 2.5 Schematic illustration of CRISPR/Cas9 mediated genome engineering .	14
Figure 3.1 Transcripts of MTHFR	25
Figure 3.2 Location of the SNP.....	26
Figure 3.3 Predicted gRNA sequences.....	26
Figure 3.4 Schematic presentation of CRISPR design with gRNAs and screening primers used for genotyping	28
Figure 3.5 Representative image of of pSpCas9(BB)-2A-Puro (PX459) vector	29
Figure 3.6 Agarose gel electrophoresis image of the sgRNA oligonucleotides.....	31
Figure 3.7 Confirmation digest for the cloning of annealed sgRNAs intoPX459 vector.....	32
Figure 3.8 Colony PCR result	34
Figure 3.9 Sequencing result of Colony-2	34
Figure 3.10 Sequencing result of Colony-8	35
Figure 4.1 Representative flow cytometry analysis of BMMSC marker expressions of Donor 1	43
Figure 4.2 RFLP assays of hBM-MSCs.....	45
Figure 4.3 Bright field microscopy images of first passage A) wild type, B) heterozygous and C) homozygous BMMSCs	46
Figure 4.4 Lipid droplets observed after Oil Red O staining of A) wild type, B) heterozygous, C) homozygous differentiated cells, respectively.....	47
Figure 4.5 Adipogenic differentiation of BMMSCs from all genotypes determined by Oil Red O staining.....	48
Figure 4.6 Comparison of adipogenic differentiation capabilities between three genotypes.	49
Figure 4.7 Calcium deposits observed after Alizarin red staining of A) wild type, B) heterozygous, C) homozygous differentiated cells	50

Figure 4.8 Osteogenic differentiation of BMMSCs from all genotypes determined by Alizarin Red staining.....	50
Figure 4.9 Comparison of osteogenic differentiation capabilities between three genotypes.	51
Figure 4.10 Representative images of chondrogenic aggregates observed after toluidine blue staining of A) differentiated wild type cells, B) differentiated homozygous cells.....	52
Figure 4.11 Fluorescent microscopy images of HEK293T cells transfected by using PEI 1:3 with PX458 vector	54
Figure 4.12 Fluorescent microscopy images of A) bright field, B)transfected HEK293T cells transfected with PX458 vector and 1.85 ug of ssODN by using PEI Max in a ratio of 1:4.....	55
Figure 4.13 Fluorescent microscopy images of A) bright field, B)transfected HEK293T cells transfected with pSpCas9(BB)-2A-GFP (PX458) vector by using PEI Max 1:4.	56
Figure 4.14 Genotyping results of mutant HEK293T colonies by RFLP assay	58
Figure 4.15 T7E1 assay of pool of transfected cell and two heterozygous (C/T) colonies	59
Figure 4.16 Fluorescent microscopy images of BMMCSs transfected with PX458 vector by using Lipofectamine with different lipofectamine:DNA amount rati.....	61
Figure 4.17 Fluorescent microscopy images of BMMCSs transfected with PX458 vector by using	62
Figure 4.18 Bright field images of BMMSCs treated with different puromycin concentrations.	64
Figure 4.19 Puromycin resistance death curve of BMMSCs	65
Figure 4.20 Fluorescent microscopy images of A) bright field, B)transfected BMMSCs transfected with PX458 vector by using PEI Max 1:4.....	66
Figure 4.21 T7E1 assay of BMMSCs	67

LIST OF TABLES

Page No

Table 3.1 gRNA sequences	27
Table 3.2 Sequence of ssODN repair template	27
Table 3.3 Annealing of sgRNA	30
Table 3.4 Annealing reaction	30
Table 3.5 Ligation reaction of sgRNA into the plasmid	31
Table 3.6 Ligation reaction condition	32
Table 3.7 Colony PCR reaction.....	33
Table 3.8 Colony PCR reaction conditions	33
Table 3.9 Primer sequences used in screening	37
Table 3.10 PCR conditions for <i>BNP</i> amplification	38
Table 3.11 PCR conditions for <i>MTHFR</i> amplification	38
Table 3.12 Thermal cyler conditions.....	39
Table 3.13 RFLP conditions.....	39
Table 3.14 Electroporation conditions for BMMSs	41
Table 4.1 Flow cytometry analysis of BMMSC marker expressions of Donors	43

SUMMARY

5,10-Methylenetetrahydrofolate reductase (MTHFR) enzyme plays an important role in folate metabolism and C677T single nucleotide polymorphism (SNP) is the most frequently seen mutation in Turkish population and it causes MTHFR enzyme activity to decrease. This SNP has been linked to many different diseases in the literature and accompanied with high homocysteine levels. The latter is considered as an indicator of bone diseases and triggers the osteoclast formation, leading to a decrease in bone density and causes apoptosis in bone marrow derived mesenchymal stem cells (MSCs). As MSCs are known to be the major source of bone, cartilage and adipose tissue regeneration, we hypothesized that there could be a link between *MTHFR* C677T polymorphism and MSC differentiation capacity. That is why in this project, we aim to investigate the effects of *MTHFR* C677T polymorphism on MSC viability, morphology, physiology and differentiation capacity. For this purpose, we obtained primary human bone marrow derived MSCs (BMMSCs) that are wild type (C/C), heterozygous (C/T) and homozygous (T/T) for *MTHFR* gene at the corresponding nucleotide position of C677T SNP. Our primary results revealed that these cells were different by their differentiation capacities. However, this may be due to different genetic backgrounds of the patients. To eliminate the differences in genetic background we designed a guide RNA and a template single stranded oligo nucleotide (ssODN) to introduce C677T polymorphism to the genomes of BMMSCs using CRISPR/Cas9 genome editing technology. However, the cells couldn't be obtained as single cells and died. As a result, this study was able to show that the C677T SNP of *MTHFR* has interference in the differentiation potentials of BMMSCs and it needs further work to investigate the underlying reasons.

Keywords: Human mesenchymal stem cells, CRISPR/Cas9, 5,10-Methylenetetrahydrofolate reductase, *MTHFR*, SNP

ÖZET

İnsan Mezenkimal Kök Hücrelerinde CRISPR/Cas9 Genom Düzenleme Yöntemi ile 5,10- Metilentetrahidrofolat Redüktaz C677T Polimorfizm Etkisinin Araştırılması

5,10-Metilenetrahidrofolat redüktaz (MTHFR) enzimi folat metabolizmasında önemli bir rol oynar ve C677T tekli nükleotit polimorfizmi(TNP), Türk popülasyonunda en sık görülen mutasyondur ve ilgili enzimin aktivitesinin azalmasına neden olur. Bu polimorfizm yüksek homosistein seviyeleri ile birlikte, literatürdeki birçok farklı hastalıkla ilişkilendirilmiştir. Ayrıca kemik hastalıklarının bir göstergesi olarak kabul edilir ve kemik yoğunluğunun azalmasına yol açarak kemik iliği kaynaklı mezenkimal kök hücrelerde (KİMKH'ler) apoptozise neden olan osteoklast oluşumunu tetikler. MKH'lerin başlıca kemik, kıkırdak ve adipoz doku rejenerasyon kaynağı olduğu bilindiğinden, *MTHFR* C677T polimorfizmi ile MKH farklılaşma kapasitesi arasında bir bağlantı olabileceği düşünülmüştür. Bu nedenle bu projede *MTHFR* C677T polimorfizminin MKH canlılığı, morfoloji, fizyoloji ve farklılaşma kapasitesi üzerine etkilerini araştırmayı hedefliyoruz. Bu amaçla, *MTHFR* geni C677T TNP'inin ilgili nükleotit pozisyonu için vahşi tip (C / C), heterozigot (C / T) ve homozigot (T / T) olan kemik iliği kaynaklı birincil insan mezenkimal kök hücrelerini (KİMKH) elde ettik. Birincil sonuçlarımız, bu hücrelerin farklılaşma kapasitelerine göre farklı olduğunu ortaya koydu. Ancak bu hastaların farklı genetik geçmişlerine bağlı olabilir. Genetik arka plandaki farklılıkları ortadan kaldırmak, C677T polimorfizmini tanıtmak ve istenen varyatı CRISPR/Cas9 genome düzenleme teknolojisini kullanarak KİMKH'lerin genomuna entegre etmek için bir kılavuz RNA ve bir şablon tek iplikli oligo nükleotidi (ssODN) tasarladık. Ancak hücreler tek hücre olarak elde edilmeye çalışıldığında elde edilemediler ve öldüler. Sonuç olarak, bu çalışma *MTHFR* C677T SNP'sinin KİMKH'lerin farklılaşma potansiyellerini etkilediğini gösterdi ve altında yatan nedenlerin ortaya çıkarılabilmesi için ileri çalışmaların gerekliliğini ortaya koydu.

Anahtar Kelimeler: İnsan mezenkimal kök hücreleri, CRISPR/Cas9, 5,10- Metilentetrahidrofolat redüktaz, MTHFR, SNP

1 AIM OF STUDY

When the function of the MTHFR enzyme and its related diseases are considered, it is concluded that it is important for normal cellular functions thus the tissue homeostasis. Accordingly as adult stem cells have important roles in providing tissue homeostasis, it was thought that *MTHFR* C677T polymorphism might be also interfering with the differentiation capacities of MSCs. However, there is no study investigating the effect of this polymorphism on the differentiation of MSCs associated with *MTHFR* C677T polymorphism. The aim of this thesis is to introduce *MTHFR* C677T polymorphism by using CRISPR/Cas9 technology to MSCs and to investigate the differentiating capacity, viability, morphological and physiological changes of MSCs bearing this polymorphism having the same genetic background with the wild type MSCs. Furthermore, there are not many studies including changes in the genome of the MSCs using the CRISPR/Cas9 system. This study aims to fill the technical deficits in the literature. Successful introduction of *MTHFR* C677T polymorphism into MSCs using CRISPR/Cas9 technology will also pave the way for the correction of a similar polymorphism by the same method and the use of gene-corrected autologous MSCs for control group. In addition, this technique will lead to the investigation of the effects of various polymorphisms on MSCs. The fact that this polymorphism can be introduced to MSCs by using CRISPR/Cas9 technology is important in terms of investigating the various disease models by filling the necessary information gap in order to study other polymorphisms which have not been studied in the literature.

2 INTRODUCTION

2.1 Stem Cells

Stem cells are cells, which have an ability to differentiate into multilineage and also have an ability to renew themselves. They form somatic cells by their differentiation abilities [1]. They undergo symmetric and also asymmetric cell divisions. When they enter symmetric cell division, they form two-daughter cells that have the same features and that are not differentiated yet but with the ability to differentiate into other somatic cells of different lineages. They can also undergo asymmetric cell division regulated by some intrinsic factors such as polarity formation and mitotic spindle orientation; as well as by extrinsic factors such as the niche of the stem cell. By this, they form progenitor cell and also non-differentiated version for maintaining the body's stem cell pool [2]. The categorization of the stem cells are done at their time of isolation. Embryonic stem cells (ESCs) are *in vitro* cells isolated from inner cell mass cells of the blastocysts, which are active in the early embryonic development time, however, the germ line cells are active in the later stages of the development, and the adult stem cells are active in post natal. Another type of categorization for the stem cells is done according to their potencies. In this type of categorization, ESCs are pluripotent cells which have an ability to form nearly all cells from all of the lineages except cells originating from trophoblast, however adult stem cells are categorized as multipotent, which can form multiple cell types.

2.1.1 Embryonic stem cells

Embryonic stem cells are cells isolated from the inner cell mass (ICM) of the embryo at blastula [3], [4]. They are pluripotent and can form all the cell types that arise from the inner cell mass. That is why they have the ability to generate cells of every three

germ layers -namely endoderm, ectoderm and mesoderm- through differentiation (**Figure 2.1**). Moreover, they keep their pluripotent ability during passages without losing their genetic integrities [5].

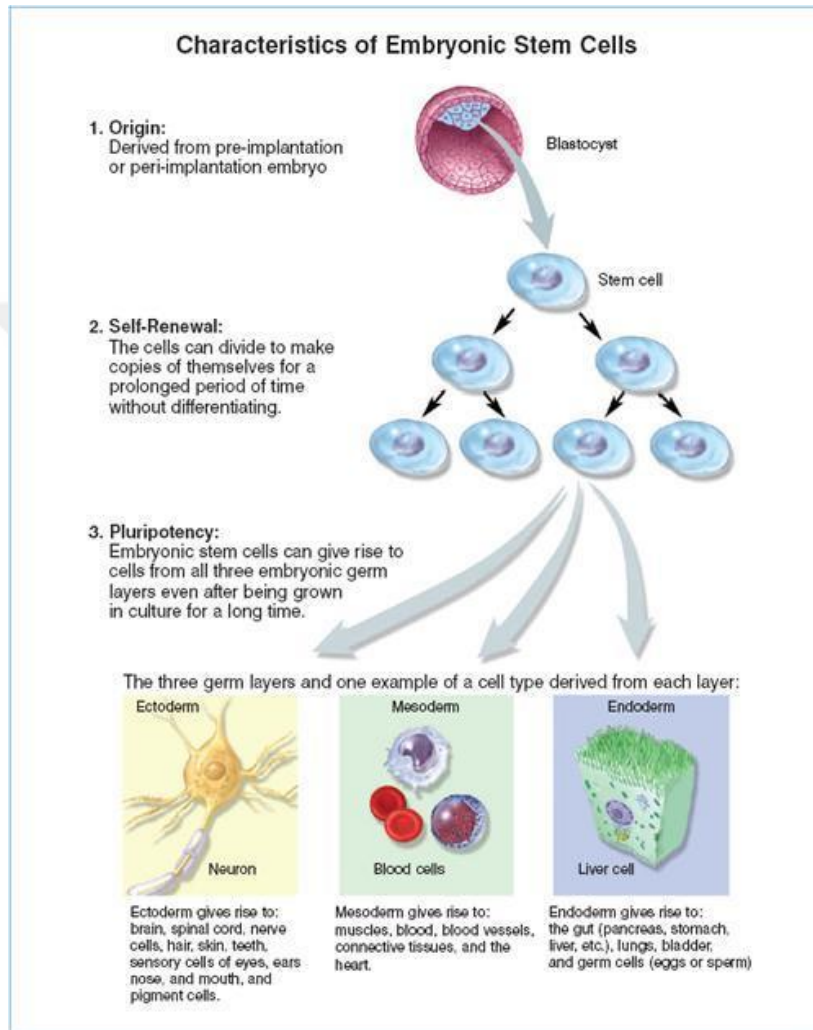


Figure 2.1 Characteristics of ESCs ©2006 Terese Winslow
(<http://stemcells.nih.gov/info/2006report/2006Chapter1.htm>)

In addition to normal embryonic development in health, ESCs are also associated with disease. Such that, teratomas are tumors that contain different cell types from all three germ layers and they are formed from undifferentiated ESCs *in vivo* [6].

Features of ESCs define their special requirements for laboratory handling. *In vitro* ESCs demand the presence of a feeder layer, which is basically usually irradiated mouse embryonic fibroblast cells (MEFs), which secrete growth factors for ESCs survival, or an extra cellular matrix, which increases ESCs' attachment [7]. Additionally, supplemented FGF2 is essential for prolonged ESCs' survival [7]. To maintain their pluripotency and undifferentiated state, endogenous expression of transcription factors like Oct4, Sox2, and Nanog are highly essential [8]. Besides these factors, SSEA 3 and SSEA 4 are expressed from human embryonic stem cells. All together, these endogenously expressed genes are regularly used as markers of pluripotency. ESC colonies, when they are cultured in suspension, form embryoid bodies (EBs), which offer extended possibilities for researchers in stem cell research.

Human ESCs can be obtained from *in vitro* fertilization clinics, however, their isolation comes with several ethical problems. In today's science, ESCs are highly important tools to investigate embryogenesis, cellular replacement therapies and the background of genetic diseases. On the contrary, they require the dissection of an embryo and also their uncontrolled usage has an increased risk of tumor formation, and possibility of immune rejection. In order to overcome these drawbacks, induced pluripotent cells (iPSCs) are invented.

2.1.2 Induced pluripotent stem cells

Because of the ethical and safety problems related with the usage of ESCs, scientists all around the World started to investigate new sources for stem cells with the same features of ESCs. In 2006, these investigations finally answered. Takahashi and Yamanaka, two scientists from Japan, published their study about creating stem cells, which are somatic cells made pluripotent by induction. In the corresponding study, it was shown that, when normal fibroblast cells isolated from mouse treated with a retroviral vector carrying cDNAs of *Oct4*, *Sox2*, *Klf4* and *c-myc* genes, cells gain

pluripotency. These cells are called as induced pluripotent stem cells and the factors mentioned are shortly named as Yamanaka factors. These newly created cells are capable of forming EBs, and teratomas just like ESCs are. In addition, they have the ability to contribute to the development of a mouse when they are injected into an ICM. When this study was revealed, a new era was opened and hopes for personalized medicine for the production of pluripotent stem cells specific for patient himself was raised. Shortly after the initial report, other studies to understand the iPSCs and their mechanisms started to be published worldwide. Although the first iPSCs were obtained by using fibroblast cells [9], [10] it was shown that other cell sources, such as keratinocytes, are also able to be used for obtaining iPSCs [11]. However, there are also some drawbacks using iPSCs. One of them is viral transfection system used in these studies, which can be mutagenic due to random integration of viral genetic material into the host cells' genome. Secondly, using c-myc can be dangerous since it can induce tumor formation. Such problems are highly important and should be solved before they are used in clinical applications such as personalized medicine and cellular therapies.

2.1.3 Adult stem cells

Adult stem cells (ASCs) are important to maintain the homeostasis of the body by locating the related tissues of organs. Their differentiation ability is more limited since they are multipotent rather than being pluripotent like ESCs. The adult stem cells are unique for the tissues they are located in and almost all tissue types have their own ASCs. Since they are tissue specific, they have special set of their own biomarkers, which can be used to identify and to categorize ASCs.

Adult stem cells are firstly discovered at 1950s during the studies after Hiroshima and Nagasaki atomic bombs related irradiation. In these studies, it was shown that, when bone marrow cells of mice were irradiated, their symptoms were highly similar with the patients surviving after atomic bombs. Whereas, when healthy bone

marrows were injected to them, their blood cells were started to proliferate again by regeneration [12], [13].

HSCs are ASCs. CD34, CD117, and Sca1 can be used as surface markers to identify them [14], [15]. They can form different cell types like cardiomyocytes, hepatocytes, muscle cells and also blood cells by differentiation [16], [17] (**Figure 2.2**). In the bone marrow transplantations, HSCs are transplanted and this treatment strategy is widely used for many diseases. In addition to their advantageous usages in clinics, HSCs transplantation has problems because of the increased possibility of immune rejection, called as graft versus host disease.

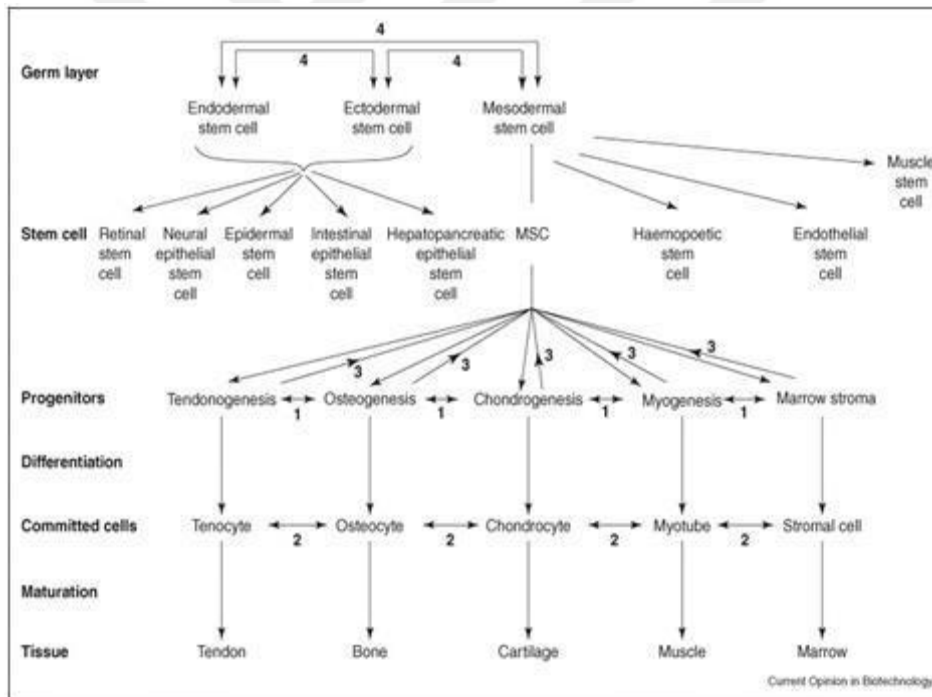


Figure 2.2 Adult Stem Cells © 2005 Elsevier Ltd.
 (<https://www.science-direct.com/science/article/pii/S0958166905001321>).

2.1.4 Mesenchymal stem cells

In bone marrow, besides HSCs, there are other adult stem cells, called mesenchymal stem cells (MSCs). MSCs are firstly discovered at 1968 by Friedenstein [19]. In the corresponding study, when the MSCs are cultured *in vitro*, it was seen that other than HSCs there were other type of cells that show fibroblastic morphology. They can attach to the culture plate surface and can form colonies. Furthermore, they can also form other cells like adipose cells, cartilage cells and also bone cells by directed differentiation (**Figure 2.3 and 2.4**). At 1988, these cells were firstly called as stromal stem cells, whereas in 1991, Caplan called them as MSCs [20]. In 1999, MSCs from bone marrow were firstly characterized by Pittenger et al. They separate bone marrow aspirates by their densities and plated them. The cells which attach to the plate was counted and checked for their colony forming abilities, which is called as colony forming unit fibroblasts (CFU-F). As a result, it was seen that only the 0.01% of the cells are able to form colonies. Also, it was seen that MSCs can specifically express CD 29, CD 90, CD 71, and CD 106 cell surface biomarkers, which can be used as surface markers for their identification. Beyond expressing specific surface markers, MSCs should lack CD 45, CD 14 and CD 34 surface expressions, which are indeed HSCs markers [21].

Different tissues can be used as a source for the isolation of MSCs. These include bone marrow -as mentioned earlier-, adipose tissue, dental pulp, umbilical cord blood and placenta. However, it was seen that the surface markers as well as the phenotypes of MSCs isolated from different tissue sources are different. For that reason, scientists defined solid criteria lists for their defined identification. According to International Society for Cellular Therapy, MSCs should express CD 73, CD 90, and CD 105; and they should not express CD 19, CD 34, CD 45, CD 11a, and HLA DR. Besides that, they should be able to attach to the surface and should be able to enter adipogenesis, osteogenesis and chondrogenesis *in vitro*. However, it also be checked the presence of tissue specific markers.

Homing capacity is the ability of the cells to migrate to injury sites. This is a highly important feature of MSCs. In the homing process, their surface receptors and also secreted chemokines and cytokines play important roles [22]. When there is an inflammation, chemokines and cytokines are secreted and MSCs start to migrate to the injury site [23]. It was seen that, between the surface receptors, CD 44 has an important role in the homing process [24]. MSCs are also anti-immunogenic cells and they have anti-apoptotic effects in the studies conducted on animal models. When there is a MSCs injection to the injured site, the apoptosis rate of the surrounding cells decrease. The reason for that anti apoptotic feature of MSCs comes from the secretion of important growth factors like VEGF, FGF 2, and TGF β , which are candidate survival signals for surrounding cells in the injured area. Additionally, it was seen that the secretion of these growth factors increase in hypoxia [25], [26].

MSCs have immunomodulatory effects as well. It was seen that when the T cells cultured with MSCs, their proliferation is inhibited [27, [28]. Besides cytotoxic and helper T cells, natural killer cells and other cells that have a role in immunity response are affected by MSCs too. However, still they have MHC receptors and may also be rejected [29]. For this reason, donor match is required for their use in therapies.

2.1.4.1 Differentiation pathways of MSCs

MSCs have differentiation ability into three lineages which are endoderm, ectoderm and mesoderm when they are cultured in specific conditions *in vitro* [30]. Differentiation of MSCs can also be controlled by transcription factors in such a way that, some genes regulate and induce the differentiation of progenitor cells to a specialized cell (**Figure 2.3 and 2.4**) [31].

2.1.4.1.1 Mesoderm differentiation

Differentiation of MSCs towards mesodermal lineage is easier when compared to differentiation into other two lineages as they share the same embryonic origin. For the induction of osteogenic differentiation, medium containing dexamethasone, ascorbic acid, and glycerophosphate is used. This type of differentiation is identified by the formation of calcium deposits, visualized by Alizarin Red staining [34].

In adipogenic differentiation, MSCs are cultured in a medium containing the chemicals insulin, dexamethasone, isobutylmethylxanthine, and indomethacin. The formation of adipocytes are detected by staining the lipid droplets with Oil Red O solution, [35], [36]. Whereas, in chondrocyte differentiation, growth factors TGF β 1 and TGF β 2 are widely administered in vitro to induce of chondrogenesis, and this is detected by toluidine blue staining.

2.1.4.1.2 Ectoderm differentiation

Notch 1 and Protein Kinase A (PKA) pathways are involved in that kind of differentiation. In order to differentiate MSCs into neurons the cells are cultured in a medium containing chemicals such as dimethyl sulfoxide, butylated hydroxyanisole and potassium chloride in addition to others. [37].

2.1.4.1.3 Endoderm differentiation

MSCs can be differentiated into pancreatic islet cells by culturing them in a medium containing nicotinamide and betamercaptaethanol like chemicals. When MSCs are differentiated into pancreatic islet cells, cells are started to secrete insulin and express nestin.[38].

In order to differentiate MSCs into liver cells, cells were cultured in a medium containing hepatocyte growth factors and oncostatin-M *in vitro* [39]. In the maturation of liver cells, mesodermal/endodermal phenotype was seen and some signaling pathways regulate this phenotype by using cytokines [40].

2.2 Genome Engineering Technologies

Genetic backgrounds and the phenotypic results have been linked by using stem cell models of diseases for years. Also, with the advent of sequencing technologies and molecular techniques, finding the links between genetic variants and diseases become possible for scientist. Furthermore, using genome engineering technologies on stem cells makes it possible to reveal the link between genetic background and phenotypic outcomes. In this, one manipulates the stem cells and reveals the effects of changes in genomic architecture on function. Thus combining of these two technologies opened new era for scientists in terms of personalized medicine.

There are various gene editing tools using artificial nucleases [41]. Firstly, there are protein based systems which bind the DNA at a specific location and create double strand breaks like meganucleases, transcription activator like effector nucleases (TALENs), and zinc finger nucleases (ZFNs) [42]. In meganucleases the systems are similar to restriction endonucleases as they have longer recognition sites on DNA [42]. TALEN and ZFN systems use engineered proteins for recognizing a desired sequence of DNA and carryinh a fused-*FokI* restriction enzyme to the target site in order to cut the DNA [42].

When ZFN technology and TALEN are compared, the DNA binding domain of TALEN consist of cys 2 his 2 sequence [43] and nearly 35 amino acid repeats, each

of which targets specific DNA nucleotide. For TALEN, when these amino acid motifs are engineered, specific DNA sequences can be targeted [30]. Such genome engineering technologies have been used to edit genomes of various organisms since their discovery. However there are also challenges of these technologies, which make them hard to use [42]. For meganucleases, their DNA binding-recognition sequence and cleavage site are intertwined [44], which makes the modification of its DNA binding sequence challenging. Whereas in TALEN and ZFN, they have separated DNA recognition sequence from their cleavage site (Fok I) [45], which makes the modification of their binding sites easier. When ZFNs and TALEN was compared, the zinc finger arrays were made to prevent unintended effects that make their creation more challenging for the laboratories. However in TALEN, despite the fact that its design is simpler than ZNF, since it has many TALE repeats, its construct cloning is more laborious and time consuming [42].

2.2.1 The CRISPR/Cas system

Because of the challenges presented by the above-mentioned genome engineering tools, a new gene editing system has been utilized in eukaryotes [46]. CRISPR/Cas system is a modified version of the natural defense mechanism in bacteria and archaea. [46] [47]. In this natural defense mechanism, foreign DNA is firstly cut into pieces and these short protospacer sequences were inserted into the bacterial genome, in the CRISPR locus exactly. This creates a cellular memory for the bacteria. If invasion of the same virus is repeated, the sequence specific CRISPR RNA (crRNA) will be transcribed and then will hybridize with the trans activating crRNA (tracrRNA) to the corresponding homology sequence of the viral genetic material. When this complex is formed, it guides a specific nuclease, Cas, to cut invading genetic material establishing a defense mechanism for the bacteria against the virus [41], [42], [48]. There are two classes of CRISPR/Cas systems using different Cas nucleases. Cas9 is the most widely used nuclease for research, which belongs to Class II, type II and it only needs one nuclease to cleave DNA[46]. This system is

firstly found in *Streptococcus pyogenes*. After nearly 20 years of its discovery, scientist started to think that this bacterial defense mechanism can be programmed to utilize for genome editing since it can induce double strand breaks in DNA and can be used for targeted genome editing. For that purpose, two components of this system should be introduced to the cells; Cas9 nuclease and a single guide RNA (sgRNA), which serves the role of crRNA and tracrRNA in a single transcript. [44].

The breaks that are created by CRISPR/Cas9 system are repaired by the DNA repair mechanisms of the host cell [44]. There are two different repair mechanisms for double strand breaks in mammalian systems, nonhomologous end joining (NHEJ) and homology directed repair (HDR). In NHEJ, the double strand break at the DNA is repaired by joining the broken ends together but during this process it introduces small insertions/deletions (indels). In case these indels are created in the reading frame of a protein-coding gene near its start codon, it is expected that they cause frame-shift mutations and create early stop codons. These mutated transcripts with early stop codons are usually destroyed by the nonsense mediated decay pathway or are sometimes translated into truncated, short and unfunctional proteins. As a result of these molecular cascades, CRISPR/Cas9 system can introduce knock-outs to the organism. In HDR, a DNA template is used to repair the DNA [41], [49]. That is why if a homology bearing sequence is introduced together with the CRISPR/Cas9 system, this repair template will be used while repairing the double strand breaks of the DNA, as a result custom made sequences can be inserted to the genome [41], [42]. Therefore, to introduce a single nucleotide polymorphism (SNP) to the genome requires the presence of three elements; Cas9 endonuclease, sgRNA and single stranded oligodeoxynucleotide (ssODN) as DNA repair template (**Figure 2.5**) [41], [42]. After these elements are delivered into the cell, sgRNA binds to the targeted DNA sequence, with a 20-nucleotide long homology, in the genome and brings about Cas9 protein, which will eventually incise both strands of the DNA at the 3bp upstream of the protospacer adjacent motif (PAM) site of the homology sequence [50] and forms a double stranded break. The host cell then will initiate its own repair mechanisms and the DNA will most likely be repaired using ssODN by HDR or in some cases without using ssODN by NHEJ.

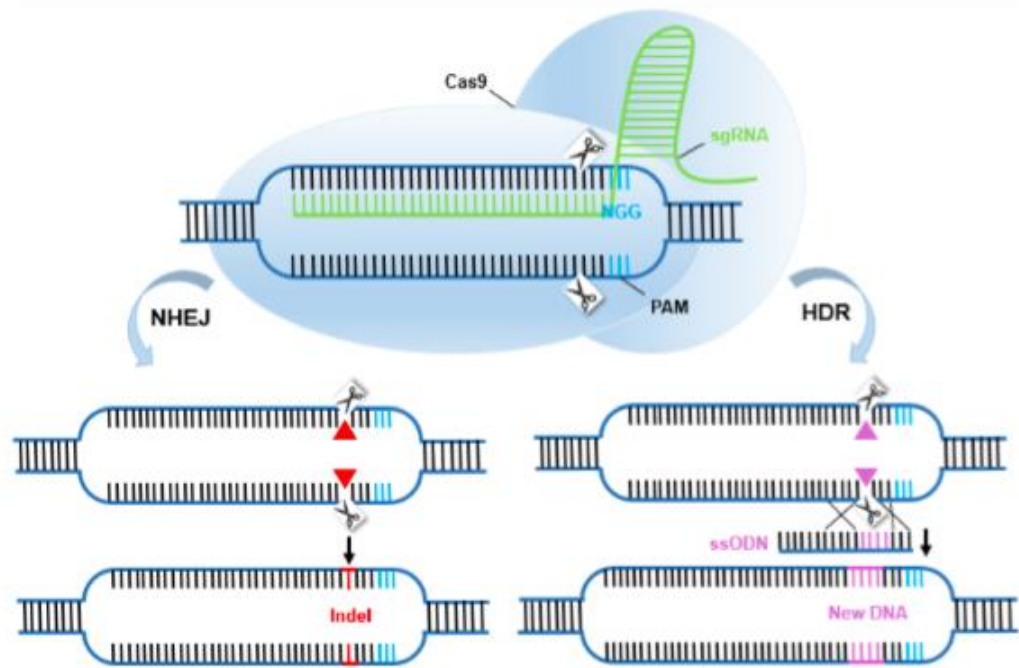


Figure 2.5 Schematic illustration of CRISPR/Cas9 mediated genome engineering © 2014, Springer Nature (<https://www.nature.com/articles/nbt.2842>)

CRISPR/Cas9 system led scientist to edit the genomes of various organisms including mammals, and it became the most widely used and studied genome engineering tool in the history of molecular biology [50], [51]. There are many new benefits of using this system. Multiple mutations can be introduced by using this editing tool to the same genome [52]. CRISPR/Cas9 is a promising tool for the treatment of genetic diseases. Furthermore, there are clinical trials using this genome editing system to treat human immunodeficiency virus (HIV) infections, various types of cancers and other diseases. Many scientists around the World are trying to understand and improve this system, as it will continue having impact in biomedical research [56-59].

There are some challenges to be solved before using this system on humans. The most important one is the off-target effects, which is the binding and cleavage of

unintended genomic loci by Cas9. This may lead to lethal problems. There are some strategies found to eliminate the possibility of off-target effects after the crystallization of Cas9-gRNA-DNA complex such as more improved bioinformatics tools to design sgRNAs. However, none of them actually prevents the problem to the full extend. Therefore novel strategies should be developed to improve CRISPR/Cas9 before being used for medical approaches [49].

2.3 Methylene tetrahydrofolate Reductase Gene

Methylene tetrahydrofolate Reductase (MTHFR) gene is located in p36.3 at chromosome 1 of human genome and encodes MTHFR enzyme which is highly important with its 656 amino acid structure. This enzyme plays role in folate metabolism [60]. Some mutations of *MTHFR* gene are considered to be risk factors for cardiovascular and cerebrovascular diseases by forming hyperhomocysteinemia and homocysteinuria [61-63]. *MTHFR* gene is conserved and present both in humans and mice. Moreover, the conserved genes have 11 exons and their exon sizes are similar bearing about 85% similarity at their coding sequences [64], [65]. The promoter region of *MTHFR* gene does not contain a TATA box, while it contains CpG islands and multiple potential specificity protein 1 (Sp1) binding sites [60]. There is alternative splicing on *MTHFR* gene generating different *MTHFR* transcripts in different tissues [65], [66], [67].

According to the studies conducted on both human and mice, it was seen that there were 15 different mutations on *MTHFR* gene [64], [68]. However, two of them were highly important since they can be seen frequently and are related with serious diseases. One of them is C677T polymorphism, affecting the catalytic domain of the enzyme and related with various diseases like vascular diseases, neural tube defects, and various cancers. The other one is A1298C polymorphism, affecting the regulator site of the enzyme and is mostly related with neural tube defects [66], [68], [69-72].

2.3.1 MHTFR enzyme

5,10-methylenetetrahydrofolate reductase enzyme is a flavoprotein and synthesized by *MTHFR* gene [60], [73], [74]. This enzyme is a cytoplasmic and it has two subunits creating a homodimer structure [75]. The studies conducted on humans showed that, it has 2 isoforms [60], [65]. One of the isoforms is 70 kDa, which is isolated from liver and the other one is 77kDa, which is isolated from other tissues [60], [65].

MTHFR enzyme is an important enzyme for folate metabolism. It has a role in the conversion of homocysteine for remethylation by using homocysteine, transsulphuration and remediation pathways [60]. MTHFR enzyme convert 5,10 methylenetetrahydrofolate (5,10-methylen THF) to 5-methyl tetrahydrofolate (5-methyl THF) [60], [61]. This formed 5-methyl THF becomes a methyl donor for DNA methylation and methionine synthesis. For this purpose, 5-methyl THF gives methyl group for the conversion of homocysteine.

There are some frequently seen mutations especially C677T mutation on *MTHFR* gene causing decrease in enzyme activity [77]. Because of this decrease in MTHFR activity, 5-methyl THF levels decrease and 5-10 methylene THF and plasma homocysteine levels increase [77]. Functional defects in MTHFR enzyme have been related with various health problems [68], [78]. In severe MTHFR deficiency in which hyperhomocysteinemia and homocysteinuria occur, clinical features such as peripheral neuropathy, growth retardation, stroke, and thrombosis are observed [68], [78]. In cases where MTHFR deficiency is mild, which is quite common throughout the population, it can be a risk factor in the occurrence of arterial diseases [68], [78].

2.3.2 C677T polymorphism

MTHFR C677T polymorphism occurs at the 4th exon at *MTHFR* gene effecting N-terminal catalytic domain of the enzyme [78], [79]. In that polymorphism, there is a point mutation at gene of *MTHFR* enzyme and causing the conversion of cytosine to thymine [68], [74], [80], [81]. This mutation, causes conversion of alanine in the protein to a valine [81], [82], [83] decreasing the enzyme activity [81], [82], [83]. Because of this decrease, 5-methyl tetrahydrofolate levels also decrease which blocks the conversion of homocysteine to methionine. These events as a result cause an increase in the homocysteine levels [71], [80-83]. There are three genotypes on *MTHFR* C677T polymorphism; CC(Alanine/Alanine) refers homozygous normal, CT(Alanine/Valine) refer heterozygous and TT (Valine/Valine) refers homozygous mutants genotypes [63], [70].

It has been revealed by metaanalysis that, the C677T polymorphism on *MTHFR* gene is a risk factor for cardiovascular diseases, neural tube defects, strokes, Down syndrome and various cancer types [71], [73]. It has also been shown that, the risks of acute leukemia, colorectal cancer and lung cancer are decreasing however the risk of endometrial cancer is increasing with the presence of the SNP [73], [84], [85].

MTHFR activity in homozygous mutants is less than heterozygous mutants and homozygous normal genotypes, with increased blood homocysteine levels [69], [86]. *MTHFR* deficiency exposes the organism to both the reduction of methionine (and S-adenosylmethionine) and the toxic effects of homocysteine accumulation [69], [71], [86]. Moreover, C677T polymorphism reduces the thermo stability and activity of the *MTHFR* enzyme at 37⁰C or higher. It has been seen that the activity of the enzyme in homozygous mutants are 60 % lower at 37⁰C and 65 % lower at 46⁰C compared to wild type controls [87], [88].

2.3.2.1 *MTHFR* C677T and cerebrovascular diseases

Studies have been shown that, in approximately 25-50% of patients with stroke, moderate hyperhomocysteinemia may occur [73]. According to the results of a metaanalysis approach performed with 24 studies, that have been conducted since 1994 with 900 patients having stroke, has showed that patients having stroke had elevated levels of homocysteine compared to control groups [73]. And also the results coming from other study done with 256 patients having stroke and 325 healthy controls, it was shown that homozygous mutant (TT) genotype and stroke is highly related [89]. In this study, the plasma homocysteine levels are higher in the patients with T/T or C/T genotype compared to patients having C/C genotype [89].

2.3.2.2 *MTHFR* C677T and venous thrombosis

It was already have been shown that, because of the sulfhydryl group of homocysteine, and its hypomethylation and acylation effects, homocysteine has dangerous effects on vein endothelium [73]. Because of that damage caused by homocysteine on veins, it increases the platelet production causing thrombosis [90]. However, there were also studies claiming T/T genotype and Venous Thrombosis are not related [73]. The mutation of *MTHFR* C677T may be an important risk factor for thromboembolism among individuals who carry another risk factor such as cystathionine beta-synthase, homozygous deficiency, which is a transsulfuration enzyme [73].

2.3.2.3 *MTHFR* C677T and neural tube defects

There are some studies claiming that, mutant T allele is a risk factor for neural tube defects [61]. Furthermore, it is well established that, decreased levels of blood folate

is a risk factor for the occurrence of neural tube defects [91]. *MTHFR* polymorphism and folate deficiency together, effect neural development and increase the risk of neural tube defects [61], [71], [91], [92].

2.3.2.4 *MTHFR* and cancer

Decreased level of enzyme activity caused by *MTHFR* polymorphism affects the tumor suppressor gene stability and also hypermethylation [71]. Studies conducted with patients having lung cancer, C677T allele is related with the elevated levels of p16 gene expression which is a tumor suppressor gene [71]. In another study, it was shown that, the decreased levels of MTHFR activity on the lymphocyte of patients having TT genotype caused the elevated levels of 5,10-methylenhydrofolate's concentration required for thymine synthesis [93]. This decreases the DNA damage by blocking the uracil formation caused by cytosine deamination [94]. In another study conducted with patients having cervical cancer, it was shown that TT and CT genotypes are strongly related with cervical cancer [95].

2.3.2.5 *MTHFR* C677T polymorphism and bone related diseases

The *MTHFR* C677T polymorphism results in increased homocysteine levels. High levels of homocysteine are thought to be an indicator of bone diseases and at the same time cause a decrease in bone density by triggering osteoclast formation [96]. In another study, high concentrations of homocysteine have been shown to induce apoptosis in BMMSCs [97].

Behcet's disease is also associated with *MTHFR* C677T polymorphism. In a study, autologous MSCs were injected into patients for treatment of Behcet's disease

vasculitis [98]. However, in this study, three patients had no improvement in their visions, and stem cell therapy was found to be unsuccessful. In another Behcet's disease study, when allogeneic MSCs were given to a patient with central nervous system damage, the damage was significantly reduced [96].

2.4 Aim of this thesis study

When the function of the MTHFR enzyme and its related diseases are considered, it is concluded that MTHFR is important for normal cellular functions thus the tissue homeostasis. Accordingly, as adult stem cells have important roles in providing tissue homeostasis, it was thought that *MTHFR* C677T polymorphism might be also interfering with the differentiation capacities of MSCs. However, there is no study investigating the effect of this polymorphism on the differentiation of MSCs associated with *MTHFR* C677T polymorphism. The aim of this thesis is to introduce *MTHFR* C677T polymorphism by using CRISPR/Cas9 technology to MSCs and to investigate the differentiating capacity, viability, morphological and physiological changes of MSCs bearing this polymorphism having the same genetic background with the wild type MSCs. Furthermore, there are not many studies including changes in the genome of the MSCs using the CRISPR/Cas9 system. This study aims to fill the technical deficits in the literature. Successful introduction of *MTHFR* C677T polymorphism into MSCs using CRISPR/Cas9 technology will also pave the way for the correction of an SNP by the same approach and the use of gene-corrected autologous MSCs for damage repair. In addition, this technique will lead to the investigation of the effects of various polymorphisms on MSCs. The fact that this polymorphism can be introduced to MSCs by using CRISPR/Cas9 technology is important in order to investigate the various disease models by filling the necessary information gap in order to study other polymorphisms which have not been studied in the literature.

3 Materials and Methods

3.1 Cell Culture

3.1.1 Maintenance of human embryonic kidney 293T cells

Human embryonic kidney 293T (HEK293T) cells (ATCC® CRL-3216™) were maintained at Dulbecco's Modified Eagle Medium (DMEM), high glucose (Gibco, 41965039) containing 10% qualified, heat inactivated fetal bovine serum (FBS) (Gibco, 10500064) in tissue culture plates in an Forma Steri-Cycle CO₂ incubator (Thermo Scientific, 51030301) set to 37⁰C and 5% CO₂. When the confluency of the cells reached 80%, cells were splitted mechanically into pre-warmed fresh DMEM (10%FBS) in a ratio of 1:10. Cells were splitted in every three days.

3.1.2 Cryopreservation of HEK293T cells

HEK293T cells were frozen for later use when they reached exponential growth phase. For freezing, cells were counted by 0.4%, liquid, sterile-filtered Trypan blue solution (Sigma-Aldrich, T8154) and approximately 1.000.000-1.500.000 cells were resuspended in ice-cold freezing medium containing 10% DMSO (Biomatik, A2424) in FBS and transferred to cryovials. Cryovials were stored at -80⁰C for 24 hours and transferred to liquid nitrogen tank for long term storage. When the cells were thawed, they were centrifuged at 300g, 3 min. and pellet was washed with pre-warmed fresh DMEM (10% FBS) to remove residual DMSO.

3.1.3 Maintenance of BMMSCs

BMMSCs were cultured in MSC medium by mixing MSC NutriStem® XF medium (Biological Industries, 05-200-1A) and MSC NutriStem® XF Supplement Mix (Biological Industries, 05-201-1U), in tissue culture plates covered with 0.1% Gelatin (Sigma, G9391) in a 5% CO₂ incubator at 37⁰C. The media of the cells were changed with pre-warmed fresh MSC medium every 2 days. When the confluency of the cells reached 80%, cells were trypsinized at 37⁰C for 3 min. with Trypsin 0.05% (1X) with EDTA (Gibco, 25300054). Trypsinization was ended by adding DMEM(10% FBS). Cell were collected to a 15mL falcon tubes and centrifuged at 300 g, 10 min. Pellet was washed with 1X Dulbecco's Phosphate Buffered Saline (DPBS)(Biological Industries, 02-023-1A) than, re-centrifuged at 300g, 5 min and resuspended at pre-warmed fresh MSC medium in a ratio of 1:2 .

3.1.4 Cryopreservation of BMMSCs

BMMSCs were frozen for later use when they reached exponential growth phase. For freezing, they were counted by trypan blue solution and approximately 1.000.000 cells were re-suspended in their culture medium containing 8% DMSO and 12% Dextran40 (Polifleks, Polifarma, PPC-1802140) and transferred to cryovials. Cryovials were stored at -80⁰C for 24 hours and transferred to liquid nitrogen tank for long term storage. When the cells were thawed, they were centrifuged at 300 g, 10 min. Pellet was washed with 1X DPBS, re-centrifuged at 300g, 5 min and re-suspended at pre-warmed fresh MSC medium to remove residual DMSO.

3.2 Differentiation of BMMSCs

3.2.1 Differentiation of BMMSCs into adipocytes

In order to differentiate BMMSCs into adipocytes, cells were counted by trypan blue and seeded into 12 well tissue culture plates to be 1×10^4 cells/cm². Cells were incubated in pre-warmed fresh MSC medium in 5% CO₂ incubator at 37⁰C until the cells were reached 90% confluency. Complete adipogenesis differentiation medium was prepared by mixing StemPro® Adipogenesis Differentiation Basal Medium (Gibco, A10410-01) and StemPro® Adipogenesis Supplement (Gibco, A10065-01). When the cells reached to desired confluency, medium was changed with pre-warmed complete adipogenesis differentiation medium. Cells were cultured for 21 days and medium was changed with pre-warmed prepared complete adipogenesis differentiation medium every 3 days. After 21 days, cells were fixed with 4% paraformaldehyde for 30 min. Fixative was washed with 1X PBS twice and 3 times with ddH₂O and the cells were covered with oil red O solution and incubated for 50 min at RT. The cells then were washed with ddH₂O 3 times. The cells were kept in ddH₂O to prevent from drying for observation. Pictures were taken on Zeiss AX10 microscope (Carl Zeiss, USA) with bright filter.

3.2.2 Differentiation of BMMSCs into osteocytes

In order to differentiate BMMSCs into osteocytes, cells were counted by trypan blue and seeded into 12 well plates to be 5×10^3 cells/cm². Cells were incubated in pre-warmed fresh MSC medium in 5% CO₂ incubator at 37⁰C until the cells were reached 90% confluency. Complete osteogenesis differentiation medium was prepared by mixing StemPro® Osteocyte/Chondrocyte Differentiation Basal Medium (Gibco, A10069-01) and StemPro® Osteogenesis Supplement (Gibco,

A10066-01). When the cells reached desired confluency, medium was changed with pre-warmed prepared complete osteogenesis differentiation medium. Cells were cultured for 21 days and medium was changed with pre-warmed complete osteogenesis differentiation medium every 3 days. After 21 days, the cells were fixed with 70% ethanol for 1h at RT and rinsed twice with ddH₂O and stained with alizarin red-s solution for 30 min at RT. The cells were washed with ddH₂O for 3 times and kept in ddH₂O to prevent from drying for observation. Pictures were taken on Zeiss AX10 microscope (Carl Zeiss, USA) with bright filter.

3.2.3 Differentiation of BMMSCs into chondrocytes

In order to differentiate BMMSCs into chondrocytes, cells were counted by typhan blue and resuspended to generate a cell suspension of 1.6×10^7 viable cells/mL in MSC medium. Micromasses were generated by seeding the cells as 5 μ L droplets in the center of each well in 12 well plates. Cells were incubated in pre-warmed fresh MSC medium in 5% CO₂ incubator at 37⁰C for 2 hours. Complete chondrogenesis differentiation medium was prepared by mixing StemPro[®] Osteocyte/Chondrocyte Differentiation Basal Medium (Gibco, A10069-01) and StemPro[®] Chondrogenesis Supplement (Gibco, A10064-01). After 2 hours, medium was changed with pre-warmed complete chondrogenesis differentiation medium. Cells were cultured for 21 days and medium was changed with pre-warmed complete chondrogenesis differentiation medium every 3 days. After 21 days, the cells were washed with 1X PBS twice and were fixed with 4% paraformaldehyde for 1 hour. After fixation, cells were washed twice and stained with freshly prepared toluidine blue solution for 30 min at RT. The cells were washed with ddH₂O for 3 times (5 min once) until the water became clean and kept in ddH₂O to prevent from drying for observation. Pictures were taken on Zeiss AX10 microscope (Carl Zeiss, USA) with bright filter.

3.3 CRISPR/Cas9 vector design for the HDR-mediated genome editing of cells to introduce C677T SNP in *MTHFR* gene

3.3.1 Bioinformatic design of the sgRNAs

In order to introduce desired SNP to *MTHFR*, firstly the suitable transcript of that gene was selected. According to literature; there were 9 transcripts of *MTHFR* [ensembl.org]. However just MTHFR-202 and MTHFR-204 transcripts had RefSeq accession numbers. That is why they were considered as suitable transcripts (**Figure 3.1**).

Name	Transcript ID	bp	Protein	Biotype	CCDS	UniProt	RefSeq	Flags
MTHFR-201	ENST00000376486.2	1135	29aa	Protein coding	-	A0A1B0GXD9	-	CDS 3' incomplete TSL:1
MTHFR-202	ENST00000376583.7	7044	697aa	Protein coding	CCDS81262	P42898	NM_001330358 NP_001317287	TSL:5 GENCODE basic APPRIS ALT1
MTHFR-203	ENST00000376585.5	5532	697aa	Protein coding	CCDS81262	P42898	-	TSL:5 GENCODE basic APPRIS ALT1
MTHFR-204	ENST00000376590.7	6232	656aa	Protein coding	CCDS137	P42898	NM_005957 NP_005948	TSL:1 GENCODE basic APPRIS P3
MTHFR-205	ENST00000376592.5	7057	656aa	Protein coding	CCDS137	P42898	-	TSL:1 GENCODE basic APPRIS P3
MTHFR-206	ENST00000413656.5	398	29aa	Protein coding	-	A0A1B0GXD9	-	CDS 3' incomplete TSL:1
MTHFR-207	ENST00000418034.1	1034	143aa	Protein coding	-	Q5SNW5	-	CDS 3' incomplete TSL:3
MTHFR-208	ENST00000423400.5	1539	52aa	Protein coding	-	Q5SNW7	-	CDS 3' incomplete TSL:1
MTHFR-209	ENST00000431243.5	870	29aa	Protein coding	-	A0A1B0GXD9	-	CDS 3' incomplete TSL:1

Figure 3.1 Transcripts of MTHFR according to databases on 03.08.2017, (ensembl.org).

Although in the literature, the SNP is called as C677T (Rs number: rs1801133), it is actually found to be at C1711T and C788T of MTHFR-204 and of 202 cDNAs respectively (NM_001330358.1:c.788C>T, NM_005957.4:c.665C>T according to databases on 03.08.2017). When MTHFR-204 and 202 transcripts were considered, the C677T SNP with the Rs number rs1801133 -causing the conversion of Alanine to Valine- is located at chromosome 1, exon 5 instead of exon 4 as cited in the literature according to databases released on 03.08.2017 (**Figure 3.2**) (ensemble.org)

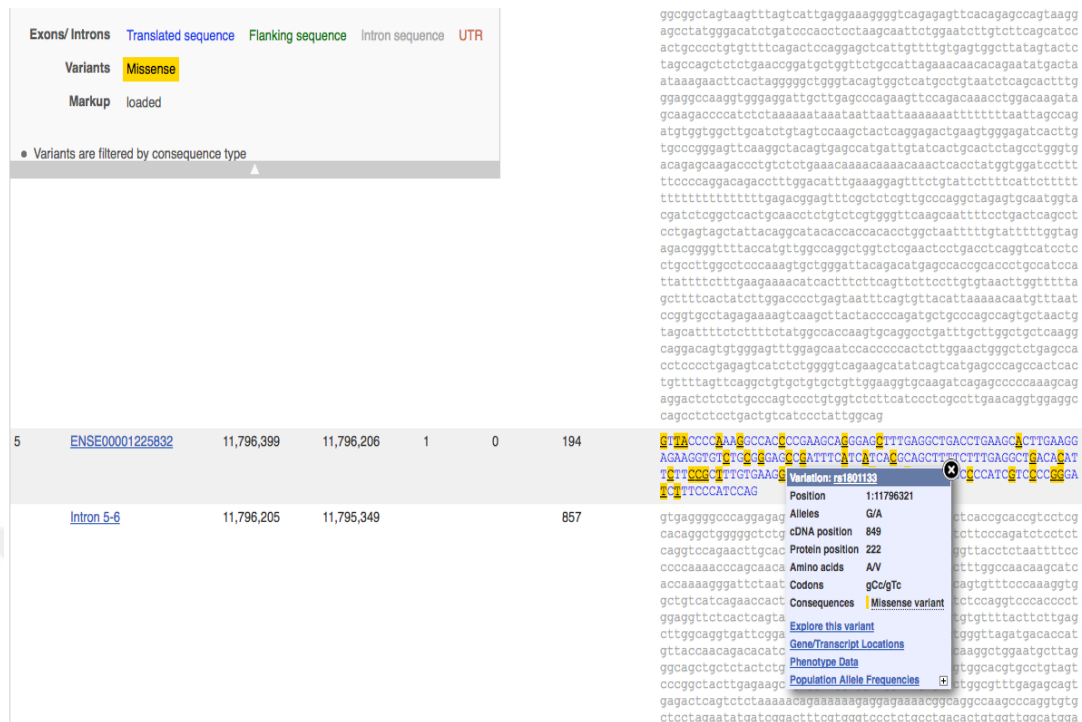


Figure 3.2 Location of the SNP(ensemble.org) (taken on 03.08.2017)

After determining the actual location of the C677T SNP, gRNAs and ssODN was designed *in silico* using crispor.tefor as an online tool. (Figure 3.3). First gRNA listed in the Figure 3.3 was selected because its location was at the targeted area.

Excel tables: Guides Off-targets Saturation-mutagenesis

Position/ Strand	Guide Sequence + PAM + Restriction Enzymes + Variants <input type="checkbox"/> Only G- <input type="checkbox"/> Only A-	Specificity Score	Predicted Efficiency Show all scores Doench '16 Mor-Mateos		Out-of-Frame score Click on score to show micro- homology	Off-targets for 0-1-2-3-4 mismatches + next to PAM	Genome Browser links to matches sorted by CFD off-target score <input type="checkbox"/> exons only <input type="checkbox"/> chr1 only
22 / rev	AAGCTGCGTGAATGAAAT CGG A- Enzymes: LmnI, TspDTI, NlaIV Cloning / PCR primers	73	57	77	72	0 - 0 - 1 - 18 - 159 0 - 0 - 0 - 1 - 4 178 off-targets	4:intron:RCAN1 4:intron:RP11-797M17.1 4:intergenic:AP000797.4-AP001891.1 show all...
52 / fw	CATCACGCAGCTTTCTTTG AGG Cloning / PCR primers	69	33	28	56	0 - 0 - 2 - 13 - 141 0 - 0 - 2 - 1 - 6	4:intergenic:RP1-309H15.2-RP1-209A6.1 4:intergenic:TRHR-NUJDC1 4:intergenic:RP11-567P19.1-XYLT1 show all...

Figure 3.3 Predicted gRNA sequences (crispor.tefor)

Table 3.1 gRNA sequences

Top oligo	caccgAAGCTGCGTGATGATGAAAT
Bottom oligo	caaaATTTTCATCATCACGCAGCTTc

3.3.1.1 ssODN design

MTHFR gene is at the reverse strand of the gDNA. For that reason, PAM sequence should be located at the forward strand and ssODN should be at the reverse strand since the enzyme will locate to the region where PAM sequence is and mediate the digestion of the other strand at the first order. For that reason, ssODN that would supposed to be used for the homologous recombination was designed as 120 bp by replacing the nucleotide to be changed at the center of the sequence, G to A (complementary to C to T). (Table 3.2). Moreover, the conversion of cytosine into thymine, also disturbs the NGG of the PAM sequence. This will prevent re-binding and possible re-cutting of Cas9 enzyme to the corresponding genomic locus after homologous recombination.

Table 3.2 Sequence of ssODN repair template

CCGAAGCAGGGAGCTTTGAGGCTGACCTGAAGCACTTGAAGGAGA AGGTGTCTGCGGGAGTCGATTTTCATCATCACGCAGCTTTTCTTTGA GGCTGACACATTCTTCCGCTTTGTGAAGG

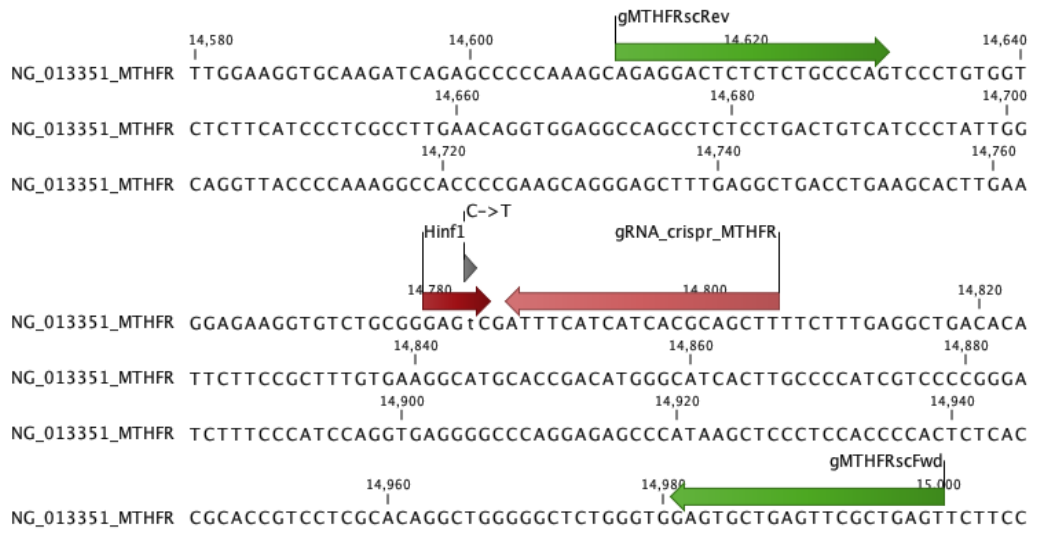


Figure 3.4 Schematic presentation of CRISPR design with gRNAs and screening primers used for genotyping

3.3.2 Construction of CRISPR/Cas9 vector

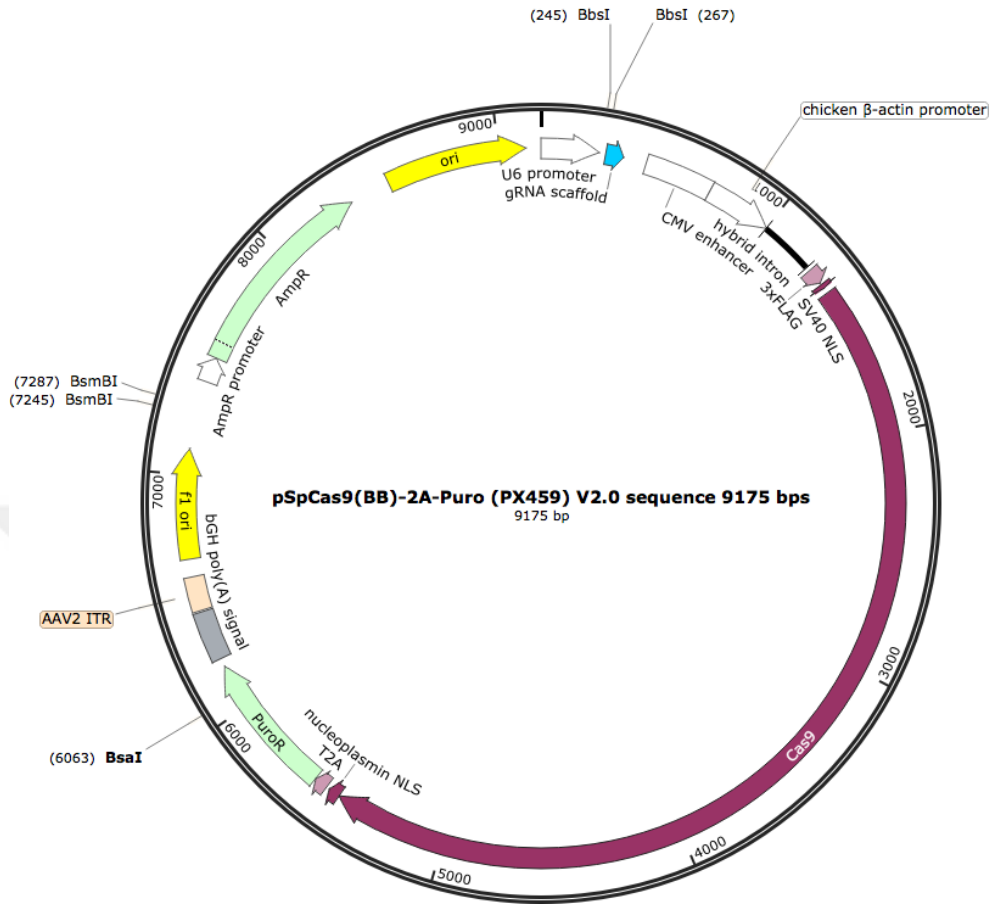


Figure 3.5 Representative image of of pSpCas9(BB)-2A-Puro (PX459) vector (addgene.org)

The designed sgRNAs were single stranded and in order to clone them into expression plasmid vector, complementary strands of sgRNAs were firstly annealed together (**Figure 3.6**) and then ligated into pSpCas9(BB)-2A-Puro vector, which is also cut with *Bbs* I enzyme simultaneously. (**Figure 3.7**).

3.3.2.1 Annealing of the sgRNAs

For the annealing of the sgRNAs following reaction indicated in **Table 3.3** were prepared in PCR tubes. PCR reactions were performed on T100™ Thermal Cycler (BioRad,1861096) with the thermal cyler conditions indicated in **Table 3.4 (Figure 3.6)**

Table 3.3 Annealing of sgRNA

Sg Top oligo (100 µM)	1 µL
Sg Bottom oligo (100 µM)	1 µL
T4 ligation buffer	1 µL
T4 PNK	1 µL
ddH ₂ O	6 µL

Table 3.4 Annealing reaction

37°C	30 min
95°C	5 min
95°C	14 min (Ramp down 0.1°C/s)

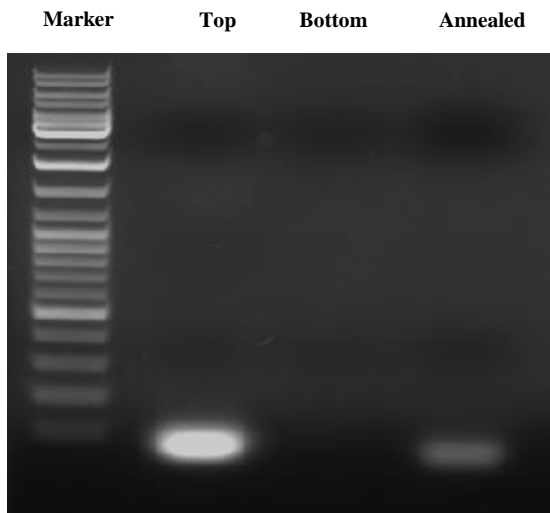


Figure 3.6 Agarose gel electrophoresis image of the sgRNA oligonucleotides. sgRNA targeting top strand was indicated as Top, sgRNA targeting bottom strand was indicated as bottom, and annealed sgRNAs were indicated as annealed.

3.3.2.2 Ligation of pspCas9-2a-Puro plasmid

For the ligation of plasmid with sgRNAs, following reaction indicated in **Table 3.5** were prepared in PCR tubes. Ligation reactions were performed on T100™ Thermal Cycler (BioRad,1861096) with the thermal cyler conditions indicated in **Table 3.6** (**Figure 3.7**)

Table 3.5 Ligation reaction of sgRNA into the plasmid

pspCas9-2a-Puro (100 ng/ μ L)	1 μ L
Diluted oligo (1:200)	2 μ L
T4 ligase buffer	2 μ L
DTT (Freshly diluted to 10 mM)	1 μ L
ATP (10 mM)	1 μ L
Bbs I	1 μ L
T4 DNA ligase	0.5 μ L
ddH2O	11.5 μ L

Table 3.6 Ligation reaction condition

37°C	5 min
21°C	x6 cycles 5 min
95°C	14 min (Ramp down 0.1°C/s)

Marker **Cut** **Uncut** **Ligated**
 plasmid **plasmid** **plasmid**

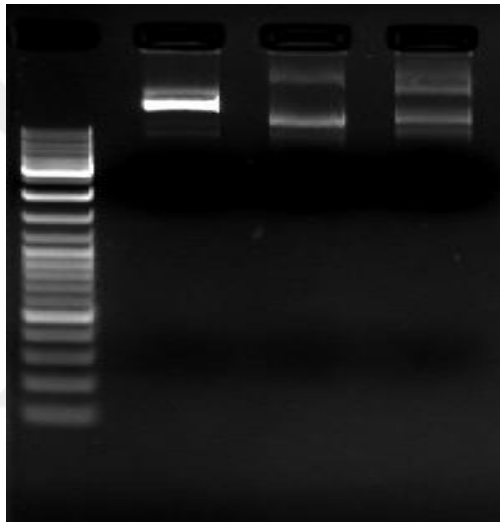


Figure 3.7 Confirmation digest for the cloning of annealed sgRNAs intoPX459 vector.

It can be seen from the agarose gel that, two sgRNAs were annealed together (**Figure 3.6**) and pSpCas9(BB)-2A-Puro vector cut with *Bbs* I enzyme ligated with annealed sgRNAs correctly (**Figure 3.7**)

3.3.2.3 Colony PCR

After the CRISPR/Cas9 vector was constructed, it was transformed into chemically competent DH5 α strain of *E.coli* cells and colony PCR was performed as described before by using a primer which can bind PX459 vector as a reverse primer and designed sgRNA targeting top strand as a forward primer so that if the vector inside the bacteria ligated with sgRNA, as a result of the PCR an approximately 120 bp sized band will be observed in the gel (**Figure 3.8**)

For the colony PCR, following reactions indicated in **Table 3.7** were prepared in PCR tubes. Transformed and grown colonies were picked by using sterile micropipette tips and firstly spread onto a replica plate than, immersed into the prepared reaction mixtures in PCR tubes. PCR reactions were performed on T100™ Thermal Cycler (BioRad,1861096) with the thermal cyler conditions indicated in **Table 3.8** Replica plate was stored at 4⁰C for later use.

Table 3.7 Colony PCR reaction

Component	10 μ l reaction
10X Standard <i>Taq</i> (Mg-free) Reaction Buffer	1.25 μ l
25 mM MgCl ₂	0.65 μ l
10 mM dNTPs	0.20 μ l
10 μ M Forward Primer	1 μ l
10 μ M Reverse Primer	1 μ l
<i>Taq</i> DNA Polymerase	0.125 μ l
ddH ₂ O	Up to 10 μ l

Table 3.8 Colony PCR reaction conditions

95 ⁰ C	3 min
95 ⁰ C	30 sec

60°C	30 sec	x28 cycles
68°C	30 sec	
68°C	5 min	

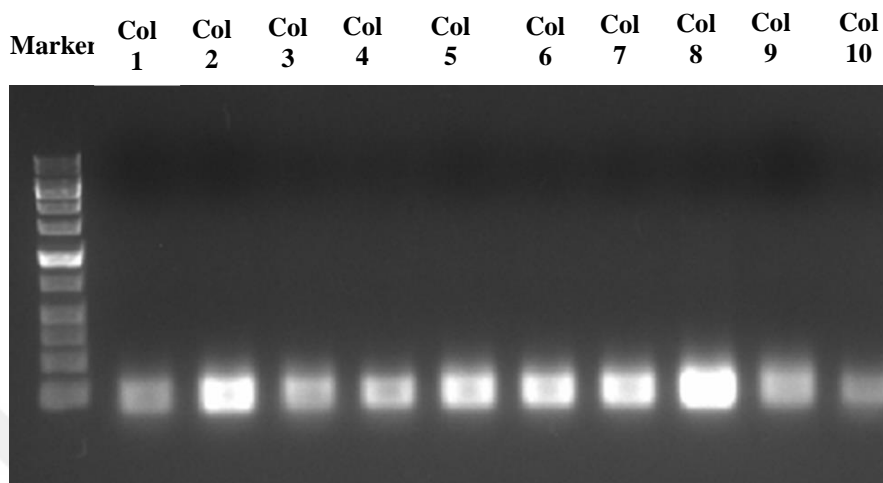


Figure 3.8 Colony PCR result

According to colony PCR, colony-2 and colony-8 were selected since their PCR bands were denser than others (**Figure 3.8**) and they were sent to sanger sequencing (MedsanTek Co.) to prove that they contained the designed sgRNAs.

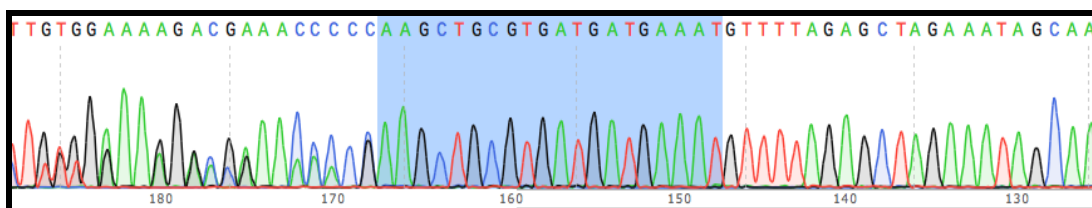


Figure 3.9 Sequencing result of Colony-2. Highlighted blue regions show the sgRNA sequence

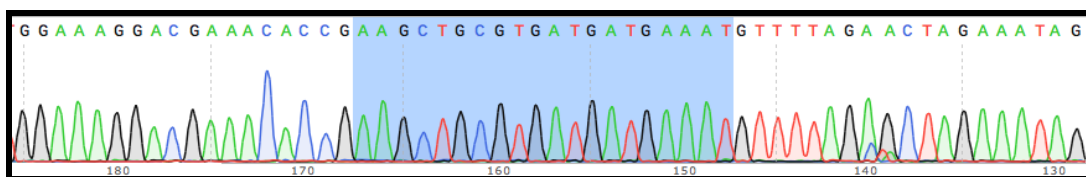


Figure 3.10 Sequencing result of Colony-8. Highlighted blue regions show the sgRNA sequence

According to the sequencing result (**Figure 3.9** and **Figure 3.10**), both the colonies contained desired sgRNAs, colony-8 was selected for further use. The plasmid isolated from this colony was pSpCas9(BB)-2A-Puro (PX459) ligated with sgRNA vector and decided to be used as a CRISPR/Cas9 vector to introduce *MTHFR* gene C677T polymorphism into HEK293T cells first and then primary human BMMSCs in later experiments will be discussed in following sections.

3.3.2.4 Bacterial culture

Escherichia coli (*E. coli*) DH5 α and HB101 strains were used for desired applications. Bacteria were cultured in LB broth (Sigma, L7659) containing Ampicillin(Neofroxx, 1728GR010) at a final concentration of 100 μ g/ml overnight at 37 $^{\circ}$ C with vigorous shaking at 180 rpm (shaker info ver). For long term storage; glycerol stocks were prepared by adding 87% glycerol to bacterial culture until final volume of glycerol was reached to 10% by mixing 115 μ l of 87% glycerol with 885 μ l of bacterial culture for 1 ml bacteria stock. Glycerol stocks of bacteria were stored at -80 $^{\circ}$ C. For single colonies, bacteria were cultured on LB agar containing final concentration of 100 μ g/ml ampicillin in petri dishes for 24 hours at 37 $^{\circ}$ C HeraTherm incubator (Thermo Scientific, 1GS60)

3.3.2.5 Transformation

For the transformation; plasmid DNA (1 μ L for ligation reaction) was mixed with competent cells taken from -80°C and incubated on ice for 30 min. After the incubation, cells were heat shocked at 42°C by using heat block for 90 sec followed by incubation on ice for 1 min. 800 μ L of LB was added on the cells and this culture was incubated at 37°C heat block for 45 min. After 45 min, cells were centrifuged at 13 000 rpm for 30 sec and pellet was resuspended with 100 μ L of LB. Cells were spread on LB agar petri dishes containing final concentration of 100 $\mu\text{g}/\text{ml}$ ampicillin by using glass beads. Petri dishes was incubated overnight at 37°C HeraTherm incubator (Thermo Scientific, 1GS60).

3.3.2.6 Plasmid DNA isolation

Plasmid DNA isolation was performed using PureLink™ HiPure Plasmid DNA Purification Kits (Invitrogen, K2100-04). For plasmid DNA isolation, bacteria were taken either from glycerol stock (-80°C) or as single colony on LB agar plate, and cultured overnight in 100 mL LB Broth containing 100 $\mu\text{g}/\text{ml}$ Ampicillin at 37°C with vigorous shaking at 180 rpm. After 24 hours, bacteria cultures were centrifuged at 4000 g for 10 min. Pellets were resuspended with resuspension buffer and lysed for 5 min with lysis buffers at RT. For the precipitation, precipitation buffer was added and samples were centrifuged at 4000 g for 30min than supernatants were loaded on equilibrated columns. After the solution in the column drained by gravity flow, columns were washed and eluted with Elution buffer. DNA was recovered with isopropanol and samples were centrifuges at 12 000g for 45 min at 4°C . Pellets were washed with 70% ethanol and after 10 min of air drying, pellets were resuspended in ddH₂O containing RNase (Macherey-Nagel, 740505). The concentration and purity of the DNA isolated were determined by using Microplate reader Varioscan Flash (Thermo Scientific, MIB#5250030)

3.4 DNA Isolation

DNA isolation was performed by using a DNA isolation from Tails-Proteinase K method by Jacks Lab, Koch Institute for Integrative Cancer Research at MIT, 2017. Tail lysis buffer (Appendix A) containing Proteinase K (Macherey-Nagel, 740506) was added to the samples. Samples were incubated in digital heating shaking drybath (ThermoFisher Scientific,88880028) adjusted to 55⁰C for 1.5 hours, then 5 M NaCl solution was added on them. Tubes were shaken and incubated on ice for 10 min. Samples were centrifuged (Thermo Scientific, MicroCl 21R) at 3000 rpm for 30 min at 4⁰C, isopropanol was added onto them and incubated on RT. DNA was recovered by centrifuge at max speed for 10 min at RT. Pellets were resuspended with 70% Ethanol, samples were re-centrifuged at max speed for 10 min at RT. Tubes were inverted on bench and air dried, pellets were resuspended with ddH₂O containing RNase The concentration and purity of the DNA isolated were determined by using Microplate reader Varioscan Flash (Thermo Scientific, MIB#5250030)

3.5 Primer Design

Primers for all the genes amplified were listed in **Table 3.9** were designed by using Primer Blast (NCBI). Ensemble and NCBI databases were used to check the specificity of the primers and product sizes they would amplify. Primers were ordered from Sentegen Biotech,Turkey.

Table 3.9 Primer sequences used in screening

Primer Name	Primer Sequence (5' - 3')
<i>MTHFR-Forward</i>	ACTCAGCGAACTCAGCACTC
<i>MTHFR-Reverse</i>	AGAGGACTCTCTCTGCCCCAG
<i>BNP-Forward</i>	CAGCCTCGGACTTGGAAC
<i>BNP-Reverse</i>	CTCCAGACACCTGTGGGAC

3.6 Polymerase Chain Reaction (PCR)

For amplifications of *MTHFR* and *BNP*, PCR was applied by using optimized PCR conditions indicated in **Table 3.10** and **Table 3.11** on T100™ Thermal Cycler (BioRad,1861096) with the thermal cycler conditions indicated in **Table 3.12**.

Table 3.10 PCR conditions for *BNP* amplification

Component	25 µl reaction
10X Standard <i>Taq</i> (Mg-free) Reaction Buffer	2.5 µl
25 mM MgCl ₂	1.5 µl
10 mM dNTPs	0.5 µl
10 µM Forward Primer	1 µl
10 µM Reverse Primer	1 µl
Template DNA	100 ng
<i>Taq</i> DNA Polymerase	0.125 µl
ddH ₂ O	Up to 25 µl

Table 3.11 PCR conditions for *MTHFR* amplification

Component	25 µl reaction
10X Standard <i>Taq</i> (Mg-free) Reaction Buffer	2.5 µl
25 mM MgCl ₂	1 µl
10 mM dNTPs	0.5 µl
10 µM Forward Primer	1 µl
10 µM Reverse Primer	1 µl
Template DNA	100 ng
<i>Taq</i> DNA Polymerase	0.125 µl
ddH ₂ O	Up to 25 µl

Table 3.12 Thermal cyler conditions

	<i>BNP</i>	<i>MTHFR</i>
Initial denaturation	95 ⁰ C, 4 min	95 ⁰ C, 4 min
Denaturation	95 ⁰ C, 30 sec.	95 ⁰ C, 30 sec.
Annealing	60 ⁰ C, 30 sec.	60 ⁰ C, 30 sec.
Extension	68 ⁰ C,30 sec.	68 ⁰ C,30 sec.
Cycles	35	35
Final Extension	68 ⁰ C, 5 min.	68 ⁰ C, 5 min.

3.7 Restriction Fragment Length Polymorphism (RFLP) Assay

RFLP assay was performed by incubating the amplified PCR samples with *HinfI* (New England Biolabs, R0155S) enzyme and CutSmart (New England Biolabs, R0155S) buffer for 1 hour at 37⁰C in T100™ Thermal Cycler (BioRad,1861096). For 25 µl of PCR sample; conditions indicated below was applied (**Table 3.13**)

Table 3.13 RFLP conditions. Cut indicates samples cut with *HinfI* enzyme, uncut indicates samples do not cut with enzyme. Uncut samples were used as a control

	Uncut	Cut
CutSmart Buffer	2.5 µl	2.5 µl
<i>HinfI</i> enzyme	-	0.5 µl (5 units)
ddH₂O	2.5 µl	2 µl

3.8 Agarose Gel Electrophoresis

Gels were prepared by dissolving the required amount of PegGOLD universal agarose (Peqlab, HD00020) (ranging from 0.5 g to 3 g) in 50 ml-150 ml (depending on the sizes of the DNA fragments in the samples) 1X TAE. 1% agarose gel was used for all experiments (PCR analysis, control of annealing and ligation of the sgRNAs etc.) except RFLP analysis. For RFLP analysis, 2% agarose gel was used. For fully dissolving the agarose, microwave oven was used. 1.5 µl ethidium bromide stock (10 mg/ml)(Sigma, E1510) per 100 ml gel solution for a final concentration of 0.15 µg/ml DNA samples were mixed with 6X DNA Loading dye (R0611, Thermo Scientific) stock solution for final concentration of loading dye in solution 1X and loaded on gel. Gels were run at 80 V, 60 min for RFLP and T7E1 assays and 100 V 60 min for PCR. The bands were visualized under UV light by using ChemiDoc Imaging System (BioRad, 1708265). Generuler DNA ladder (Thermo Prizma,LSG-SM0331)

3.9 Transient Transfection of Human Cell Lines

3.9.1 Transient transfection of cell lines using polyethylenimine (PEI)

The day before the transfection, cells were split as previously described in section 2.1.1 and 2.1.3 into 10 cm tissue culture plates. Transfection mixtures were prepared by mixing totaly 10 µg DNA (plasmid DNA and ssODN) in 1 mL serum free DMEM with (1µg/µL) PEI MAX -Transfection Grade Linear Polyethylenimine Hydrochloride (MW 40,000) (Polysciences, 24765-1) at a desired ratio. Mixture was immediately vortexed and incubated at RT for 15 min, then mixture was added onto the cells drop by drop.

3.9.2 Transient transfection of BMMSCs with electroporation

For the electroporation, 1×10^6 cells were transferred into the 2 mm electroporation cuvettes and pulsed at the following conditions **Table 3.14**. GenePulser Xcell (Biorad, 1652660) was used for the electroporation.

Table 3.14 Electroporation conditions for BMMSCs

Amount of DNA used in the transfection (μg)	Conditions
60 μg DNA	350 V, 950 μF 200 Ω
50 μg DNA	150 V, 1050 μF , 200 Ω
10 μg DNA	90 V, 5.5 to 5.7 msec duration
50 μg DNA	200 V, 0.500 μF

3.9.3 Transient transfection of cell lines with lipofectamine

The day before the transfection, cells were split as previously described in section 2.1.1 and 2.1.3 into 10 cm tissue culture plates. Transfection mixtures were prepared by mixing totally 10 μg DNA (plasmid DNA and ssODN) in 1 mL serum free DMEM with Lipofectamine™ 3000 Transfection Reagent (Invitrogen, L3000015) at a desired ratio. Mixture was immediately vortexed and incubated at RT for 15 min, then mixture was added onto the cells drop by drop.

4 RESULTS

4.1 Characterization of BMMSCs by Stem Cell Marker Expressions

BMMSCs previously were isolated from human donors' bone marrow and were characterized for their MSCs marker expressions using flow cytometry by Labcell (Acibadem Health Group Co.). MSCs marker expressions and validation reports of the cells were shown below (**Table 4.1, Figure 4.1**). Figure 4.1. given below is a representative flow analysis result showing the gates and the quadrans. All the donor cells were analyzed accordingly and their specific quantitated results were given at the Table 4.1 As can be seen from the table, all the BMMSCs are expressing universal MSC markers validated by ISCT including CD73, CD90 and CD 105 and excluding the hematopoietic markers (CD 34, CD45 and HLA DR) [99] (**Figure 4.1**) (**Table 4.1**). The actual names of the donors were hidden for their privacy and for the ethical reasons and in this study they were simply referred as donor1, donor2, and donor3.

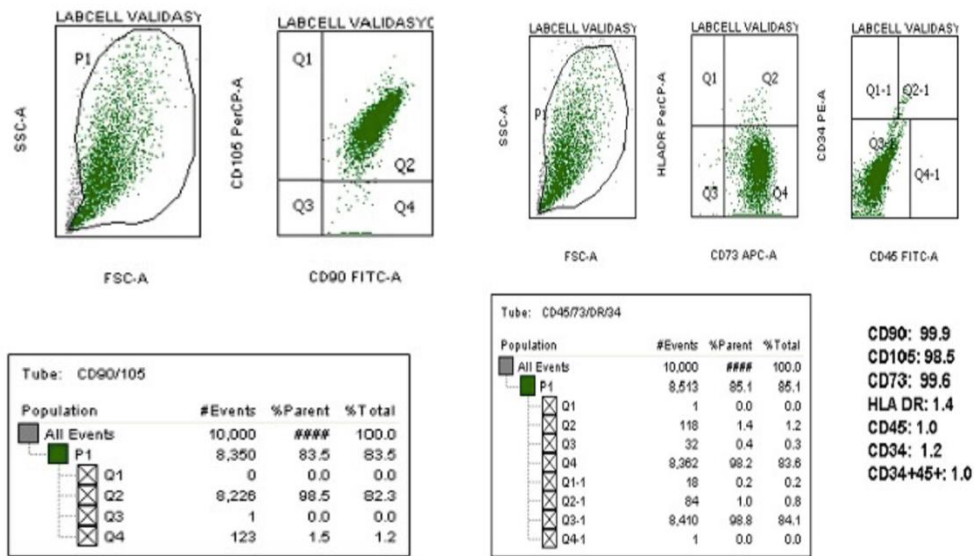


Figure 4.1 Representative flow cytometry analysis of BMMSC marker expressions of Donor 1

Table 4.1 Flow cytometry analysis of BMMSC marker expressions of Donors

	CD90	CD105	CD73	HLA-DR	CD34	CD45
Donor1	99,9	98,5	99,6	1,4	1,2	1,0
Donor2	99,8	99,5	99,3	0,1	0,7	0,1
Donor3	99,9	99,9	99,3	0,2	0,4	0,1

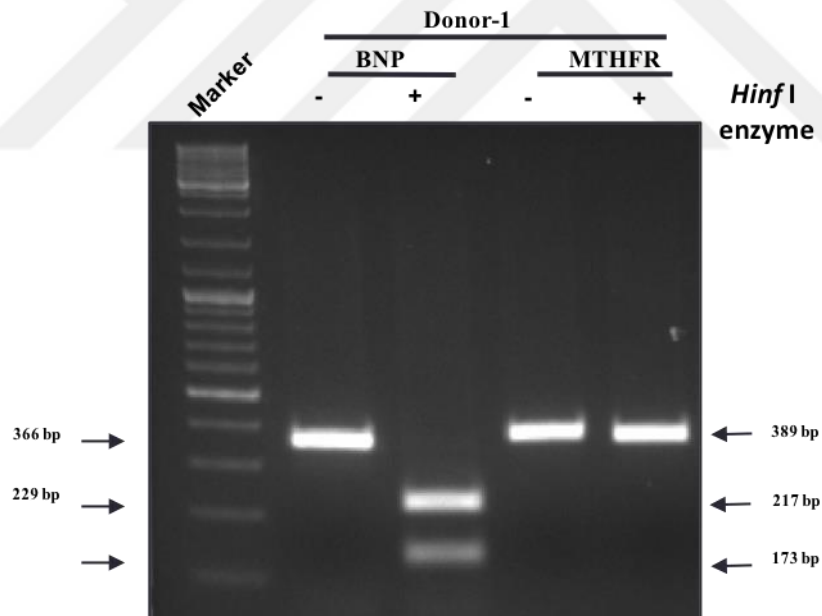
4.2 Evaluating the Effect of C677T Polymorphism on Mesenchymal Stem Cell Properties

4.2.1 Genotyping of the BMMSCs

In order to determine the genotypes of the BMMSCs, restriction fragment length polymorphism (RFLP) assay was applied to the cells. The C677T mutation in *MTHFR* gene, generates a restriction site for *Hinf*I restriction enzyme (5'- GANTC-

3'). That is why the SNP region was first amplified by PCR and then digested with *Hinf* I to identify homozygous (T/T) , heterozygous(C/T) and wild type (C/C) donors. The expected PCR product size for the amplified *MTHFR* gene region is 389 base pairs and *Hinf* I digests this product into two fragments having the size of 173 bp and 217 bp if C677T SNP is present. For this reason, after the enzyme treatment the expected band sizes for wild type is 1 band sized 389bp, for homozygous 2 bands sized 173 bp and 217 bp and for heterozygous 3 bands sized 173 bp, 217 bp and 389bp. Also in this assay, *BNP* gene PCR amplicon (366 base pairs) was used as a control since this region has a *Hinf* I digest site and is suitable to use in RFLP assay to test the efficiency of the enzyme. *BNP* PCR product is 366 bp and when treated with *Hinf* I, two fragments are observed at the size of 137 base pairs and 229 base pairs.

A



B

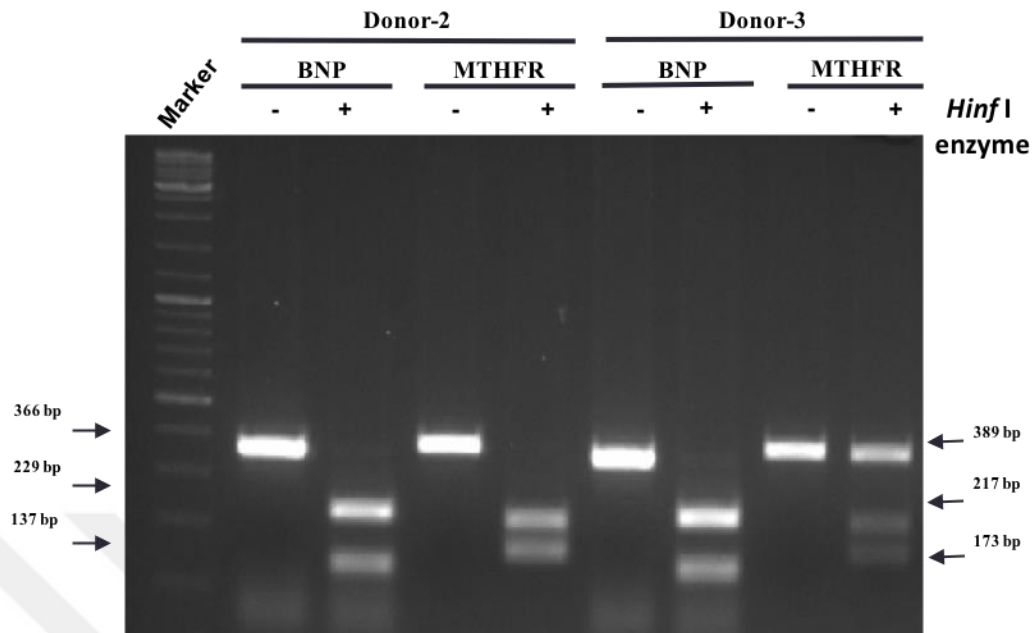


Figure 4.2 RFLP assays of hBM-MSCs **A**) isolated from Donor 1, **B**) isolated from Donor 2 and Donor 3, respectively

As a result of these assays (**Figure 4.2**), the BMMSCs taken from Donor-1 (**Figure 4.2 A**) was identified as wild type (C/C), BMMSCs taken from Donor-2 (**Figure 4.2 B**) was identified as homozygous (T/T) and BMMSCs taken from Donor-3 (**Figure 4.2 B**) was selected as heterozygous (C/T) to be used in the studies conducted to evaluate the effect of C677T polymorphism on MSC properties.

4.2.2 The effect of *MTHFR* C677T polymorphism on BMMSC morphology

After genotyping, the BMMSCs were seeded in to 10 cm tissue culture plates covered with gelatin to investigate their morphological properties *in vitro* and cultured in a humidified incubator as described before. 3 population doublings (PD) were performed with these cells and each passage was performed at the same time for all three donors' BMMSCs. Our results revealed that *MTHFR* C677T polymorphism did not have any observable effects on the morphology of the cells under these conditions (**Figure 4.3**).

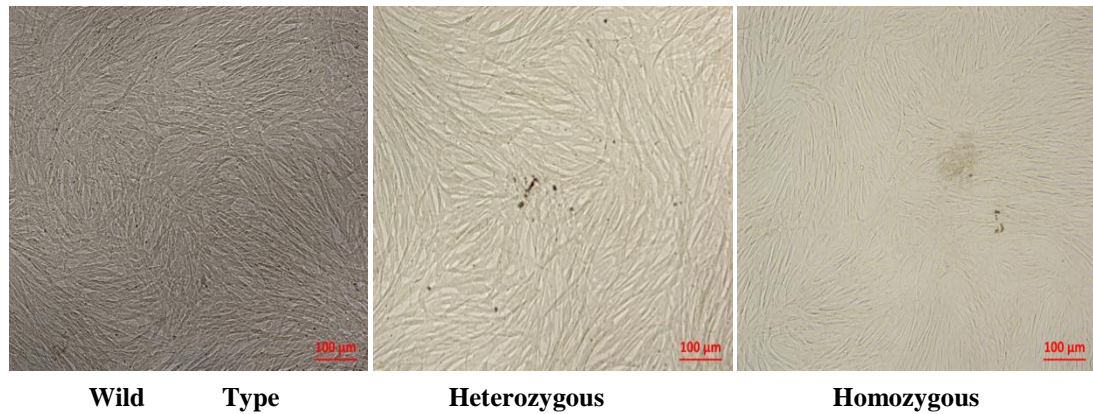


Figure 4.3 Bright field microscopy images of first passage A) wild type, B) heterozygous and C) homozygous BMMSCs

4.2.3 The effect of *MTHFR* C677T polymorphism on differentiation of BMMSCs

Multipotency is a very important feature for MSC regenerative capacities. For this reason, the effect of *MTHFR* C677T polymorphism on BMMSC differentiation potential was investigated by performing adipogenic, osteogenic and chondrogenic differentiation protocols.

4.2.3.1 Adipogenic differentiation

The cells were treated with Stem Pro Adipogenic differentiation medium to induce adipocyte differentiation for 21 days and stained with Oil Red O to visualize the lipid droplets. Lipid droplets were observed (**Figure 4.4 A, B and C**) at all BMMSCs regardless of their genotypes.

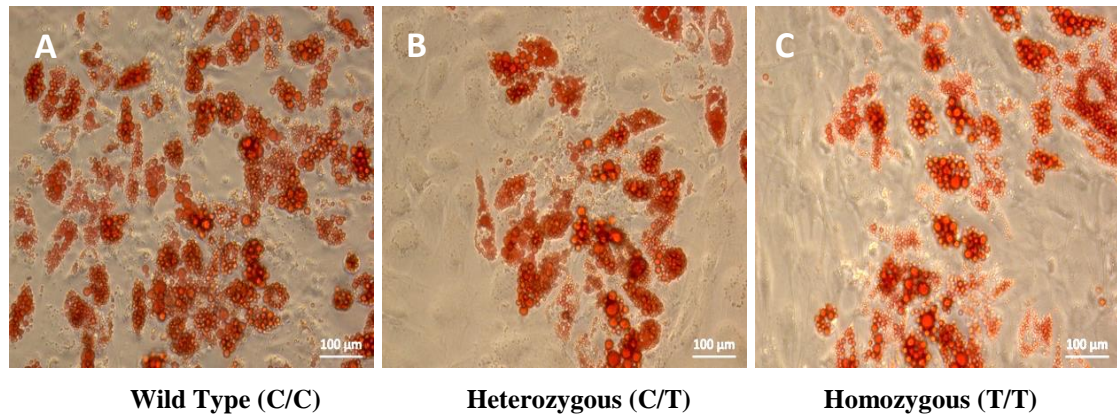


Figure 4.4 Lipid droplets observed after Oil Red O staining of A) wild type, B) heterozygous, C) homozygous differentiated cells, respectively

However, the differentiation potential of each genotype was different. The adipocytic differentiation capacity of the BMMSCs were seem to decrease with the presence of the SNP (Figure 4.5 and 4.6) So that when compared with the wild type heterozygous and homozygous BMMSCs had lower differentiation capacity. These results can be interpreted as, C677T SNP on MTHFR gene may have an effect on adipogenic differentiation capacity of BM-MSCs.

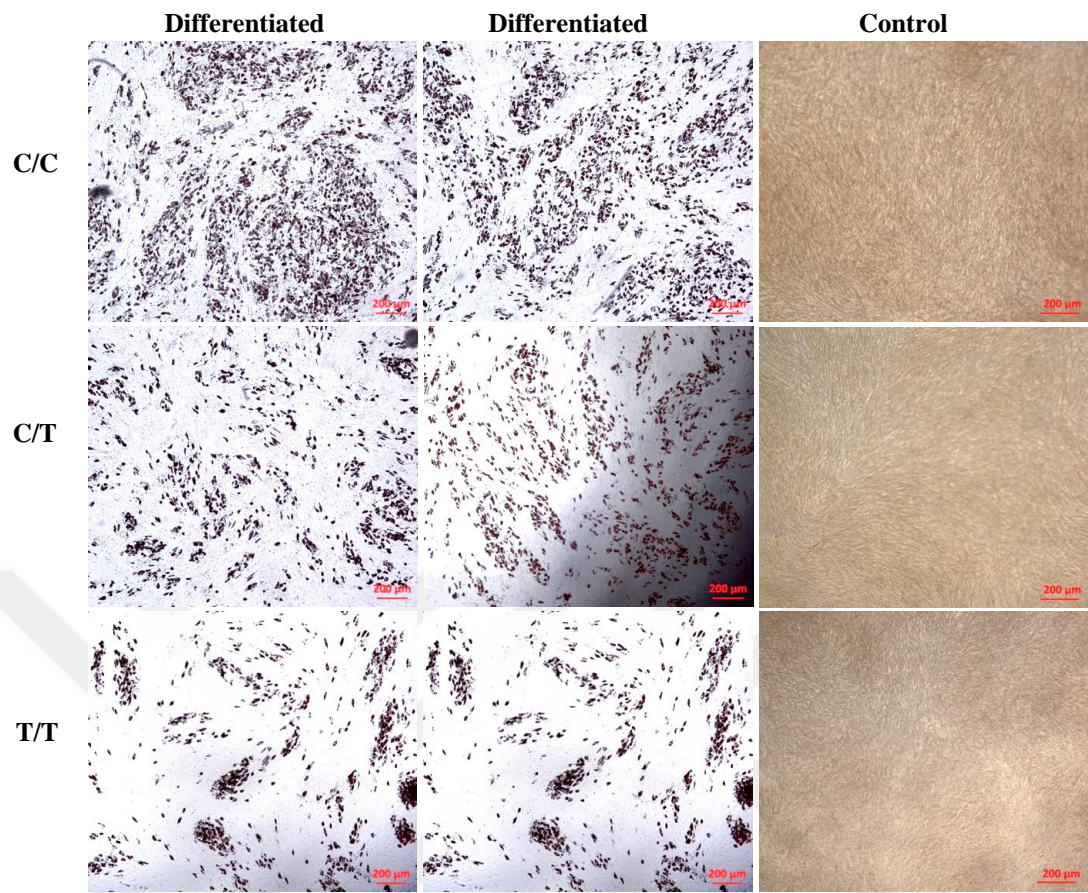


Figure 4.5 Adipogenic differentiation of BMMSCs from all genotypes determined by Oil Red O staining. Undifferentiated BMMSCs were stained and used as a control.

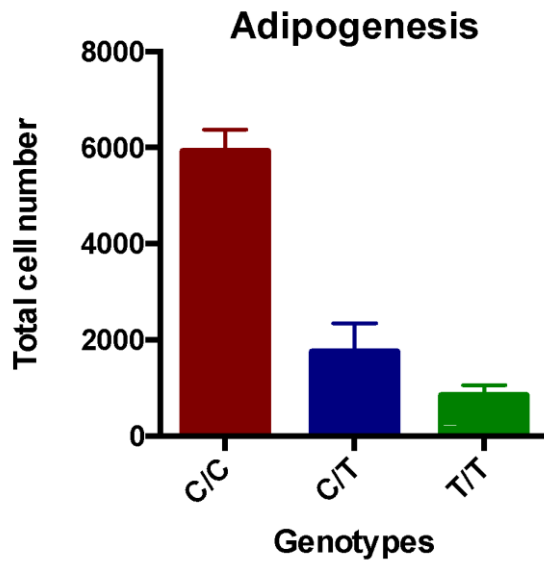


Figure 4.6 Comparison of adipogenic differentiation capabilities between three genotypes. According to ordinary one-way ANOVA test, differences among means statistically significant ($P < 0.05$) ($P < 0.0001$) (****)

4.2.3.2 Osteogenic differentiation

The cells were treated with Stem Pro Osteogenic differentiation medium to induce osteocyte differentiation for 21 days and stained with Alizarin Red to visualize the calcium deposits. Calcium deposits were observed (**Figure 4.7 A, B and C**) in all BMSCs regardless of their genotypes although at different levels.

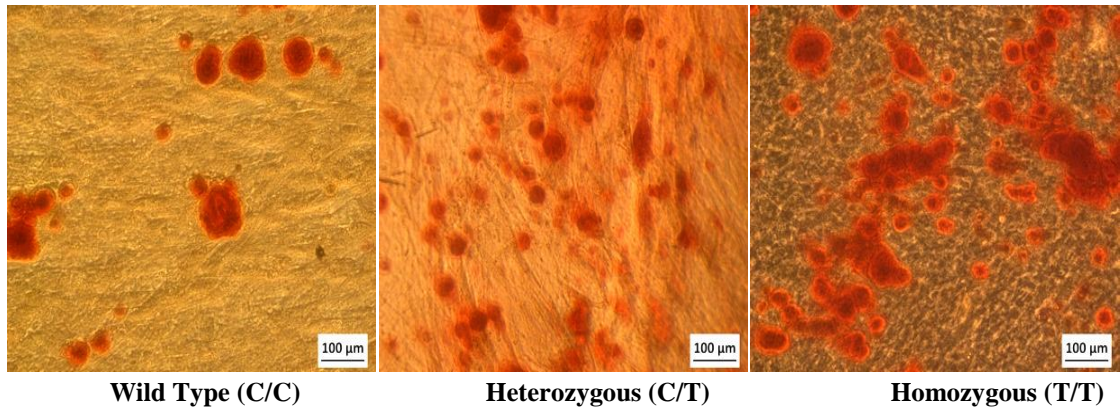


Figure 4.7 Calcium deposits observed after Alizarin red staining of A) wild type, B) heterozygous, C) homozygous differentiated cells, respectively

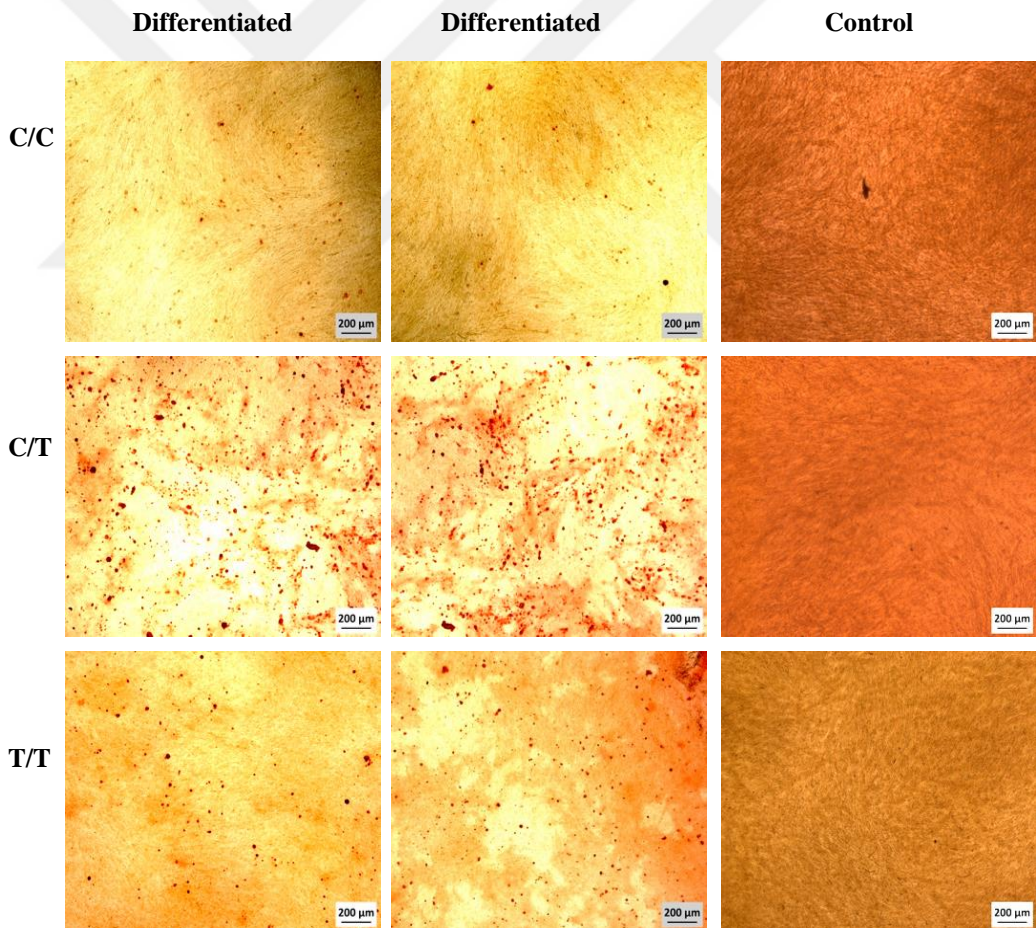


Figure 4.8 Osteogenic differentiation of BMMSCs from all genotypes determined by Alizarin Red staining. Undifferentiated BMMSCs were stained and used as a control.

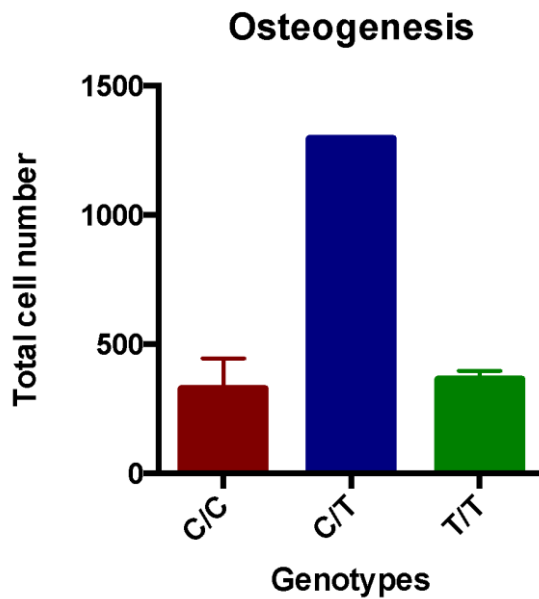


Figure 4.9 Comparison of osteogenic differentiation capabilities between three genotypes. According to ordinary one-way ANOVA test, differences among means statistically significant ($P < 0.05$) ($P = 0.0001$)(***)

The differentiation potential of each genotype was different in terms of their efficiency to form osteocytes, heterozygous BMMSCs have the highest differentiation capacity (**Figure 4.8 and 4.9**) among all genotypes. These results can be interpreted that, C677T SNP on *MTHFR* gene may have an affect on osteogenic differentiation capacity of BMMSCs.

4.2.3.3 Chondrogenic differentiation

For chondrogenesis, cells were cultured as micro masses and differentiation was induced by using chondrogenic differentiation medium(Stem Pro). Firstly, cells were seeded on non-coated tissue culture plates, and, after 24 hours, they formed 3D aggregates floating in medium in homozygous and wild type cells. However the cells needed to attach to the surface for differentiation. For that reason, aggregates were

transferred into plates coated with gelatin and induced to become chondrocytes for 21 days. After 21 days of differentiation, it was seen that, there were no viable cell in heterozygous and control (undifferentiated BMMSCs) plates. Aggregates were observed only with the wild type and the homozygous BMMSC samples. (**Figure 4.10 B**) (**Figure 4.10 A**)

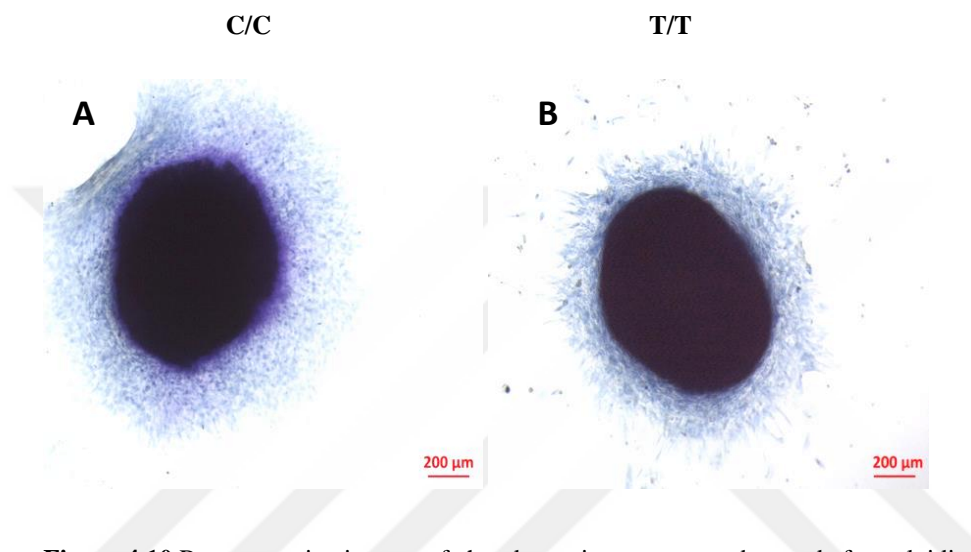


Figure 4.10 Representative images of chondrogenic aggregates observed after toluidine blue staining of A) differentiated wild type cells, B) differentiated homozygous cells, respectively

According to our observations the chondrogenic differentiation potential of BMMSCs does not change with the presence of the homozygous mutation. However as the heterozygous (C/T) cells died and the differentiation potential of each genotype can be different (**Figure 4.10**).

4.3 Introducing the *MTHFR* gene C677T polymorphism to HEK293T cells with CRISPR/Cas9 gene editing system

4.3.1 Transient transfection of HEK293T cells

Since the introduced SNP to *MTHFR* gene will affect the MTHFR enzyme activity, and betaine is a methyl donor for the conversion of homocysteine to methionine in the homocysteine pathway. For this reason, betaine supplement should be added to medium to rescue T/T mutant cells. Because, Firstly, because the growth medium contained betaine, it was highly important to evaluate the effect of betaine on transfection efficiency. In order to evaluate that, HEK293T cells were transfected with pSpCas9(BB)-2A-GFP (PX458) vector, which carries a GFP marker cDNA, by using PEI reagent in a ratio of 1:3 (DNA:PEI ratio in weight) in two conditions: with or without 10mM betaine (final concentration). After the transfection, GFP expression of HEK293T cells were investigated under fluorescent microscope using appropriate filters (**Figure 4.11**).

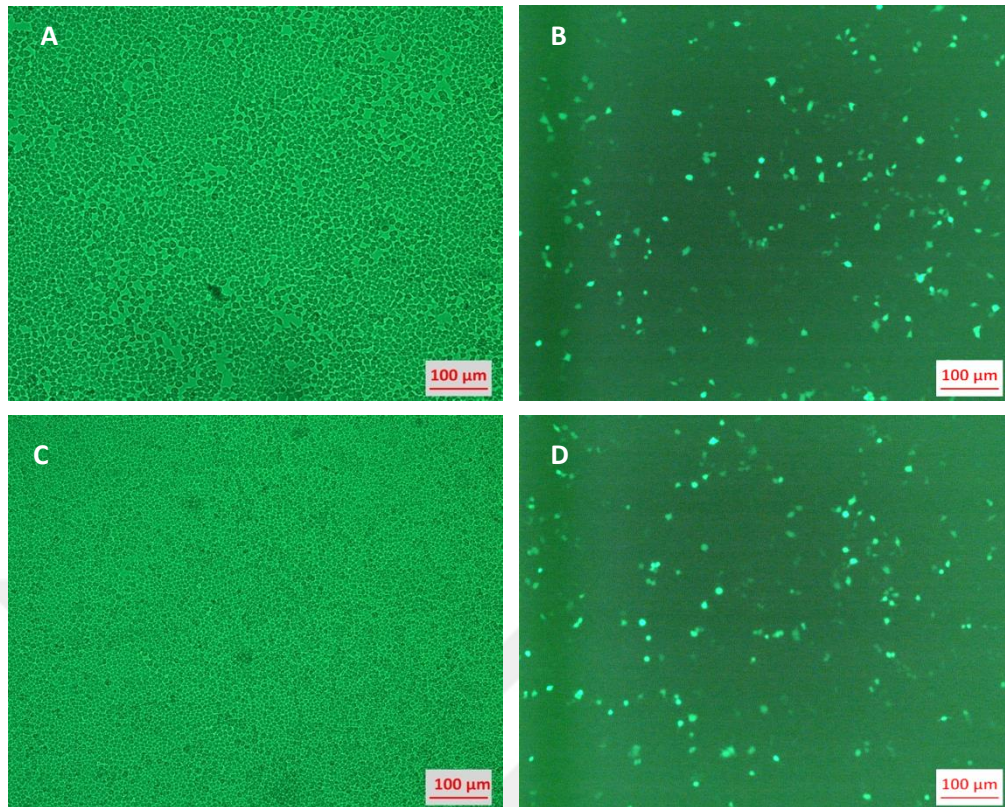


Figure 4.11 Fluorescent microscopy images of HEK293T cells transfected by using PEI 1:3 with PX458 vector A) and B) incubated in DMEM (with 10%FBS) (bright field), C) and D) incubated in DMEM(with 10% FBS) containing 10 mM betain.

Since the transfection of the cells were done simultaneously, GFP⁺ cells also indicates the transfection efficiency and not much difference was observed among samples having different media contents. However, the efficiency of the transfection in two conditions were still not as high as expected

Introducing ssODN mediated *MTHFR* targeted modification requires co-transfection of the designed ssODN together with with pSpCas9(BB)-2A-PURO (PX459) carrying the designed sgRNA sequence into the corresponding cells.. In that purpose, HEK293T cells were transfected with pSpCas9(BB)-2A-GFP (PX458) vector and ssODN by using PEIMAX in a ratio of 1:4 (DNA:PEI ratio in weight) (**Figure 4.11 A and B**). GFP positive cells were observed after 24h with fluorescent microscopy. (**Figure 4.12**)

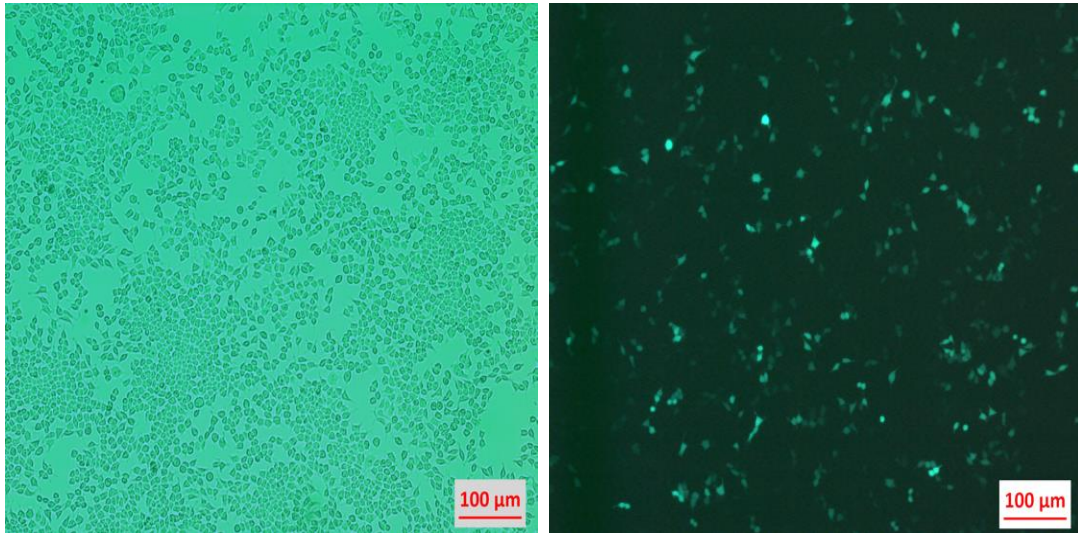


Figure 4.12 Fluorescent microscopy images of A) bright field, B)transfected HEK293T cells transfected with PX458 vector and 1.85 µg of ssODN by using PEIMax in a ratio of 1:4

As higher number of GFP expressing cells were obtained after transfection with pSpCas9(BB)-2A-GFP (PX458) vector by using PEIMAX with a ratio of 1:4 (**Figure 4.12 B**) than PEI with a ratio of 1:3 (**Figure 4.11 B**), using PEIMAX in 1:4 ratio was selected to be continued for transfection of HEK293T cells.

After necessary optimization studies mentioned above, HEK293T cells were seeded into two plates in DMEM (10% FBS) containing 10 mM betain and the cells in one of the plate were transfected with the vector pSpCas9(BB)-2A-PURO (PX459) carrying *MTHFR* sgRNA and 1.85 µg ssODN in 10 cm cell plate. In order to evaluate the transfection efficiency, a separate plate was transfected with pSpCas9(BB)-2A-GFP (PX458) vector. Both transfections were performed at optimized conditions with PEIMax 1:4, simultaneously. GFP positive cells were observed after 24h with fluorescent microscopy (**Figure 4.13 B**).

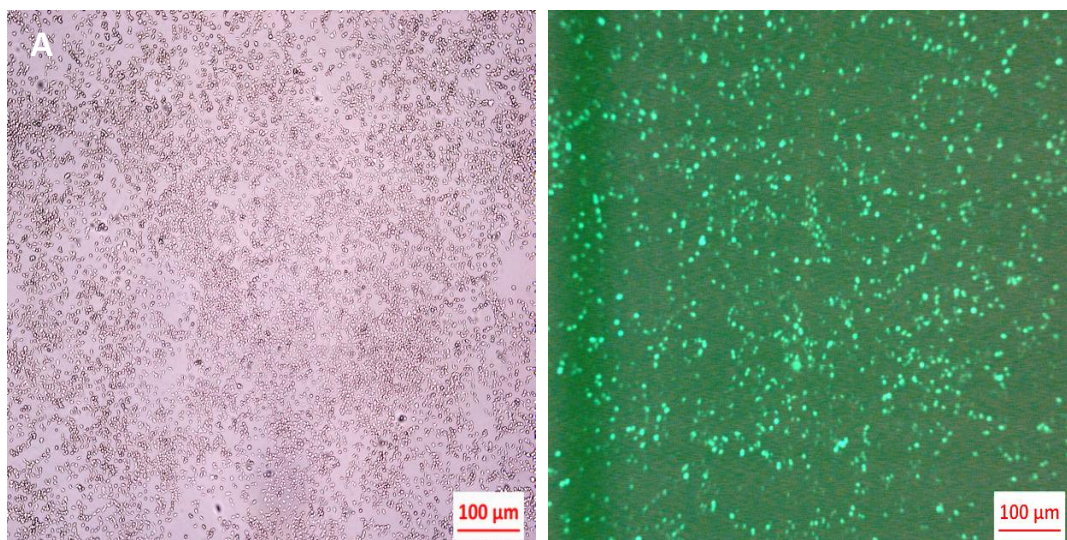


Figure 4.13 Fluorescent microscopy images of A) bright field, B)transfected HEK293T cells transfected with pSpCas9(BB)-2A-GFP (PX458) vector by using PEI_{Max} 1:4.

Florescent microscopy images of GFP positive cells indicate that approximately 80% of the cells were transfected with pSpCas9(BB)-2A-GFP (PX458) vector (**Figure 4.13**). It was assumed that approximately the same percent of the cells were transfected with pSpCas9(BB)-2A-PURO (PX459) -*MTHFR* sgRNA vector. In order to select transfected cells puromycin selection was applied to both plates until all the cells transfected with pSpCas9(BB)-2A-GFP (PX458) vector were death. pSpCas9(BB)-2A-PURO (PX459) vector contains puromycin resistance gene while pSpCas9(BB)-2A-GFP (PX458) vector does not. That is was gfp expressing cells are expected to die under puromycin selection. This serves as a control for the success of the selection. After the puromycin selection, remaining cells were accepted as cells carrying the pSpCas9(BB)-2A-PURO (PX459).

4.3.2 Genotyping of the mutant HEK 293T colonies with RFLP

When the CRISPR/Cas9 plasmids are transfected into the cells, a heterogeneous population is created, in which there might be cells that do the desired genomic

modification or cells that do unexpected genomic modifications or cells that do not do any genomic modifications. Therefore, in the aforementioned transection, HEK293T cells had to be seeded as single cells to select the cell clones that had the desired genomic modification. Single cells were grown as colonies approximately for 3 weeks in the wells of 96-well plate. During this period, betain supplement was always available for the cells. 20 colonies were survived. Genotyping of these colonies were performed by RFLP assay to separate them as wild type (C/C), homozygous (T/T) and heterozygous (C/T) colonies. The gene editing system transfected to the HEK293T cells was designed to create a DNA break at the specific point of the *MTHFR* gene region and it was expected that this DNA break will be repaired using by ssODN as the template DNA, cotransfected to the cells. If this break will repaired in both alleles, homozygous alleles (T/T) will be obtained, however if one of the alleles is repaired by HDR, heterozygous cells (C/T) will be obtained and unaffected colonies will appear as wild type. In addition to that, some colonies might present a genotype having random mutations (insertions/deletions - indels) due to NHEJ. The C677T mutation on *MTHFR* gene generates a restriction site for *Hinf* I. That is why the genomic locus surrounding the targeted SNP region was first amplified by PCR and then the PCR product was digested with *Hinf* I. The expected PCR product size for the amplified *MTHFR* gene region is 389 base pairs and *Hinf* I digests this product into two fragments having the size of 173 bp and 217 bp if C677T SNP is present. For this reason, after the enzyme treatment the expected band sizes for homozygous 2 bands sized 173 bp and 217 bp and for heterozygous 3 bands sized 173 bp, 217 bp and 389bp. Also in this assay, *BNP* gene PCR amplicon (366 base pairs) was used as a control since this region has a *Hinf* I digest site and is suitable to use in RFLP assay to test the cutting efficiency of the enzyme. *BNP* PCR product is 366 bp and when digested with *Hinf* I, two fragments are observed at the size of 137 base pairs and 229 base pairs. (Figure 4.14)

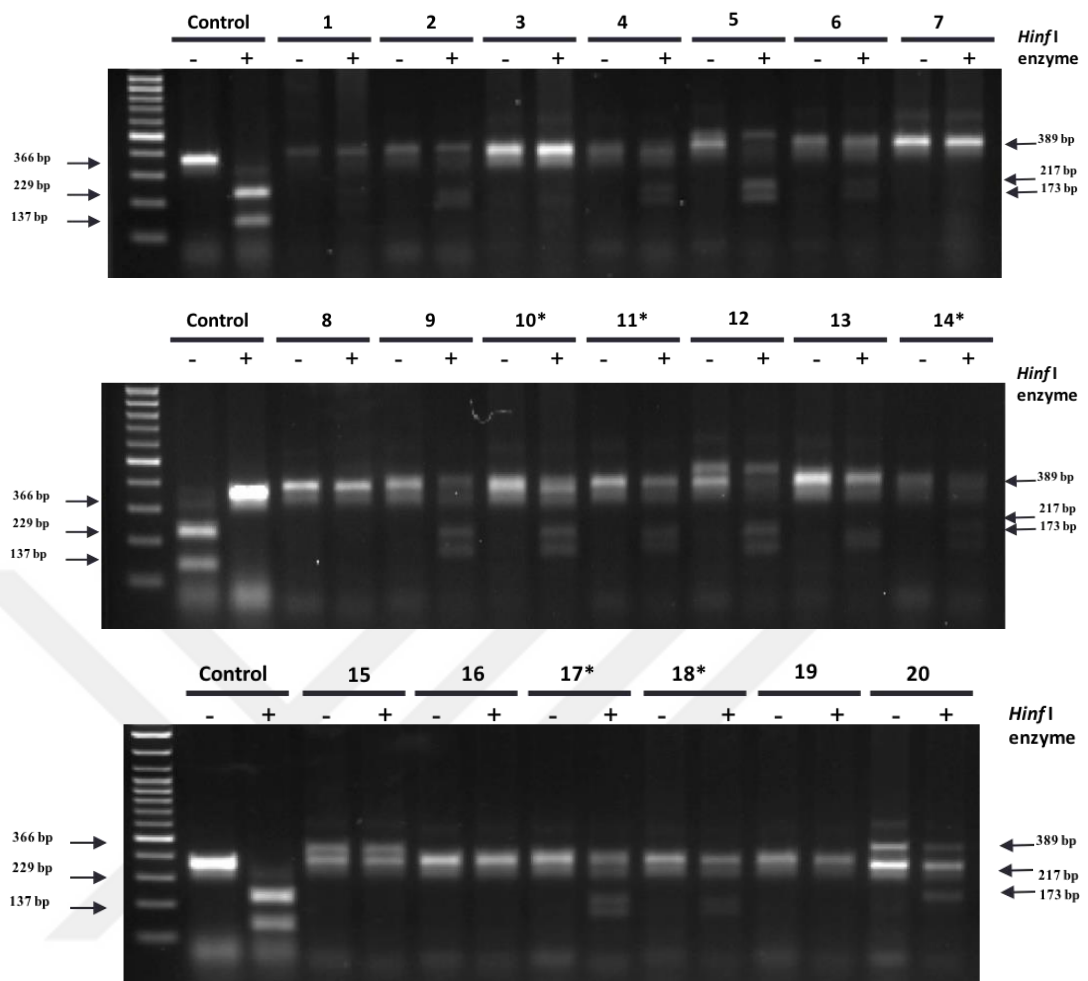


Figure 4.14 Genotyping results of mutant HEK293T colonies by RFLP assay. Possible heterozygous colonies (C/T) were indicated by the star(*). Control indicates *BNP* gene PCR amplicon.

The genotyping results of transfected colonies indicated that, in the group of 20 colonies, only five of them (colony number 10, 11, 14, 17 and 18) were chosen as possible heterozygous colonies (C/T) according to their RFLP assay results as one of their alleles was repaired by HDR and the other allele stayed as the same (**Figure 4.14**). Regarding the band numbers and sizes, some of the colonies (Colony number 5, 9 and 20), represented both HDR and NHEJ upon CRISPR/Cas9 engineering.

The transfection of HEK293T cells yielded with only heterozygous mutants rather than homozygous mutants. Furthermore, after the transfection, only 20 colonies were survived, grown and screened. This indicates that the survival capacity of the colonies was highly decreased after the transfection. Moreover, the growing rates of the colonies were highly slow compared to wild type HEK293T cells.

4.3.3 Genotyping of the mutant HEK 293T colonies with T7 endonuclease1 assay

After the genotyping, successfully transfected colonies were chosen and possibly heterozygous colonies were seeded and grown for further investigations. However before going further, *MTHFR* region was amplified by PCR and T7E1 assay was applied to two possibly heterozygous mutants (colony number 10 and 17) and also the pool of the cells obtained after transfection. This assay was applied in order to be sure that the chosen colonies were heterozygous and also, SpCas9 of the PX459 vector used in the transfection works fully (**Figure 4.15**).

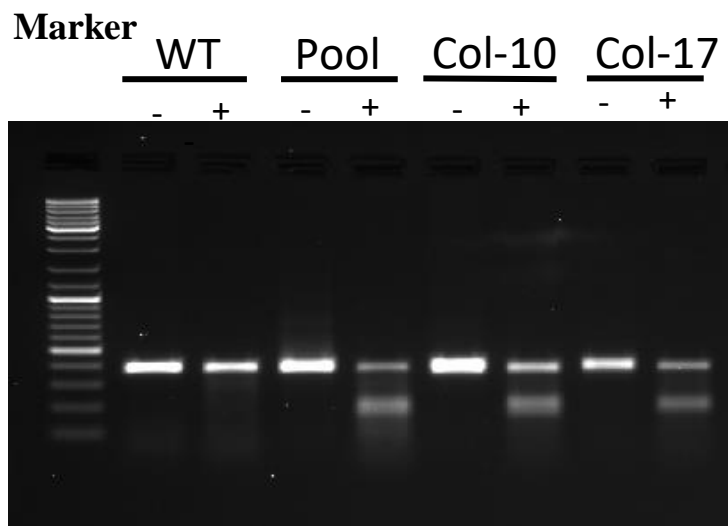


Figure 4.15 T7E1 assay of pool of transfected cell and two heterozygous (C/T) colonies (Colony 10 and 17). Untransfected Hek293T cells were used as a control (WT).

In T7E1 assay, T7 endonuclease recognizes and cleaves non perfectly annealed DNA complementary strands. When the *MTHFR* PCR product was incubated with T7 endonuclease, it cleaved from the positions mismatches/indels from NHEJ repair. It was seen that, there was mismatches for pool and heterozygous colonies compared to wild type (**Figure 4.15**). Thus, the cleavage was effective proved that, chosen colonies were heterozygous and also, SpCas9 of the PX459 vector used in the transfection works fully.

4.4 Introducing the *MTHFR* C677T polymorphism to BMMSCs by using CRISPR/Cas9 gene editing system

4.4.1 Optimization of transfection of BMMSCs

It was seen that C677T mutation in *MTHFR* can change the differentiation capacities and multipotency of BMMSCs isolated from different donors (**Figure 4.5, 4.8, 4.10**). On the other hand the cells bear different genetic backgrounds and it can be an important factor affecting the differentiation potentials of the cells. In order to eliminate the effect of genetic background and better understand the effect of the SNP on the differentiation potentials of BMMSCs, the designed CRISPR/Cas9 gene editing system, which was shown to work on HEK293T cells, was also used for BMMSCs (**Figure 4.13**). Moreover, although previous experiments showed that, PEI_{Max} in a ratio of 1:4 is the best transfection agent for HEK293T cells (**Figure 4.13**), MSCs and HEK293T cells have different cell properties. That is why different transfection methods were investigated on BMMSCs

Firstly, electroporation with different conditions was used to transfect the vector and ssODN to the BMMSCs however, cells were death right after transfection. So, it was decided that electroporation was not a suitable way to transfect primary BMMSCs

isolated from adults. Moreover, BMMSCs were transfected with pSpCas9(BB)-2A-GFP (PX458) vector by using Lipofectamine with different DNA:Lipofectamine ratios (in weight) in order to find the optimum transfection efficiency with the lowest number of dead cells possible. 24 h and 48 h after the transfection, GFP expression of BMMSCs were investigated under fluorescent microscope to assess the transfection efficiency (**Figure 4.16**).

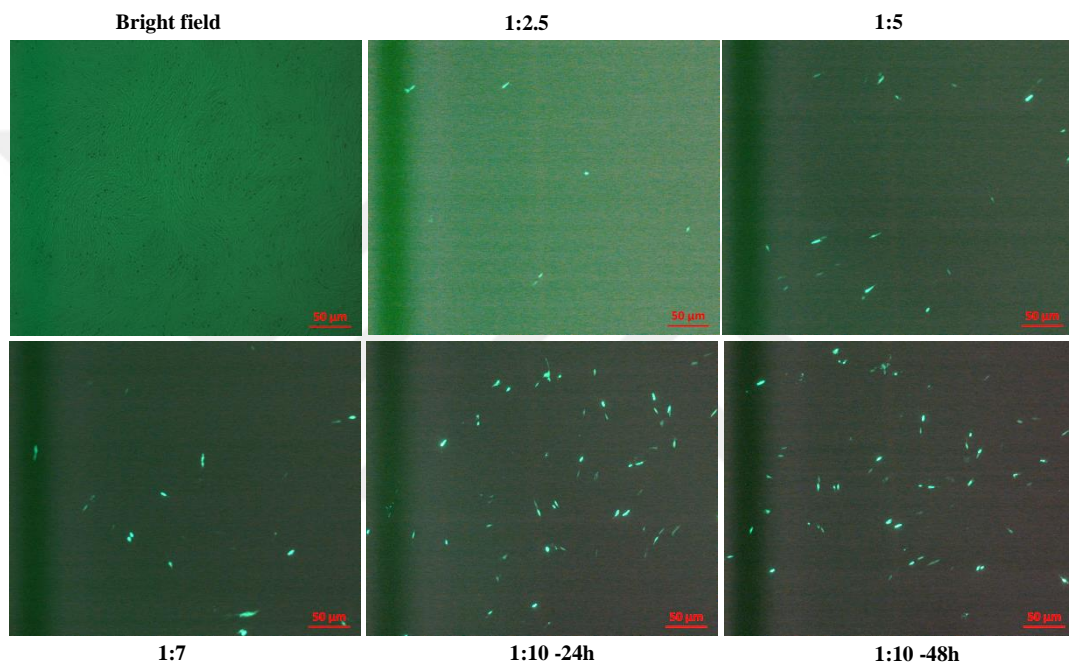


Figure 4.16 Fluorescent microscopy images of BMMSCs transfected with PX458 vector by using Lipofectamine with different lipofectamine:DNA amount ratio; A) bright field image of the cells, B) the GFP expression of the GFP⁺ cells 24 hours after transfected with Lipofectamine by using ratio of 1:2.5 C) the GFP expression of the GFP⁺ cells 24 hours after transfected with Lipofectamine, 1:5, D) the GFP expression of the GFP⁺ cells 24 hours after transfected with Lipofectamine, 1:7, E) the GFP expression of the GFP⁺ cells 24 hours after transfected with Lipofectamine, 1:10, F) the GFP expression of the GFP⁺ cells 48 hours after transfected with Lipofectamine by using ratio of 1:10 as DNA:Lipofectamine.

Highest number of GFP expressing cells were observed 48 hours after transfection with Lipofectamine at a ratio of 1:10 (**Figure 4.16 F**) when compared with the other ratios (1:2.5, 1:5, 1:7). However, Lipofectamine was toxic to BMMSCs and most of the cells died after the transfection.

BMMSCs were then transfected with pSpCas9(BB)-2A-GFP (PX458) vector by different PEI_{Max} ratios (**Figure 4.17 A and B**) Moreover Chloroquine addition to transfection medium was also investigated (**Figure 4.17 C and D**), since it was shown to increase the transfection efficiency up to 20 folds for Chinese hamster ovary (CHO) cells [100].

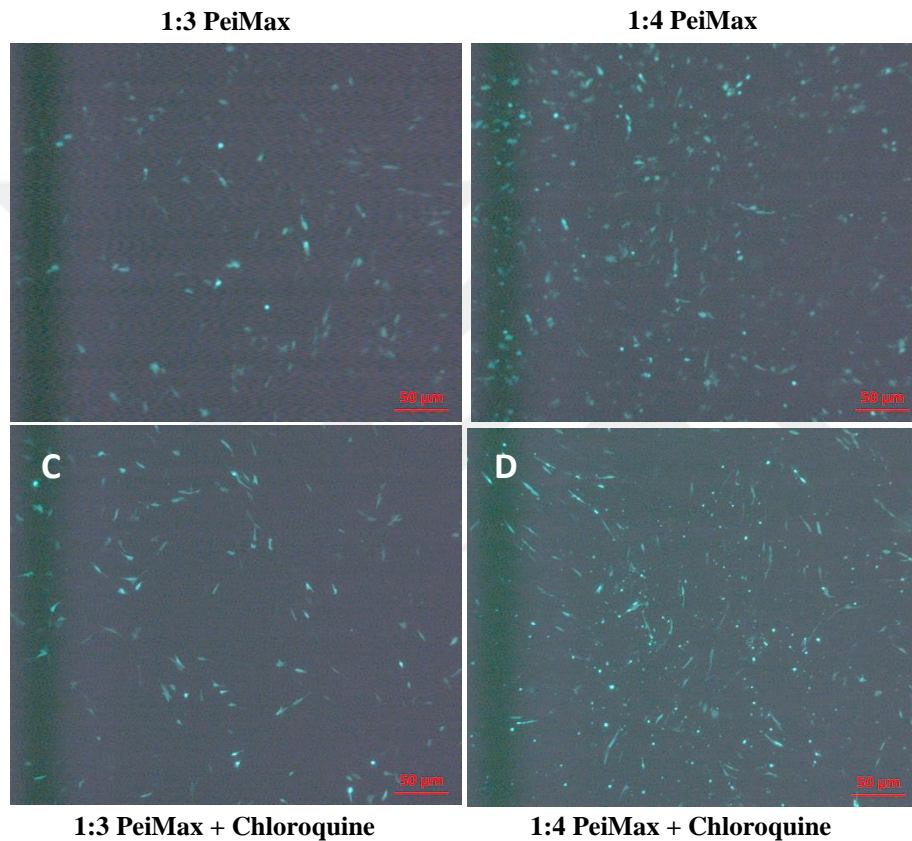


Figure 4.17 Fluorescent microscopy images of BMMSCs transfected with PX458 vector by using; A) PEI_{Max} with the ratio of 1:3, B) PEI_{Max} with the ratio of 1:4, C) PEI_{Max} with the ratio of 1:3 in a medium containing chloroquine D) PEI_{Max} with the ratio of 1:4 in a medium containing chloroquine

Higher number of GFP positive cells were obtained after transfection with pSpCas9(BB)-2A-GFP (PX458) vector by using PEI_{Max} in a ratio of 1:4 (in weight) (**Figure 4.17 B**) with lowest number dead cells. In addition, contrary to the information in the literature [100], using chloroquine in the transfection medium did not increase transfection efficiency on BMMSCs (**Figure 4.17 D**) according to our

observations. It may be because of the unique characteristics of BMMSCs or the concentration of chloroquine was not optimal.

The pSpCas9(BB)-2A-PURO (PX459) vector contains puromycin resistance gene. For this, optimum concentration and application time range of puromycin for the selection of the transfected colonies are highly important. Excess amount of puromycin in the medium can be toxic by causing stress and leading apoptosis. On the other hand, less amount of puromycin will not be enough to identify and select the mutant colonies after transient transfection. Because of these reasons, BMMSCs were treated with different puromycin concentrations for a period of time until nearly all cells died. Medium was changed with fresh medium containing puromycin and cells were observed under light microscope (**Figure 4.18**) and a death curve for puromycin was plotted (**Figure 4.19**).

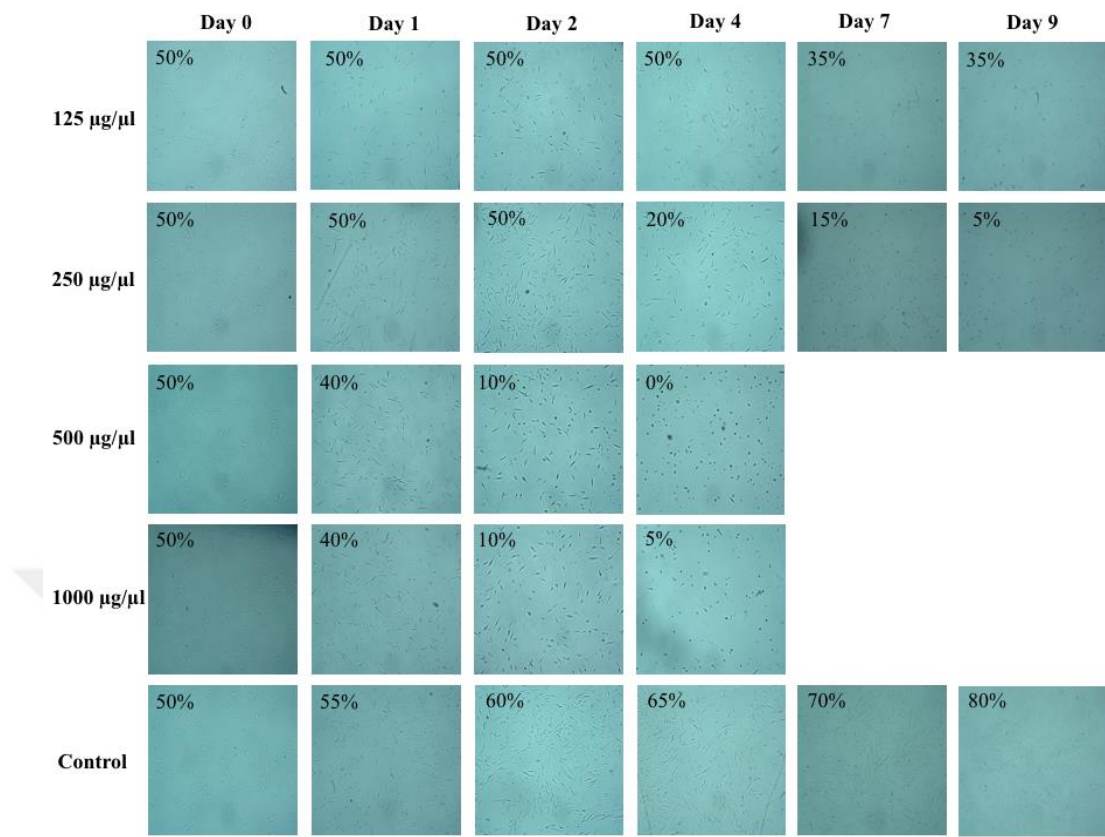


Figure 4.18 Bright field images of BMMSCs treated with different puromycin concentrations. Concentration of the puromycin used in the selection medium, the time range of the application and confluences of the cells were indicated.

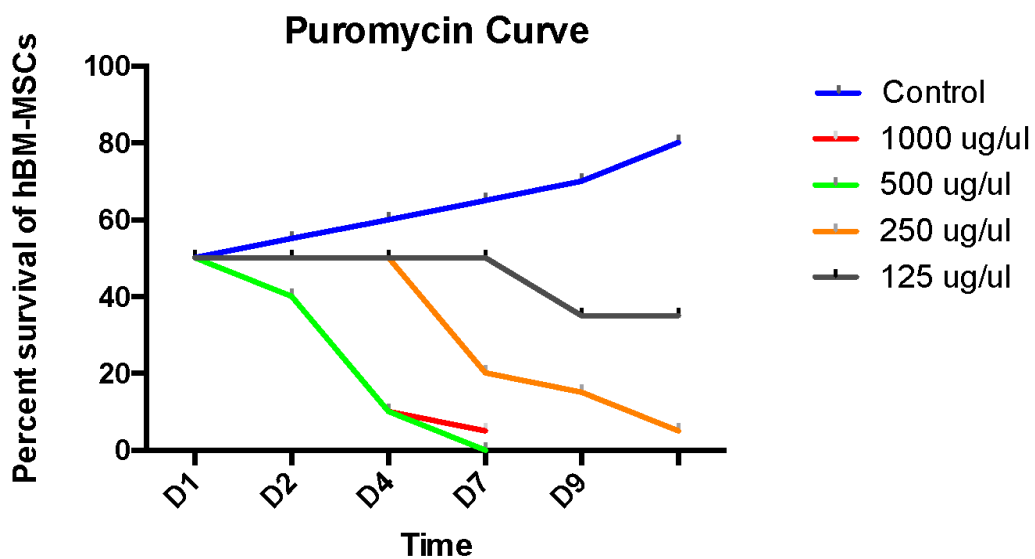


Figure 4.19 Puromycin resistance death curve of BMMSCs

It was seen from the puromycin death curve (**Figure 4.19**) that using 500 $\mu\text{g}/\mu\text{l}$ puromycin for the selection of mutant colonies for 2 days was enough for BMMSCs when it compared to 100 $\mu\text{g}/\mu\text{l}$, excess amount of that concentration can be toxic for these cells.

4.4.2 Transient transfection of BMMSCs with the CRISPR/Cas9 system

After all the necessary optimization studies were performed, BMMSCs were seeded into two plates and the cells in one of the plates were transfected with pSpCas9(BB)-2A-PURO (PX459) -MTHFRsgRNA vector and ssODN. The cells in second plate were transfected with pSpCas9(BB)-2A-GFP (PX458) vector. Both transfections were performed with PEIMax 1:4, simultaneously and GFP positive cells were observed after 24h with fluorescent microscopy (**Figure 4.20 B**).

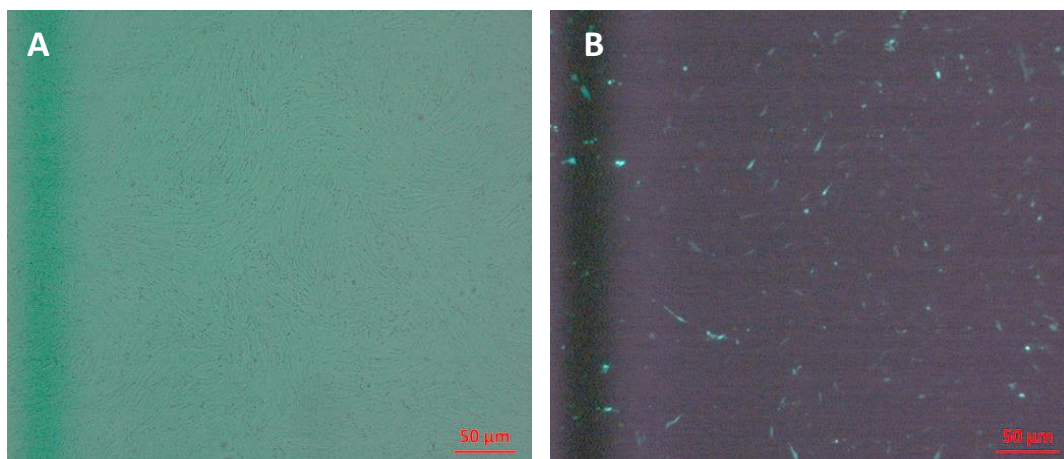


Figure 4.20 Fluorescent microscopy images of A) bright field, B)transfected BMMSCs transfected with PX458 vector by using PEIMax 1:4

Florescent microscopy images of the GFP positive cells indicated that approximately 50% of the cells were transfected with pSpCas9(BB)-2A-GFP (PX458) vector (**Figure 4.20 B**). That can be interpreted that, approximately same percent of the cells were transfected with pSpCas9(BB)-2A-PURO (PX459) carrying the sgRNA for MTHFR SNP region. Afterwards, transfected cells were selected with 500 µg/µl puromycin for 4 days. After the puromycin selection, the confluency of the pSpCas9(BB)-2A-PURO (PX459) MTHFR sgRNA transfected plate was approximately 40%. The selected cells were trypsinized and some of the cells were separated for T7 endonuclease assay (T7E1) and the rest of the cells were seeded to 96 well plates for single colonies.

The result of the BMMSC T7 endonuclease assay is presented at (**Figure 4.21 A, B**). Previously created CRISPR/Cas9 MTHFR sgRNA transfected HEK293T pool gDNA was used as a positive control of T7E1. Another control of the assay was PCR derived from C/T BMMSCs gDNA, however, T7E1 did not work as efficiently for this sample. For this reason, we compared our T7E1 results of all BMMSC samples among each other but not with HEK293T. When wild type BMMSC T7E1 digested bands were observed, a very clean neat undigested MTHFR band at the expected size was seen. However, when CRISPR/Cas9 transfected BMMSC T7E1 band is compared with untransfected wild type band, there a smear was observed underneath

the main band. Furthermore, this smear is also present at the T7E1 digested bands of C/T and T/T samples. Observing such a smear was not expected at T/T samples however our interpretation is the presence of other SNPs at the same region of the amplified PCR product.

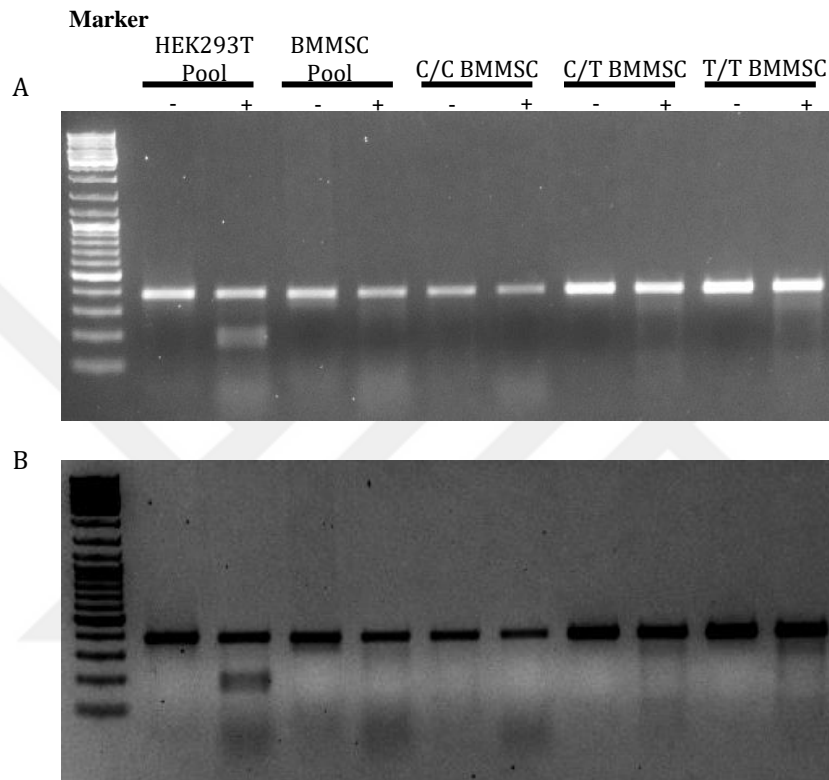


Figure 4.21 T7E1 assay of BMMSCs A) T7E1 assay of pool of transfected HEK293T cells, pool of transfected BMMSCs, wild type, heterozygous and homozygous BMMSCs, respectively. B) contrast enhanced image of (A)

In order to obtain single cell clones, remaining cells were seeded into 96 well plates and monitored for 2-3 weeks. However, none of them started proliferating, because they did not survived. Because these cells require survival signals coming from other cells, transfection was repeated, and this time cells were cultured with medium containing 10 μ M Y-27632 which is required for survival. However none of the cells were able to survive out of the single cell cloning.

5 DISCUSSION AND CONCLUSION

When the function of the MTHFR enzyme and its related diseases are considered, it is concluded that, MTHFR is highly important for normal cellular functions for the tissue homeostasis. Accordingly, as adult stem cells have important roles in providing tissue homeostasis, we thought that *MTHFR C677T* polymorphism might be also interfering with the differentiation capacities of BMMSCs. To this end, there is no study investigating the effect of this polymorphism on the differentiation capacities of BMMSCs. For this reason, in this study the effect of *MTHFR C677T* on BMMSCs was investigated.

There are important parameters of MSCs in order to maintain tissue homeostasis. The ability to form colonies *in vitro* that supports hematopoiesis is one of the main features that define MSCs. According to Kuznetsov et al. colony forming efficiency (CFE) values may provide useful insights into bone and bone marrow pathophysiology and CFE was significantly altered in patients with several skeletal and metabolic disorders. Since *MTHFR C677T* has been associated with several skeletal and metabolic dysfunctions, we investigated the morphologic properties of the three genotypes. Our results revealed that *MTHFR C677T* polymorphism did not have any observable effects on the colony forming abilities of the cells and we were able to observe colonies under light microscope. Also, their growth rates were highly similar and all the cells were passaged and treated for all experiments at the same time. That's why it was concluded that, *C677T* SNP on *MTHFR* do not affect growth and phenotypic characters of BMMSCs. However for further experiments and quantitative assays could be performed to better identify these properties.

Moreover, multipotency is a very important feature for MSC regenerative capacities. For this reason, the effect of *MTHFR C677T* polymorphism on BMMSC differentiation potential was also investigated by performing adipogenic, osteogenic

and chondrogenic differentiation protocols. Firstly, all BMMSCs regardless of their genotypes were successfully differentiated into adipocytes, osteocytes and chondrocytes. However, the differentiation potential of each genotype was different.

Adipose tissue is an active endocrine organ, which plays a central role in lipid and glucose metabolisms. Dysfunctions in adipogenesis lead to dysfunctioning adipose tissue which produces a large number of hormones and cytokines that both play important roles in the development of metabolic syndrome, diabetes mellitus, and vascular diseases. According to our results, the adipocytic differentiation capacity of the BMMSCs were seem to decrease with the presence of the SNP, which directs us to think that, C677T *MTHFR* may have an effect on adipogenesis. Furthermore this defect can be linked with the increasing risk of diabetes mellitus and frequently seen cancers in patients having this SNP. According to Yang et al. there is an increased risk seen in the Caucasian populations with type 2 Diabetes having *MTHFR* C677T, also in another study it was demonstrated that C677T significantly associated with diabetes in Arabic population according to Al-Rubeaan et al. and might be a risk genetic factor of Type 2 diabetes mellitus in the Chinese Han population. The association of this polymorphism and diabetes mellitus and its complications were also reported in two studies conducted by Settin et al. and Zhong et al. In addition, adipokines are cytokines (cell signaling proteins) secreted by adipose tissue and dysregulated production or secretion of these adipokines leading to adipose tissue dysfunctions can lead to the pathogenesis of obesity linked complications. Thereby, adipokines produced by the placenta regulate the maternal metabolic adaptation to pregnancy and dysfunction in the production of adipokines. These dysfunctions in the production of adipokines can be the main reason behind the meta-analysis indicating that C677T *MTHFR* is associated with recurrent pregnancy loss (Yang et al.). Furthermore, *MTHFR* C677T is also significantly associated with many psychiatric disorders like Schizophrenia, Bipolar Disorder and Unipolar Depressive Disorder (Gilbody et al. and Peerbooms et al.) There is another study revealing that, *MTHFR* C677T had a significant association with the risk of Parkinson's disease according to Wu et al. And it was also revealed that disturbances in adipokine

secretion are important in the pathogenesis, clinical presentation and outcome of mental disorders. It can be hypothesized that, dysfunctions in adipogenesis causing form C677T can cause these complications, however, further investigations should be done in order to understand the mechanism and prove that hypothesis. Moreover although we have performed three technical replicates for each biological sample our results must be repeated with a higher number of donor cells.

Additionally, the differentiation potential of each genotype was different in terms of their efficiency to form osteocytes and chondrocytes. There are many studies related to bone fracture risks and dysregulated bone mineral density with *MTHFR* C677T. The main reason of this correlation can be related with the altering osteogenesis and chondrogenesis related with the existence of the SNP. Also, altering osteogenic and chondrogenic differentiation capacity of BMMSCs can be the reason behind the improved central nervous system damage of the patients having Behcet's disease transplanted with allogeneic mesenchymal stem cells instead of autologous mesenchymal stem cells [96,98].

Our results demonstrated that, C677T SNP on *MTHFR* affects differentiation capacity of BMMSCs. On the other hand, these cells were isolated from different donors so the cells bear different genetic backgrounds. Also, diseases related with *MTHFR* C677T are complex diseases meaning that, the occurring of the diseases are not only caused by the mutation on a single gene, it can be due to multigene interactions or environmental factors as well. Our results have enough technical replicas, however they are not supported by the presence of biological replicas. For that reason, in order to correlate the C677T mutation and the altered differentiation ability of BMMSCs with a greater confidence, our study should be repeated multiple times with cells isolated from different donors. Increasing the sample size may help normalizing and generalizing our findings but still it will not be enough to eliminate the background differences to the fullest extent. For that reason, in order to eliminate the effect of genetic background and better understand the effect of the SNP on the

differentiation potentials of BMMSCs, CRISPR/Cas9 genome editing system was designed *in silico* in order to introduce C677T SNP on BMMSCs.

We chose CRISPR/Cas9 system since it is less time consuming and its design is simpler than the other genome editing systems. However, there are some challenges to be solved before using this system on humans. The most important one is the off-target effect, which is the binding and cleavage of untargeted sites by Cas9 that can lead to lethal problems. In order to reduce the possibility of off-target cleavage and recombination, we choose gRNAs having slightly less off target effects compared to others while performing the *in silico* design of our genome editing system. Successful introduction of *MTHFR* C677T into BMMSCs using CRISPR/Cas9 technology will also pave the way for the correction of a similar polymorphism by the same method and the use of gene-corrected autologous MSCs for damage repair. The fact that this polymorphism can be introduced to MSCs by using CRISPR/Cas9 technology is important in order to investigate the various disease models by filling the necessary information gap in order to study other polymorphisms which have not been studied in the literature. Many of the studies related with MSCs do not include gene editing. The few studies that used CRISPR/Cas9 system on MSCs employed viruses to transfect the cells. However, this kind of transfection system can not be used in this study since the result can be used as a guideline in personalized medicine in the future and viral transfection systems are not suitable to be used in humans. Also, technically, it is impossible to deliver the donor DNA template through viral infections in the case of a desired HDR modification such as in this study. Because of all these factors, this study serves as a guide for employing CRISPR/Cas9 genome editing of BMMSCs by transient transfection methods. One of the main challenges in this study was the limited availability of BMMSCs isolated from donors. Therefore, we first used HEK293T cells to prove that our design works. After that we continued with BMMSC transfection experiments.

We investigated the efficiency of different transfection reagents. From the pool of cells we indirectly demonstrated that, BMMSCs could be transfected with a chemical agent, PEI_{max} instead of viral transfection systems. According to our T7E1 results we expected to see a band at low intensity at the C/T BMMSC lane corresponding to the *MTHFR* PCR digest sizes however instead of that we observed a smear underneath the main band. These results were not comparable with our HEK293T CRISPR/Cas9 *MTHFR*sgrNA treated pool. The reason for this discrepancy is most probably because of the very low transfection efficiency and large cell size of BMMSCs. In a confluent 10cm tissue culture plate we could obtain $5 \cdot 10^6$ BMMSCs. The transfection efficiency was 40% in our experiments that means approximately $2 \cdot 10^6$ BMMSCs were transfected. The modification efficacy is approximately 1/100 with ssODNs, which gives us a yield of 20000 cells that could possibly carry the correct mutation. The other reason is the presence of high number of indel bearing HEK293T cells within the pool after CRISPR/Cas9 modification due to high transfection efficiency with a higher population size that is approximately $8 \cdot 10^6$ cells. CRISPR/Cas9 *MTHFR*sgrNA treated pool of BMMSCs gave similar results with C/T and T/T primary BMMSCs. Furthermore the C/C wild type was clearly negative according to our results. The presence of the smear at T/T could be explained by the presence of other mutations at the PCR amplicon as exon 5 of *MTHFR* gene bears many other mutations reported in the literature that could be followed via ENSEMBLE genome browser. Due to the very clear difference between the wild type BMMSCs and the CRISPR/Cas9 *MTHFR*sgrNA treated wild type BMMSCs we expected that our modification system successfully but not efficiently worked in BMMSCs.

However still, the major challenge after the transfection was that, BMMSCs should be seeded as single cells in order to obtain the clones harboring the specific C677T mutation. When cells were seeded as single cells and grown at very low numbers, unfortunately none of the cells were survived. The possible reason for that could be anoikis which is a type of programmed cell death induced when anchorage-dependent cells like BMMSCs detach from their surrounding ECM. According to Fujii et al. BMMSCs need essential growth factors and survival signals provided by

neighboring cells and the ECM. Several methods have been tested, including seeding them as 10-cell-subpopulations or culturing them in the presence of Y-27632, a ROCK inhibitor. The role of Y-27632 is not yet fully known but it improves the survival of certain cells in the cell culture when they are seeded as single cells like human ESCs. Unfortunately none of the tested methods were successful in our hands. These results indicated that further optimization is required to obtain single cell colonies out of BMMSC transient transfection experiments.

To conclude, our study demonstrated that C677T SNP on *MTHFR* may have an important effect on differentiation ability of BMMSCs into adipocytes, osteocytes and chondrocytes. However in order to prove this, either sample size should be increased or BMMSCs with the same genetic background should be used. For the gene editing of these cells, chemical agents can be used for the transfection however in order to select transfected cells, techniques should be improved.

6 REFERENCES

1. Morrison SJ, Shah NM, Anderson DJ. Regulatory mechanisms in stem cell biology. *Cell* 1997; 88(3):287-98.
2. Venkei, ZG and Yamashita, YM. Emerging mechanisms of asymmetric stem cell division *Journal of Cell Biology* 2018; 7(3): 72-80
3. Evans MJ, Kaufman MH. Establishment in culture of pluripotential cells from mouse embryos. *Nature* 1981; 292(5819):154-6
4. Reubinoff BE, Pera MF, Fong CY, Trounson A, Bongso A. Embryonic stem cell lines from human blastocysts: somatic differentiation in vitro. *Nat Biotechnol* 2000; 18(4):399-404
5. Keller G. Embryonic stem cell differentiation: emergence of a new era in biology and medicine. *Genes Dev* 2005; 19(10):1129-55
6. Wobus AM, Boheler KR. Embryonic stem cells: prospects for developmental biology and cell therapy. *Physiol Rev* 2005; 85(2):635-78
7. Amit M, Margulets V, Segev H, Shariki K, Laevsky I, Coleman R, Itskovitz-Eldor J. Human feeder layers for human embryonic stem cells. *Biol Reprod* 2003; 68(6):2150-6
8. Mitsui K, Tokuzawa Y, Itoh H, Segawa K, Murakami M, Takahashi K, Maruyama M, Maeda M, Yamanaka S. The homeoprotein Nanog is required for maintenance of pluripotency in mouse epiblast and ES cells. *Cell* 2003; 113(5):631-42.
9. Park IH, Zhao R, West JA, Yabuuchi A, Huo H, Ince TA, Lerou PH, Lensch MW, Daley GQ. Reprogramming of human somatic cells to pluripotency with defined factors. *Nature* 2008; 451(7175):141-6
10. Takahashi K, Yamanaka S. Induction of pluripotent stem cells from mouse embryonic and adult fibroblast cultures by defined factors. *Cell* 2006; 126(4):663-76
11. Aasen T, Raya A, Barrero MJ, Garreta E, Consiglio A, Gonzalez F, Vassena R, Bilić J, Pekarik V, Tiscornia G, Edel M, Boué S, Izpisua Belmonte JC. Efficient and rapid generation of induced pluripotent stem cells from human keratinocytes. *Nat Biotechnol* 2008; 26(11):1276-84
12. Nowell PC, Cole LJ, Habermeyer JG, Roan PL. Growth and continued function of rat marrow cells in x-irradiated mice. *Cancer Res* 1956; 16(3):258-61.
13. Gengozian N, Urso IS, Congdon CC, Conger AD, Makinodan T. Thymus specificity in lethally irradiated mice treated with rat bone marrow. *Proc Soc Exp Biol Med* 1957;96(3):714-20.
14. Kim M, Cooper DD, Hayes SF, Spangrude GJ. Rhodamine-123 staining in hematopoietic stem cells of young mice indicates mitochondrial activation rather than dye efflux. *Blood* 1998; 91(11):4106-17
15. Negrin RS, Atkinson K, Leemhuis T, Hanania E, Juttner C, Tierney K, Hu WW, Johnston

- LJ, Shizurn JA, Stockerl-Goldstein KE, Blume KG, Weissman IL, Bower S, Baynes R, Dansey R, Karanes C, Peters W, Klein J. Transplantation of highly purified CD34+Thy-1+ hematopoietic stem cells in patients with metastatic breast cancer. *Biol Blood Marrow Transplant* 2000; 6(3):262-71.
16. Ferrari G, Cusella-De Angelis G, Coletta M, Paolucci E, Stornaiuolo A, Cossu G, Mavilio F. Muscle regeneration by bone marrow-derived myogenic progenitors. *Science* 1998; 279(5356):1528-30
 17. Jackson KA, Majka SM, Wang H, Pocius J, Hartley CJ, Majesky MW, Entman ML, Michael LH, Hirschi KK, Goodell MA. Regeneration of ischemic cardiac muscle and vascular endothelium by adult stem cells. *J Clin Invest* 2001; 107(11):1395-402
 18. Raghunath J, Salacinski HJ, Sales KM, Butler PE, Seifalian AM. Advancing cartilage tissue engineering: the application of stem cell technology. *Curr Opin Biotechnol* 2005; 16(5):503-9.
 19. Friedenstein AJ, Petrakova KV, Kurolesova AI, Frolova GP. Heterotopic of bone marrow. Analysis of precursor cells for osteogenic and hematopoietic tissues. *Transplantation* 1968; 6(2):230-47
 20. Caplan AI. Mesenchymal stem cells. *J Orthop Res* 1991; 9(5):641-50
 21. Pittenger MF, Mackay AM, Beck SC, Jaiswal RK, Douglas R, Mosca JD, Moorman MA, Simonetti DW, Craig S, Marshak DR. Multilineage potential of adult human mesenchymal stem cells. *Science* 1999; 284(5411):143-7.
 22. da Silva Meirelles L, Caplan AI, Nardi NB. In search of the in vivo identity of mesenchymal stem cells. *Stem Cells* 2008; 26(9):2287-99.
 23. Salem HK, Thiemermann C. Mesenchymal stromal cells: current understanding and clinical status. *Stem Cells* 2010; 28(3):585-96
 24. Sackstein R, Merzaban JS, Cain DW, Dagia NM, Spencer JA, Lin CP, Wohlgemuth R. Ex vivo glycan engineering of CD44 programs human multipotent mesenchymal stromal cell trafficking to bone. *Nat Med* 2008; 14(2):181-7.
 25. Tögel F, Weiss K, Yang Y, Hu Z, Zhang P, Westenfelder C. Vasculotropic, paracrine actions of infused mesenchymal stem cells are important to the recovery from acute kidney injury. *Am J Physiol Renal Physiol* 2007; 292(5):F1626-35.
 26. Block GJ, Ohkouchi S, Fung F, Frenkel J, Gregory C, Pochampally R, DiMattia G, Sullivan DE, Prockop DJ. Multipotent stromal cells are activated to reduce apoptosis in part by upregulation and secretion of stanniocalcin-1. *Stem Cells* 2009; 27(3):670-81.
 27. Di Nicola M, Carlo-Stella C, Magni M, Milanese M, Longoni PD, Matteucci P, Grisanti S, Gianni AM. Human bone marrow stromal cells suppress T-lymphocyte proliferation induced by cellular or nonspecific mitogenic stimuli. *Blood* 2002; 99(10):3838-43.
 28. Krampera M, Glennie S, Dyson J, Scott D, Laylor R, Simpson E, Dazzi F. Bone marrow mesenchymal stem cells inhibit the response of naive and memory antigen-specific T cells to their cognate peptide. *Blood* 2003; 101(9):3722-9.

29. Berglund AK, Schnabe LV. Allogeneic major histocompatibility complex-mismatched equine bone marrow-derived mesenchymal stem cells are targeted for death by cytotoxic anti-major histocompatibility complex antibodies. *Equine Vet. J* 2017; 49:4,539-544.
30. Oishi K, Noguchi H, Yukawa H, Hayashi S. Differential ability of somatic stem cells. *Cell Transplant* 2009;18(5): 581–589.
31. Dennis JE, Carbillet JP, Caplan AI, Charbord P, The STRO-1⁺marrow cell population is multipotential. *Cells Tissues Organs* 2002; 170(2–3):73–82.
32. Ding DC, Shyu WC, Lin SZ. Mesenchymal Stem Cells. *Cell Transplantation* 2011; 20, 5–14.
33. Uccelli A, Moretta L, Pistoria V. Mesenchymal stem cells in health and disease. *Nature Reviews Immunology* 2008; 8, 726–736.
34. Ouyang HW, Goh, JC, Thambyah, A, Teoh SH, Lee EH. Knitted polylactide-co-glycolide scaffold loaded with bone marrow stromal cells in repair and regeneration of rabbit Achilles tendon. *Tissue Eng* 2003; 9(3): 431–439.
35. Hung SC, Chang CF, Ma HL, Chen TH, Lowtone Ho, L. Gene expression profiles of early adipogenesis in human mesenchymal stem cells. *Gene* 2004; 340(1):141– 150.
36. Sekiya I, Larson BL, Smith JR, Pochampally R, Cui JG, Prockop DJ. Expansion of human adult stem cells from bone marrow stroma: Conditions that maximize the yields of early progenitors and evaluate their quality. *Stem Cells* 2002; 20(6):530–541.
37. Qian L, Saltzman WM. Improving the expansion and neuronal differentiation of mesenchymal stem cells through culture surface modification. *Biomaterials* 2004; 25(7–8):1331– 1337.
38. Chen, LB., Jiang, XB., Yang, L. Differentiation of rat marrow mesenchymal stem cells into pancreatic islet beta- cells. *World J. Gastroenterol* 2004; 10(20):3016–3020.
39. Lee KD, Kuo TK, Whang-Peng J, Chung YF, Lin CT, Chou SH, Chen JR, Chen YP, Lee OK. In vitro hepatic differentiation of human mesenchymal stem cells. *Hepatology* 2004; 40(6):1275–1284.
40. Inada M, Follenzi A, Cheng K, Surana M, Joseph B, Benten D, Bandi S, Qian H, Gupta S. Phenotype reversion in fetal human liver epithelial cells identifies the role of an intermediate mesoendodermal stage before hepatic maturation. *J. Cell Sci* 2008; 121(7):1002–1013.
41. Zhang F, Wen Y, Guo X. CRISPR/Cas9 for genome editing: Progress, implications and challenges. *Hum Mol Genet* 2014; 23,40–46.
42. Sander JD, Joung JK. CRISPR-Cas systems for genome editing, regulation and targeting. *Nat Biotechnol* 2014; 32, 4,347–355.
43. Kim YG, Cha J, Chandrasegaran S. Hybrid restriction enzymes: zinc finger fusions to Fok I cleavage domain, *Proc. Natl. Acad. Sci.* 1996; 93, 1156–1160.
44. Silva G. Meganucleases and other tools for targeted genome engineering: perspectives and challenges for gene therapy. *Curr Gene Ther* 2011;11, 11–27.
45. Urnov FD, Rebar EJ, Holmes MC, Zhang HS, Gregory PD. Genome editing with engineered

- zinc finger nucleases. *Nat Rev Genet* 2010; 11, 636– 646.
46. Jinek M, Chylinski K, Fonfara I, Hauer M, Doudna JA, Charpentier E. A programmable dual-RNA-guided DNA endonuclease in adaptive bacterial immunity. *Science* 2012; 80, 337, 816–821.
 47. Fineran PC., Charpentier, E. Memory of viral infections by CRISPR-Cas adaptive immune systems: Acquisition of new information. *Virology* 2012; 434, 202–209.
 48. Deltcheva, E. CRISPR RNA maturation by trans-encoded small RNA and host factor RNase III. *Nature* 2011; 471, 602–607
 49. Zhang, JH, Adikaram, P., Pandey, M., Genis, A., Simonds, WF. Optimization of genome editing through CRISPR-Cas9 engineering. *Bioengineered* 2016; 7, 3, 166–174.
 50. Weninger A, Hatzl AM, Schmid C, Vogl T, Glieder A. Combinatorial optimization of CRISPR/Cas9 expression enables precision genome engineering in the methylotrophic yeast *Pichia pastoris*. *J. Biotechnol* 2016; 7(3): 72-80.
 51. Calarco J, Friedland A. Creating genome modifications in *C. elegans* using the CRISPR/Cas9 system. *Methods Mol. Biol* 2015; 1327, 59–74.
 52. Cong L. Multiplex genome engineering using CRISPR/Cas systems, *Science* 2013; 80, 819–823
 53. Vojta A. Repurposing the CRISPR-Cas9 system for targeted DNA methylation, *Nucleic Acids Res* 2016; 8(5): 96-110
 54. Dominguez AA, Lim WA, Qi LS. Beyond editing: repurposing CRISPR- Cas9 for precision genome regulation and interrogation. *Nat. Rev. Mol Cell Biol* 2015; 17, 5–15.
 55. Xue HY, Ji LJ, Gao AM, Liu P, He JD, Lu XJ. CRISPR-Cas9 for medical genetic screens: applications and future perspectives, *J. Med. Gene* 2015; 0, 1– 7.
 56. Savic N, Schwank G. Advances in therapeutic CRISPR/Cas9 genome editing, *Transl. Res.* 2015; 967.
 57. Müller M. *Streptococcus thermophilus* CRISPR-Cas9 systems enable specific editing of the human genome. *Mol. Ther*; 2015.
 58. Wojtal D. Spell checking nature: Versatility of CRISPR/Cas9 for developing treatments for inherited disorders, *Am. J. Hum. Genet* 2016; 98, 1–12
 59. White MK, Khalili K. CRISPR/Cas9 and cancer targets: future possibilities and present challenges, *Oncotarget* 2016; (7)11, 12305–12317.
 60. Homberger G, Linnebank M, Winter C, Genomic structure and transcript variants of the human methylenetetrahydrofolate reductase gene. *Eur J Hum Genet* 2000; 8:725-729.
 61. Weisberg I, Tran P, Christensen, B, A second genetic polymorphism in methylenetetrahydrofolate reductase (MTHFR) associated with decreased enzyme activity. *Mol Genet Metab* 1998; 64: 169- 172
 62. Daly SF, Molloy AM, Mills JL. The influence of 5,10 methylenetetrahydrofolate reductase

- genotypes on enzyme activity in placental tissue. *Brit J Obstet Gynae* 1999; 106:1214-1218.
63. Stern LL, Bagley PJ, Rosenberg IH. Conversion of 5-formyltetrahydrofolic acid is unimpaired in folate-adequate persons homozygous for the C677T mutation in the methylenetetrahydrofolate reductase gene. *J Nutr* 2000; 130: 2238-2242.
 64. Goyette P, Pai A, Milos R. Gene structure of human mouse methylenetetrahydrofolate reductase (MTHFR). *Mammalian Genome* 1998; 9:652-656.
 65. Rozen R. Methylenetetrahydrofolate reductase in vascular disease, neural tube defects and colon cancer; 1998.
 66. Botto LD, Yang Q. 5,10-Methylenetetrahydrofolate reductase gene variants and congenital anomalies: *Am J Epidemiol* 2000; 151, 862-77
 67. Tonetti C, Burtscher A, Bories D. Methylenetetrahydrofolate reductase deficiency in four siblings: A clinical, biochemical, and molecular study of the family. *Am J Med Genet* 2000; 91:363-367.
 68. Goyette P, Pai A, Milos R. Gene structure of human mouse methylenetetrahydrofolate reductase (MTHFR). *Mammalian Genome* 1998; 9:652-656
 69. Bagley PJ, Jacob S. A common mutation in the methylenetetrahydrofolate reductase gene is associated with an accumulation of formylated tetrahydrofolates in red blood cells. *Med Sci* 1998;95:13217-13220.
 70. Molloy AM, Daly S, Mills JL. Thermolabile variant of 5,10-methylenetetrahydrofolate reductase associated with low red-cell folates: Implications for folate intake recommendations. *The Lancet* 1997; 49: 1591-1593.
 71. Schmitz C, Lindpainter K, Verhoef P. Genetic polymorphism of methylenetetrahydrofolate reductase and myocardial infarction. *Circulation* 1996; 94: 1812-1814.
 72. Shpichinetsky V, Raz I, Friedlander Y, et al. The association between two common mutations C677T and A1298C in human methylenetetrahydrofolate reductase gene and the risk for diabetic nephropathy in type II diabetic patients. *J Nutr* 2000; 130: 2493-2497.
 73. Fodinger M, Horl WH, Sunder-Plassman G. Molecular biology of 5,10-methylenetetrahydrofolate reductase. *J Nephrol* 2000; 13(1):20-33.
 74. Goyette P, Rozen R. The thermolabile variant 677CT can further reduce activity when expressed in cis with severe mutations for human methylenetetrahydrofolate reductase. *Hum Mutat* 2000; 16:132-138.
 75. Sibani S, Christensen B, O'Ferrall E, et al. Characterization of six novel mutations in the methylenetetrahydrofolate reductase (MTHFR) gene in patients with homocystinuria. *Hum Mutat* 2000; 15: 280-287.
 76. Liew SC, Gupta ED. Methylenetetrahydrofolate reductase (MTHFR) C677T polymorphism: Epidemiology, metabolism and the associated diseases. *European Journal of Medical Genetics* 2014; 1-10.
 77. Peng F, Labelle LA, Rainey B, et al. Single nucleotide polymorphisms in the

- methylenetetrahydrofolate reductase gene are common in US Caucasian and Hispanic American populations. *Int J Mol Med* 2001; 8: 509-511.
78. Rady PL, Tying SK, Hundnall SD, Methylenetetrahydrofolate reductase (MTHFR): The incidence of mutations C677T and A1298C in the Ashkenazi Jewish population. *Am J Med Genet* 1999; 86:380-384.
 79. Tonetti C, Burtscher A, Bories D. Methylenetetrahydrofolate reductase deficiency in four siblings: A clinical, biochemical, and molecular study of the family. *Am J Med Genet* 2000; 91:363- 367.
 80. Schneider JA, Rees DC, Liu YT. Worldwide distribution of a common methylenetetrahydrofolate reductase mutation. *Am J Hum Genet* 1998; 62: 1258-1260.
 81. Sell SM, Lagemwa PR. Development of a highly accurate, rapid PCR-RFLP genotyping assay for the methylenetetrahydrofolate reductase gene. *Genet Test* 1999; 3:287-289.
 82. Demuth K, Moatti N, Hanon O,. Opposite effects of plasma homocysteine and the methylenetetrahydrofolate reductase C677T mutation on carotid artery geometry in asymptomatic adults. *Thromb Vasc Biol* 1998; 18:1838-1843.
 83. Lee H, Choi J, Ha K,. Influence of 5,10- methylenetetrahydrofolate reductase gene polymorphism on plasma homocysteine concentration in patients with end-stage renal disease. *Am J Kidney Dis* 1999; 34: 259-263.
 84. Bova I, Chapman J, Sylantiev C,. The A677C methylenetetrahydrofolate reductase gene polymorphism and carotid atherosclerosis . *Stroke* 1999; 30: 2180-2182.
 85. Kang S, Wong PWK, Susmano A. Thermolabile methylenetetrahydrofolate reductase: An inherited risk factor for coronary artery disease. *J Hum Genet* 1991; 48: 536-545.
 86. Lievers KJA, Boers GHJ, Verhoef V, et al. A second common variant in methylenetetrahydrofolate reductase (MTHFR) gene and its relationship to MTHFR enzyme activity, homocysteine and cardiovascular disease risk. *Journal of Molecular Medicine* 2011; 73-87.
 87. Kang S, Zhou J, Wong P, Kowalisyn J, Strokosch G. Intermediate homocysteinaemia: a thermolabile variant of methylenetetrahydrofolate reductase. *Am J Hum Genet* 1998; 43:414-21.
 88. Rozen R. Genetic predisposition to hyperhomocysteinaemia: deficiency of methylenetetrahydrofolate reductase (MTHFR). *Thromb Haemost* 1997; 78:523-6.
 89. Morita H, Kurihara H, Tsubaki S,. Methylenetetrahydrofolate reductase gene polymorphism and ischemic stroke in Japanese. *Arterioscler Thromb Vasc Biol* 1998; 18:1465-1469.
 90. Donnelly JG, Rock GA. Genetic determinants of heritable venous thrombosis: Genotyping methods for factor V_{LEIDEN} A1691G, methylenetetrahydrofolate reductase C677T, prothrombin G20210A mutation, and algorithms for venous thrombosis investigations. *Clin Biochem* 1999; 32: 223-228.
 91. van der Put NM, Gabreels F, Stevens EMB. A second common mutation in the

- methylenetetrahydrofolate reductase gene: An additional risk factor for neural-tube defects. *Am J Hum Genet* 1998; 62:1044-1051.
92. Dean JCS, Moore SJ, Osborne A, Fetal anticonvulsant syndrome and mutation in the maternal MTHFR gene. *Clin Genet* 1999; 56: 216- 220.
 93. Crott JW, Mashiyama ST, Ames BN, The effect of folic acid deficiency and MTHFR C677T polymorphism on chromosome damage in human lymphocytes in vitro. *Cancer Epidem Biomar* 2001;10(10):1089-1096.
 94. Güneş HV. *Moleküler Hücre Biyolojisi* 2003; 1,223-224.
 95. Piyathilake CJ, Macaluso M, Johanning GL, et al. Methylenetetrahydrofolate reductase (MTHFR) polymorphisim increases the risk of cervical intraepithelial neoplasia. *Anticancer Res* 2000; 20:1751-1757.
 96. Behera J, Bala J, Nuru M, Tyagi SC, Tyagi N, Homocysteine as a Pathological Biomarker for Bone Disease, *Journal of Cellular Physiology* 2016; 17: 23-35.
 97. Cai B, Li X, Wang Y, Liu Y, Yang F, Chen H. Apoptosis of Bone Marrow Mesenchymal Stem Cells Caused by Homocysteine via Activating JNK Signal. *PLoS ONE* 2013; 8(5): 63561.
 98. Davatchi F, Nikbin B, Shams H, Sadeghi Abdollahi B, Mohyeddin M, Shahram F, Mesenchymal stem cell therapy unable to rescue the vision from advanced Behcet's disease retinal vasculitis: report of three patients, *International Journal of Rheumatic Diseases* 2013; 16: 139–147.
 99. Horwitz E, Le BK, Dominici M. Clarification of the nomenclature for MSC: the International Society for Cellular Therapy position statement. *Cytotherapy* 2013; 7:393 5.
 100. Chang TY, Subbaroyan R, Hasan MT. High-efficiency stable gene transfection using chloroquine-treated Chinese hamster ovary cells. *Somat. Cell Mol Genet* 1991; 17, 5,513-7.

7 CURRICULUM VITAE

Personal Information

Name	Burcu	Surname	Taluğ
Birth of place	İstanbul	Date of birth	18.03.1992
Nationality	T.C.	Telephone number	
E-mail	burcutalug@gmail.com		

Educational Level

	Institution Name	Graduate Year
Master	Mehmet Ali Aydınlar Acibadem University	2019
Undergraduate	Yeditepe University	2016
High-School	Kadir Has Anadolu Lisesi	2010

Work Experience

	Position	Enterprise	Duration
1.	Long Term R&D Internship (Project based)	TAYF Biotechnology	4/2014 – 8/2014
8	Yeditepe University	Assistant student in Regenerative Biology laboratory	9/2015 – 6/2016
3.	NCMM Center for Molecular Medicine Norway, University of Oslo	Internship	06/2018- 09/2018

Foreign Languages	Reading*	Speaking*	Writing*
English	Very good	Very Good	Very Good

Foreign Languages Exams•

YÖK- DİL	UDS	IELTS	TOEFL IBT	TOEFL PBT	TOEFL CBT	FCE	CAE	CPE
92/100		6.5/9						

	Quantitative	Equally Weighted	Verbal
ALES Exam	77,66	80,74	73,65

Projects				
	Granted Program	Active Years	Position	Project Name
1.	TÜBİTAK 1003 (216S404)	2017-2019	Burslu	Genome-Wide Screening With CRISPR/Cas9 and Modeling of Resistance Mechanisms Developed Against Cytotoxic Drugs in Cancer Treatment

Presentations & Awards			
	Organization	Presentation Type	Title of the Presentation
1.	5th International Congress of Molecular Biology Association of Turkey, Bogazici University	Poster	Investigating The Effects Of 5,10-Methylenetetrahydrofolate Reductase C677t Polymorphism On Mesenchymal Stem Cells By Using Crispr/Cas9 System As A Gene Editing Tool
2.	5th International Congress of Molecular Biology Association of Turkey, Bogazici University	Poster	The Role Of Long Noncoding Rna Dancr In The Dna Damage Response
3.	Adv Exp Med Biol	Publication	Induced Pluripotent Stem Cells in Disease Modeling and Regeneration